University of Milano-Bicocca

Department of Quantitative Methods for Economics and Business
Doctoral Thesis in Mathematics for Financial Markets Analysis

Spread and Basket Option Pricing: an Application to Interconnected Power Markets

Author:
Ruggero Caldana

Supervisor:
Gianluca Fusai

Milan, October 2012

Dedicated to my family.

Abstract. An interconnector is an asset that gives the owner the right, but not the obligation, to transmit electricity between two locations each hour of the day over a prefixed time period. The financial value of the interconnector is given by a series of options that are written on the price differential between two electricity markets, that is, a strip of European options on an hourly spread. Since the hourly forward price is not directly observable on the market, Chapter 1 proposes a practical procedure to build an hourly forward price curve, fitting both base load and peak load forward quotations. One needs a stochastic model, a valuation formula, and a calibration method to evaluate interconnection capacity contracts. To capture the main features of the electricity price series, we model the energy price log-returns for each hour with a non-Gaussian mean-reverting stochastic process. Unfortunately no explicit solution to the spread option valuation problem is available. Chapter 2 develops a method for pricing the generic spread option in the non-Gaussian framework by extending the Bjerksund and Stensland (2011) approximation to a Fourier transform framework. We also obtain an upper bound on the estimation error. The method is applicable to models in which the joint characteristic function of the underlying assets is known analytically. Since an option on the difference of two prices is a particular case of a basket option, Chapter 3 extends our results to basket option pricing, obtaining a lower and an upper bound on the estimated price. We propose a general lower approximation to the basket option price and provide an upper bound on the estimation error. The method is applicable to models in which the joint characteristic function of the underlying assets and the geometric average is known. We test the performance of these new pricing algorithms, considering different stochastic dynamic models. Finally, in Chapter 4, we use the proposed spread option pricing method to price interconnectors. We show how to set up a calibration procedure: A market-coherent calibration is obtained, reproducing the hourly forward price curve. Finally, we present several examples of interconnector capacity contract valuation between European countries.

Introduction

The White Rabbit put on his spectacles. "Where shall I begin, please your Majesty?" he asked. "Begin at the beginning," the King said gravely, "and go on till you come to the end: then stop."

Lewis Carroll (1832–1898)

Electricity markets have been liberalized worldwide over the last 20 years. Before this period, electricity prices were generally determined by the regulatory authorities controlled by the government of each individual country. Now many countries have reformed their power sector, leaving the price determination to the market principles of supply and demand. One important consequence of this is the trade of electricity delivery contracts on exchanges or through over-the-counter markets. Energy has thus become an important asset class of investments, attracting not only traditional actors in the energy markets, but also speculators such as banks and investment funds. However, the new power market setting brings an increased uncertainty to the electricity price dynamic and many markets exhibit very high rates of volatility, which are hardly found in any other assets. Energy spot prices have several typical features, such as mean reversion toward a seasonally varying mean level driven by the balance between demand and production. Another important characteristic is the frequent occurrence of spikes, resulting from an imbalance between supply and demand. This extreme behavior is also present in the difference between the prices of two locations. This price difference is an economic incentive to transport electric power between countries, explaining why an interconnection between two markets could be profitable. In the European power market, interconnections between different countries play an important role in obtaining energy balance and maintaining security of supply. Countries are connected by a complex web of transmission lines and the exchange of electricity between European states is increasing. An interconnector is an asset that gives the owner the right, but not the obligation, to transmit electricity between two locations each hour of the day over a prefixed time period. The financial value of the interconnector is given by a series of options that are written on the price differential between two electricity markets, that is, a strip of European options on an hourly spread.

Evaluating interconnections between power markets is a very recent issue and requires financial modeling and pricing tools. First, a stochastic model is required to describe the price dynamics. A natural class of stochastic models to describe the log-price dynamics is a non-Gaussian mean-reverting stochastic process in which specification jumps and seasonality must be included. We model the price log-returns. Second, a pricing formula is required. Unfortunately, no explicit solution to the spread option valuation problem has been available up to now and very little is

discussed in the literature about pricing spread options in the non-Gaussian setup. Furthermore, we would like to use a general enough pricing method, for example requiring only that the joint characteristic function of the log-returns of the assets is known; we could thus change the price dynamics without changing the pricing method, provided the joint characteristic function of the log-returns of the assets is known for the model in question. Hurd and Zhou (2009) have proposed the best technique we are aware of, but their method has a drawback: It requires a bivariate Fourier inversion. The **first contribution** of the present work is the derivation of a lower bound to the value of an option on the spread of two prices, extending the method of Bjerksund and Stensland (2011) to general processes. Our lower approximation turns out to be extremely accurate for many stochastic dynamics, as confirmed by several numerical tests. The computation of our lower bound requires a univariate Fourier inversion, versus the bivariate inversion required in the work of Hurd and Zhou (2009). We also derive a general upper bound.

An option on the difference between two prices is a particular case of a more general contract, a basket option. Basket options are hard to price and hedge as well as spread options and existing pricing methods are not totally satisfying. Many of the methods have limited scope because they require a basket value that is always positive and can be applied only in a geometric Brownian motion setting. The study of pricing methods for general price dynamics is still underdeveloped. The **second contribution** of the present work is the derivation of a lower bound for the value of a basket option for general price processes, allowing the basket value to be negative. The only quantity we need to know explicitly is the joint characteristic function of the log-returns of the assets and the geometric average. The computation of our lower bound requires a univariate Fourier inversion and an optimization. Numerical experiments show that the performance of our lower approximation is comparable to that of the best methods in a geometric Brownian motion setting. A comparison with Monte Carlo simulations shows the quality of the method even in the non-Gaussian case. In addition, we derive a general upper bound.

Let us return to the valuation of interconnection contracts. Once we have chosen the model and the spread option pricing method, we only need a calibration procedure to set the pricing method according to market information. Regardless of the calibration procedure we could construct, a remark is necessary. The interconnections are priced under a risk-neutral measure. However, the underlying cannot be used to replicate derivative products in energy markets due to the non-storability of electricity. The market is incomplete; thus arbitrage arguments do not immediately lead to a unique price for derivatives. Moreover, liquid energy option markets are still rare and data from average-based forward contracts are often the only information available. We need to use historical data to overcome this issue. To calibrate the model, we obtain data from the real-world probability measure $\mathbb{P}$ and transfer their information to an equivalent risk-neutral measure $\mathbb{Q}$ setting. Since the market is incomplete, the measure $\mathbb{Q}$ is not uniquely determined and needs to be chosen according to some criteria. Irrespective of the criteria chosen, it is important to fit the only market information that is usually available on liquid markets, that is, forward contract quotations. On the other hand, the inability to store electricity makes its price a pure flow variable and hence all contracts need to specify a delivery period, so the electricity forward contract does not just pay at a fixed date but over a period of time. Such delivery periods can differ from the settlement period of each option composing an interconnection capacity contract. How can an hourly pricing model incorporate the information given by contracts with longer delivery periods? A common solution is to represent the forward prices by a term structure. We need a bootstrapping procedure to extrapolate hourly forward prices from forward contract quotations.

The most important paper concerning how to fit a forward price curve in the energy market is that of Benth et al. (2007b). The authors derive a smooth instantaneous forward curve modeling the forward price as the sum of a seasonality function and a polynomial spline. Given an instantaneous forward curve, it is straightforward to compute an hourly curve. However, we do not directly use the method of Benth et al. (2007b). The proposed method deals only with base load quotations. Although from a theoretical point of view the method is still applicable even if we want to consider peak load quotations, from a practical perspective this task is very challenging to implement. Furthermore, hourly electricity prices in day-ahead markets do not follow a time series process but are a panel of 24 cross-sectional hours that vary from day to day. This is because the microstructure of many day-ahead markets is such that prices for all hours are quoted at the same moment in a day. Therefore, hourly prices within a day behave cross-sectionally and hourly dynamics over days behave according to time-series properties. Since the method of Benth et al. (2007b) is based on a maximum smoothness criterion, each computed point depends on other points of the generated curve and is set to determine the smoothest configuration. We decide to use the maximum smoothness criterion only to mimic the time dependency. We compute a daily forward curve fitted to base load forward quotations. Then, using the computed daily forward curve, an hourly shape is achieved using statistical tools. The **third contribution** of the present work is the discussion of a practical method to obtain an hourly forward price curve fitting both base load and peak load forward quotations.

Once we choose the model and spread option pricing method and calibrate the model to market data, we can finally evaluate the interconnection capacity contracts. Few studies discuss such issue. The most valuable paper is that of Cartea and Pedraz (2012), who model the spread between markets directly with a mean-reverting jump diffusion process, splitting the data between peak and off-peak hours. We use a different approach and set up 24 models for each interconnected market, describing the price of a specific hour of the day. We thus have many more parameters to calibrate than Cartea and Pedraz (2012), but we do so for three reasons. First, we model the price and not the spread because it is useful to have a model able to price not only spread options but also other options written on the hourly price. We therefore do not need to change the model if we want to price a different derivative contract, only the pricing method. Furthermore, a model for the price could be useful for calibration purposes. A liquid energy option market is still in the distant future for Europe, but things can change. If a liquid market were available for energy options on a single asset, it would be possible to calibrate the model to option prices, obtaining a more detailed estimation of the probability measure describing market prices. Second, splitting prices between peak and off-peak hours is a strong approximation. Huisman et al. (2007) state that the statistical characteristics of day-ahead prices do not exactly follow a peak/off-peak structure. The authors show that the speed of mean reversion is different over the hours, with the lowest mean reversion estimates for the hours 18:00 through 22:00. In addition, despite Huisman et al. (2007) identifying a cross-sectional correlation structure between peak and off-peak prices within the same day, the boundaries of such correlation blocks do not perfectly match the market definitions of peak and off-peak hours. Third, modeling each hour separately allows us to fit the forward market information reproduced by the bootstrapped hourly forward curve, adopting a risk-neutral pricing. Cartea and Pedraz (2012) prefer to price the interconnectors under the real probability measure $\mathbb{P}$ and discount cash flows by a risk-adjusted rate. However, they do not discuss how to choose the risk-adjusted rate depending on the available forward market quotations; using forward market data, they only provide no-arbitrage lower bounds for the value of a bidirectional interconnector. The **fourth**

contribution of our work is a new approach to interconnection capacity contract valuation that outperforms that of Cartea and Pedraz (2012) for the three reasons underlined above.

This work is organized as follows. Chapter 1 provides an introduction to energy markets and energy forward contracts. It discusses the method of Benth et al. (2007b) and propose a procedure to obtain an hourly forward curve, fitting both base load and peak load forward quotations. All the steps of the procedure are discussed with the help of a practical curve construction example on the German EEX (European Energy Exchange) market. Chapters 2 and 3 discuss options on the spread of two assets and basket options, respectively. Providing a lower bound and an estimation of the error, we propose general pricing methods in both cases and test their performance with numerical experiments. Finally, Chapter 4 describes interconnection capacity contracts. It sets up a model and discusses how to calibrate it. This study concludes with several examples of interconnection valuations between European countries.

CHAPTER 1

Hourly Forward Price Curve Fitting

The purpose of models is not to fit the data but to sharpen the questions.

Samuel Karlin (1923–2007)

Modeling the energy forward price dynamics or marking an over-the-counter (OTC) product to the market inevitably deals with the issue of representing forward prices by a term structure curve. The settlement periods of OTC financial contracts traded in the market can differ from those traded on the exchange. In marking to market, investors need to combine market prices to reflect the "market" value of the OTC product. A forward curve that can be used to price electricity futures with any settlement period is an essential tool.

Fitting a yield curve to market data in a fixed income market is a topic that has been extensively studied. The seminal paper in this field is that of McCulloch (1971) and a survey of different methods for constructing yield curves is provided by Anderson and Deacon (1996). The first application to curve fitting in the energy market was that of Fleten and Lemming (2003), who smoothen an electricity futures curve based on a bottom–up model called the MPS model. The MPS model calculates weekly equilibrium prices and production quantities based on fundamental factors for demand and production (e.g., temperature, fuel costs, snow levels, capacities). The approach of Fleten and Lemming (2003) is non-parametric, in the sense that they derive a sequence of daily (or any other appropriate time resolution) forward prices minimizing the least-squares distance to the output from the MPS model. The optimization is constrained on the bid–ask spreads of market prices and the curve is appropriately smoothened by a penalty term. Hildmann et al. (2011) propose a method for the construction of an hourly forward price curve and fit a curve applying statistical techniques such as LAD-lasso regression and median estimation to develop a robust calculation method. The most important paper concerning how to fit forward price curve in the energy market is that of Benth et al. (2007b). These authors derive a smooth instantaneous forward curve modeling the forward price as the sum of a seasonality function and a polynomial spline. The proposed method deals only with base load quotations. Although from a theoretical point of view their method is still applicable even when considering peak load quotations, from a practical perspective this task is very challenging to implement. We fill this gap with the methodology proposed in this chapter.

We propose a procedure to obtain an hourly forward curve, fitting both base load and peak load forward quotations. Section 1 introduces energy markets and describes how electricity forward contracts work. Section 2 focuses on a daily seasonality function to be used in the derivation of a daily forward curve. The method of Benth et al. (2007b) is the kernel of the daily curve computation and is described in Section 3. Once the daily forward curve is derived, we give it an hourly shape to

consider both historical and peak load information. Section 4 models hourly seasonality and Section 5 computes the hourly forward curve. All the steps of the procedure are discussed with the help of a practical curve construction example on the European Energy Exchange (EEX), implemented in the Matlab computing environment. Section 6 presents backtesting results and how to set calibration parameters.

1. Forward contracts in energy markets

Electricity has been called a flow commodity because of its non-storability. Electrical power is only useful for practical purposes if it can be delivered during a period of time. Deregulated power markets have market mechanisms to balance supply and demand where electricity is traded in an auction system for standardized contracts. All contracts guarantee the delivery of a given amount of power for a specified future time period. Some contracts prescribe physical delivery, while others are financially settled. While the specifications and rules of trading for financial electricity contracts vary among the different power exchanges, we briefly describe here some general features of energy markets, referring the interested reader to Benth et al. (2008) for a detailed introduction.

By physical electricity contracts we mean contracts with actual consumption or production as part of contract fulfillment. The contracts for physical delivery are usually organized between two different markets: the real-time market and the day-ahead market (a two-settlement system). The spot day-ahead price is a common reference price for financial energy contracts. On such markets, hourly power contracts are traded daily for physical delivery in the next day's 24-hour period (midnight to midnight). Each morning, the players submit their bids for purchasing or selling a certain volume of electricity for the different hours of the following day. Once the spot market is closed for bids, at noon each day, the day-ahead price is derived for each hour next day. Strictly speaking, the day-ahead market trades in electricity forward contracts with delivery over a specified hour the next day.

Financial power contracts are linked to reference electricity spot prices (e.g. day-ahead prices) and are settled in cash. One difference between physical electricity markets and financial markets is that the latter is open to speculators, since the consumption or production of electricity is not required to participate in the market. Basic exchange traded contracts are written on the (weighted) average of the (hourly) reference price over a specified delivery period. During the delivery period the contract is settled in cash against the system price. The specified reference price is typically the day-ahead price. Contracts are not traded during the delivery period and market participants typically close their positions beforehand. Let us see how to mathematically describe such contracts. Let $S(t)$ be the (day-ahead) spot price at time t. The strike price F at time t of an instantaneous zero-cost forward contract paying $S(T) - F$ at time T is denoted by $f(T)$ and given by the risk-neutral expectation

$$f(T) = \mathbb{E}[S(T)].$$

In electricity markets the forward contract does not just pay at time T but over a time period $[\tau^b, \tau^e]$. The strike of a zero-cost forward depends on the precise specification of when the money is paid. There are two kinds of payouts for forward contracts: instant settlement and settlement at maturity. In an instant settlement the contract pays $(S(t) - F)\Delta t$ at time t. In a settlement at maturity the payment of the whole amount is due at the end of the delivery period τ^e. By definition of a forward contract, the strike F has to be set so that the contract is of zero cost at the time t

we enter into it. So for settlement at maturity we have

$$\mathbb{E}\left[\int_{\tau^b}^{\tau^e}(S(u)-F)du\right]=0,$$

which leads to

$$F=\frac{1}{\tau^e-\tau^s}\int_{\tau^b}^{\tau^e}f(u)du.$$

In the case of an instant settlement the money received can be invested in a riskless bank account, so

$$\mathbb{E}\left[\int_{\tau^b}^{\tau^e}(S(u)-F)e^{r(\tau^e-u)}du\right]=0.$$

Solving the equation in F yields

$$F=\frac{r}{e^{r(\tau^e-\tau^s)}-1}\int_{\tau^b}^{\tau^e}e^{r(\tau^e-u)}f(u)du.$$

In both cases, the strike price F of an average-based forward contract turns out to be a weighted average of all instantaneous forwards in that period, but for small delivery periods we can make the first-order approximation

$$\frac{re^{r(\tau^e-u)}}{e^{r(\tau^e-\tau^s)}-1}\approx\frac{1}{\tau^e-\tau^s}. \tag{1}$$

It therefore only makes a small difference whether the money is settled at the end of the period or on a daily basis.

Forward contracts are described above in continuous time. However, in practice, they are not settled continuously over the delivery period but, rather, at discrete times. These discrete times are usually days or hours. When a contract settlement period comprises all the hours in a day, we call it a base load forward contract. A contract can even involve only a subset of the hours of a day. The most common such contract is the peak load forward contract, where the settlement period consists of the peak load hours between τ^b and τ^e. Peak load hours are a subset of the hours of a day in which the energy demand is supposed to be highest. The complementary set of hours is called off peak. The definition of peak and off peak depends on the market. For example, the EEX defines it as the average price over 8:00–20:00 and the APX Power UK defines it as the average over 7:00–19:00, Monday to Friday. For simplicity, we consider markets in which peak hours are from 8:00 to 20:00. Assuming time is measured in hours and assuming a settlement in N days with $\tau^b=t_1,\tau^e=t_N$, the strike price relations for base load and peak load contracts become

$$F^{base}=\frac{1}{24N}\sum_{i=1}^{N}\sum_{h=1}^{24}\hat{f}(t_i,h),\quad F^{peak}=\frac{1}{12\sharp BD}\sum_{i=1}^{\sharp BD}\sum_{h=9}^{20}\hat{f}(t_i,h),$$

where $\hat{f}(t_i,h)$ is the forward price for hour h of day t_i and $\sharp BD$ is the number of business days of the forward settlement period. In this setting we do not consider that some days present with 23 or 25 hours when going from a legal to a solar hour count or vice versa. The following sections describe a methodology to obtain $\hat{f}(t_i,h)$, starting from market data. For a better understanding, we present a numerical example of an hourly forward curve construction on the German market (EEX). We build a curve at the valuation date $t_0=22/05/2012$. Base load and peak load forward

TABLE 1. EEX forward market data.

Start Date	End Date	F^{base}	F^{peak}
22/05/12	22/05/12	42.750	49.000
23/05/12	23/05/12	42.450	47.880
24/05/12	24/05/12	38.380	43.250
25/05/12	25/05/12	36.980	41.130
26/05/12	27/05/12	28.350	N.A.
02/06/12	03/06/12	27.500	N.A.
28/05/12	03/06/12	35.125	41.625
04/06/12	10/06/12	36.850	43.875
11/06/12	17/06/12	39.400	47.500
18/06/12	24/06/12	40.625	49.000
25/06/12	01/07/12	40.210	50.500
01/07/12	31/07/12	40.175	49.025
01/08/12	31/08/12	38.775	47.250
01/09/12	30/09/12	44.475	53.000
01/09/12	31/12/12	50.600	63.300
01/01/13	31/03/13	51.900	65.000
01/01/13	31/12/13	48.725	60.250

quotations in euros per megawatt–hour (€/MWh) are listed in Table 1 and consists of contracts of different lengths: days, weeks, weekends[1], months, quarters, and calendar years.

2. Daily seasonality estimation

Due to the fact that forward contracts give information about time periods, such information may obscure seasonality if the settlement period is long. This means we must specify a seasonal function $\Lambda(t)$ based on more information than can be read off the market prices. As do Benth et al. (2007b), we base the estimation of $\Lambda(t)$ on spot price data, which can be linked to forward prices. However, since there is no clear arbitrage-free connection between spot prices and the forward curve in the electricity market, the choice of seasonal function is ad hoc to some degree.

We begin by recording the hourly spot prices that are identified in day-ahead quotes. For our numerical example, we consider the EEX hourly price from January 1, 2005, to May 22, 2012. Should such data be missing, we replace it by the last available quote preceding the hour in question. This occurs, for instance, when going from a legal to a solar hour count. In regression analysis, classical estimation routines such as ordinary least squares are very sensitive to extreme observations and outliers. One way to improve the robustness of the model is by cleaning the data with some reasonable procedure to reject outliers. The outlier selection method we describe is proposed by Truck et al. (2007), although they consider lower-performance filters than the Hodrick–Prescott filter (see Hodrick and Prescott (1997)). Selection of the parameter λ in the filter definition follows the method proposed by Pedersen (2001), who provides with an optimal selection of the Hodrick–Prescott parameter to filter components with a period equal to or greater than a chosen figure.

[1]All the hours of the period are base load hours because weekend quotations refer to Saturday and Sunday.

Appendix A briefly describes the Hodrick–Prescott filter and Pedersen's criterion for the optimal λ.

Here $S_h^{raw}(t)$ denotes the spot price of hour h on day t. Hourly prices $S_h^{raw}(t)$ lead to daily quotes $S^{raw}(t)$ by averaging the former over the day. The resulting time series of daily prices undergoes a procedure to filter out outliers and replace them by "normal values." We estimate a *filtering trend* component whose purpose is to identify data outliers. This filtering trend is calculated using a Hodrick–Prescott filter with a parameter λ set to perform a monthly smoothing, that is, filtering out recurrent components with period equal to or exceeding a month. An outlier is then defined as either a negative price or a price corresponding to an extreme deviation from the trend. The extreme deviation is set equal to three times the standard deviation of the sample distribution of discrepancies between the actual price and the trend. Once an outlier is identified, it is replaced in the original series by the value estimated through the Hodrick–Prescott filter, the so-called normal value referred to above. The filtering trend serves only to filter out data outliers. Figure 1 plots the outliers detected for our EEX market example. We see how the German market changed its behavior over the years and how the frequency of daily price spikes was higher during the first years considered. In the last years of our analysis, the prices have a more regular pattern.

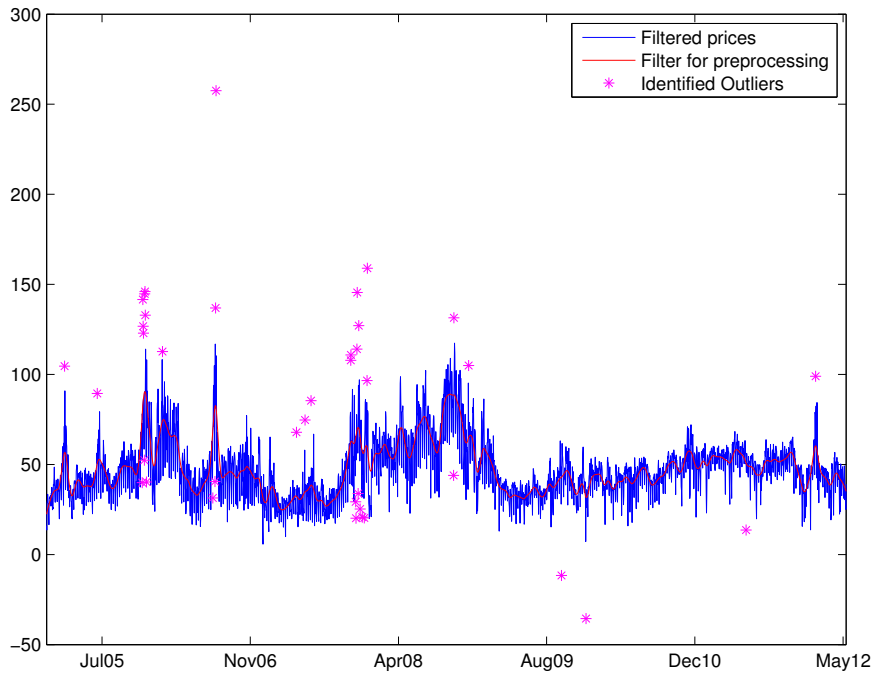

FIGURE 1. EEX daily prices after replacement of the spikes and original observations classified as outliers, using the Hodrick–Prescott filter technique.

The spot prices obtained after the outlier filtering procedure are denoted $S(t)$. Each of the resulting spot prices is then assumed to be represented as the sum of three additive components:

$$S(t) = trend + seasonality + noise. \tag{2}$$

We want to extract the seasonality component to analyze and estimate it using a suitable parametric function $\Lambda(t)$. To do so, we estimate a *cyclical trend* component. This component aims to reproduce the first additive term in formula (2). The cyclical trend is calculated using a Hodrick–Prescott filter. The parameter λ is set to filter out recurrent components with a period equal to or exceeding a year and a half. The rationale behind this choice is that economic movements with more than one year are supposed to be related to macroeconomic phenomena, while pure seasonalities must be searched in shorter periods. Furthermore, the longest settlement period quoted on the market is the calendar year, so shorter period seasonalities should be hidden within them. The practical choice of setting the period to a year and a half instead of just one year is to avoid any risk, while filtering a time series, of introducing distortions near the cutoff frequency. Figure 2 estimates the cyclical trend for EEX market daily prices.

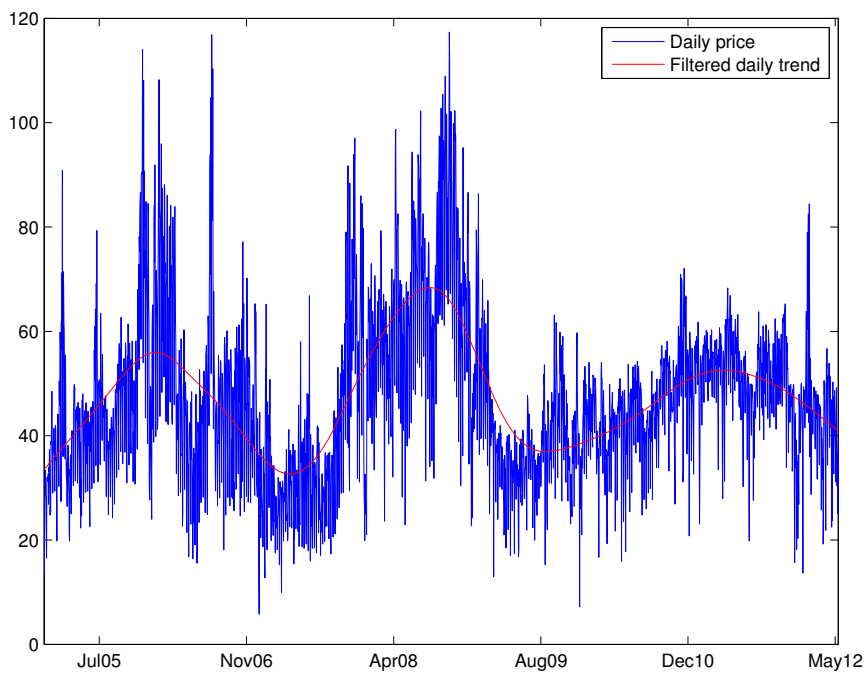

FIGURE 2. Filtered trend $S^{trend}(t)$ and EEX daily price time series $S(t)$.

We indicate the filtered trend with $S^{trend}(t)$. The resulting detrended series

$$Z(t) = S(t) - S^{trend}(t)$$

constitutes the basis for our seasonal components analysis. We look for a parametric function to fit $Z(t)$. We use the following functional form:

$$\Lambda(t) = a\cos\left(\frac{4\pi}{365}t + b\right) + \mathbf{D}_{day}\mathbf{d} + \mathbf{D}_{month}\mathbf{m}, \tag{3}$$

where the dummy variables $\mathbf{D}_{day}$ and $\mathbf{D}_{month}$ are defined for each of the twelve months and each of the seven days under analysis respectively. Official holidays are treated as if they were a typical

Sunday. The function $\Lambda(t)$ reproduces a semiannual periodicity plus daily and monthly dummies. We even add a cosine with a six-month period. An analysis of periodicities is conducted using a periodogram. We fit $\Lambda(t)$ by minimizing the weighed discrepancy to the target path $Z(t)$. This goal amounts to solving the optimization problem

$$\min_{\theta_i} ||e^{-\alpha(t_{end}-t)}(Z(t) - \Lambda(t))||_2^2. \tag{4}$$

and the parametric vector θ_i gathers all parameters defining the function $\Lambda(t)$. For the example of the German electricity market, we set $\alpha = 0.4$. Figure 3 plot one year of the estimated $\Lambda(t)$. The estimated $\Lambda(t)$ shows that prices are lower during Sundays and holidays than during weekdays. Monthly prices seem to be lower when people usually have more holidays, such as during December, January, July, and August.

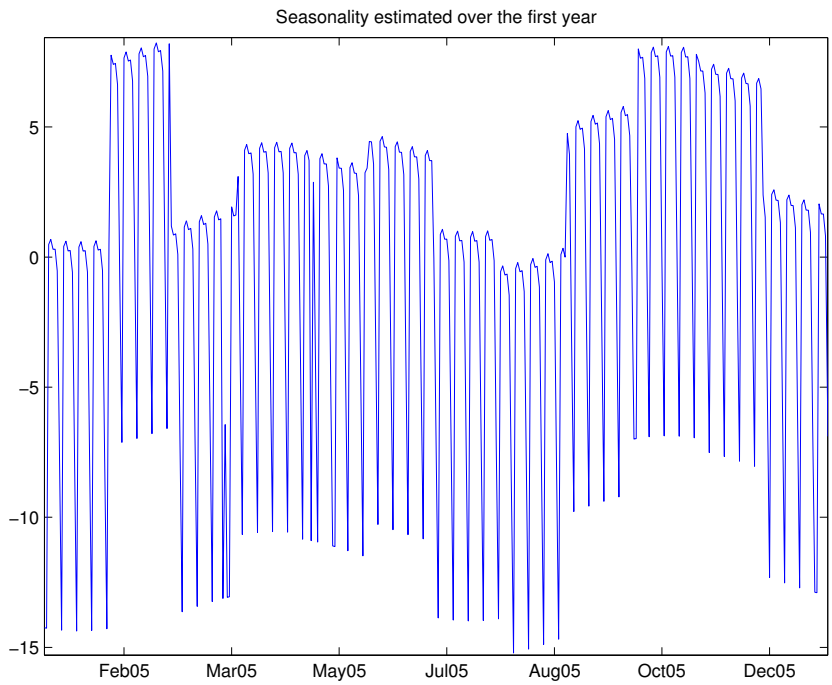

FIGURE 3. The function $\Lambda(t)$ is computed over the first year of estimation.

3. From an instantaneous to a daily forward curve

The first step of our procedure to obtain an hourly forward price curve is to derive an instantaneous forward price curve. To do so, we use the technique proposed by Benth et al. (2007b), which we cover in this section.

Let

$$\mathcal{S} = \{[\tau_1^b, \tau_1^e], [\tau_2^b, \tau_2^e], \ldots, [\tau_m^b, \tau_m^e]\}$$

be a list of start and end dates for the settlement periods of m average-based forward contracts. Assume that for $k = 1, \ldots, m$ base load F_k^{base} and peak load F_k^{peak} forward contracts are quoted.[2] Periods can overlap, so we construct a new list $t_1, ..., t_n$, as illustrated in Figure 4. We assume that time is measured in days. The new list consists of the elements in $\mathcal{S}$ sorted in ascending order,

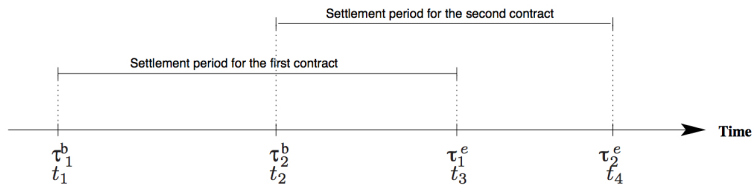

FIGURE 4. Splitting overlapping contracts.

with duplicate elements removed. At time u the instantaneous forward price curve $f(u)$ is modeled as

$$f(u) = \Lambda(u) + \varepsilon(u)$$

for the two continuous functions $\Lambda(u)$ and $\varepsilon(u)$, where $\Lambda(u)$ represents the seasonality of the forward curve and $\varepsilon(u)$ is an adjustment function that captures the forward curve's deviation from seasonality. The adjustment function ε is assumed to be the following polynomial spline of order four:

$$\varepsilon = \begin{cases} a_1u^4 + b_1u^3 + c_1u^2 + d_1u + e_1, & u \in [t_0, t_1], \\ a_2u^4 + b_2u^3 + c_2u^2 + d_2u + e_2, & u \in [t_1, t_2], \\ \vdots & \\ a_nu^4 + b_nu^3 + c_nu^2 + d_nu + e_n, & u \in [t_{n-1}, t_n]. \end{cases}$$

Moreover, the splines are assumed to be twice continuously differentiable. and with zero derivative in t_n. The parameter vector

$$\mathbf{x}^\top = [a_1, b_1, c_1, d_1, e_1, a_2, b_2, c_2, d_2, e_2, \ldots, a_n, b_n, c_n, d_n, e_n]$$

is found by solving the convex quadratic programming problem

$$\min_{\mathbf{x}} \int_{t_0}^{t_n} [\varepsilon''(u; \mathbf{x})^2] du \tag{5}$$

subject to the following constraints of continuity and smoothness at the knots, $j = 1, \ldots, n-1$:

$$(a_{j+1} - a_j)u_j^4 + (b_{j+1} - b_j)u_j^3 + (c_{j+1} - c_j)u_j^2 + (d_{j+1} - d_j)u_j + e_{j+1} - e_j = 0, \tag{6}$$

$$4(a_{j+1} - a_j)u_j^3 + 3(b_{j+1} - b_j)u_j^2 + 2(c_{j+1} - c_j)u_j + d_{j+1} - d_j = 0, \tag{7}$$

$$12(a_{j+1} - a_j)u_j^2 + 6(b_{j+1} - b_j)u_j + 2(c_{j+1} - c_j) = 0, \tag{8}$$

[2]Benth et al. (2007b) propose a procedure to constrain the curve between the bid and ask prices. We do not treat this case, limiting our description to a curve obtained from mid or closing price quotations.

and

$$\varepsilon'(u_n;\mathbf{x}) = 0, \tag{9}$$

$$F_i^{base} = \frac{1}{\tau_i^e - \tau_i^b}\int_{\tau_i^b}^{\tau_i^e} \left(\varepsilon(u;\mathbf{x}) + \Lambda(u)\right) du. \tag{10}$$

Equations (6) to (10) can be written in the form $\mathbf{Ax} = \mathbf{b}$. In writing equation (10), the kind of settlement of the forward contract does not really matter, as seen in formula (1). Benth et al. (2007b) show that the maximum smoothness problem (5) is equivalent to solving the linear equation problem

$$\begin{bmatrix} 2\mathbf{H} & \mathbf{A}^\top \\ \mathbf{A} & \mathbf{0} \end{bmatrix} \begin{bmatrix} \mathbf{x} \\ \lambda \end{bmatrix} = \begin{bmatrix} \mathbf{0} \\ \mathbf{b} \end{bmatrix}, \tag{11}$$

where the dimension of the left matrix is $(8n+m-2)\times(8n+m-2)$ and the solution vector and the rightmost vector both have dimension $(8n+m-2)$. Here $\lambda^\top = [\lambda_1, \lambda_2, ..., \lambda_{3n+m-2}]$ is a Lagrange multiplier vector and the matrix $\mathbf{H}$ is defined as

$$\mathbf{H} = \begin{bmatrix} \mathbf{h}_1 & & 0 \\ & \ddots & \\ 0 & & \mathbf{h}_n \end{bmatrix}, \quad \mathbf{h}_j = \begin{bmatrix} \frac{144}{5}\Delta_j^5 & 18\Delta_j^4 & 8\Delta_j^3 & 0 & 0 \\ 18\Delta_j^4 & 12\Delta_j^3 & 6\Delta_j^2 & 0 & 0 \\ 8\Delta_j^3 & 6\Delta_j^2 & 4\Delta_j^1 & 0 & 0 \\ 0 & 0 & 0 & 0 & 0 \\ 0 & 0 & 0 & 0 & 0 \end{bmatrix},$$

and

$$\Delta_j^l = t_j^l - t_{j-1}^l.$$

Solving formula (11) numerically is standard, using LU factorization. Indicating with $\mathbf{x}^*$ the solution of the problem stated above, the instantaneous forward curve reads as

$$f(u) = \Lambda(u) + \varepsilon(u;\mathbf{x}^*).$$

Once we obtain the instantaneous forward curve, the daily forward price computes as the arithmetic average of instantaneous forward prices over day i:

$$\hat{f}(t_0+i) = \int_{t_0+i}^{t_0+i+1} f(u)du, \tag{12}$$

for $i = 1, \ldots, N$, where N is the number of days between the starting date and the last end date. Therefore $N = t_n - t_0$. This quantity is important in market practice because it represents a prediction, under a risk-neutral probability measure, of the future spot price and is the starting point from the hourly shaping described in the following sections. We deal with peak load quotations when shaping the curve to an hourly profile. The daily curve computed for the EEX market example with data in Table 1 is shown in Figure 5.

4. Hourly seasonality estimation

We now need to extrapolate the seasonality from the hourly prices to give the curve an hourly shape. As pointed out by Huisman et al. (2007), hourly electricity prices in day-ahead markets do not follow a time series process but comprise, instead, a panel of 24 cross-sectional hours that vary from day to day. This is because the microstructure of many day-ahead market prices is such that all hours are quoted at the same moment in a day. A trader uses exactly the same

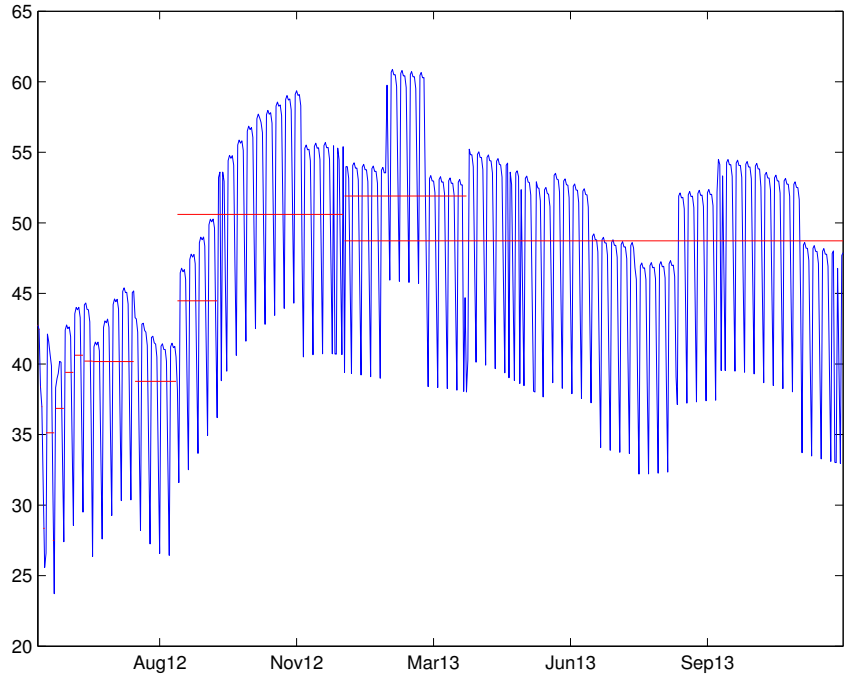

FIGURE 5. The computed daily forward price curve (blue line) and base load contract quotations (red line).

information to set the price for hour h as to set the price for hour s (h being different from s). The next day, the information set updates, but it updates simultaneously for hours 1 through 24. Therefore, hourly prices within a day behave cross-sectionally and hourly dynamics over days behave according to time series properties. However, we consider separately each hourly time series in the outlier identification step due to difficulties in handling multidimensional time series. The procedure followed for estimating hourly seasonality mimics that described above for daily quotes, with a few amendments. The following briefly describes the approach.

For each hour h, we compute a normalized hourly deviation from the day-ahead price, defined as the average of the 24 hourly quoted prices:

$$\frac{S_h(t) - S(t)}{S(t)} = trend_h + seasonality_h + noise_h,$$

where $h = 1, \ldots, 24$. As in the daily price case, we identify a *filtering trend* using a Hodrick–Prescott filter with an optimal parameter for each hour, remove *outliers*, and then filter a *cyclical trend*, again using a suitable Hodrick–Prescott filter.

We want to examine the normalized price deviation trends displayed in Figure 6 before modeling market seasonality. In recent years, Germany has significantly increased its share of electricity produced from renewable sources, mainly due to the Renewable Energy Act. The Renewable Energy Act substantially impacts the dynamics of intra-day electricity. In the first years of our

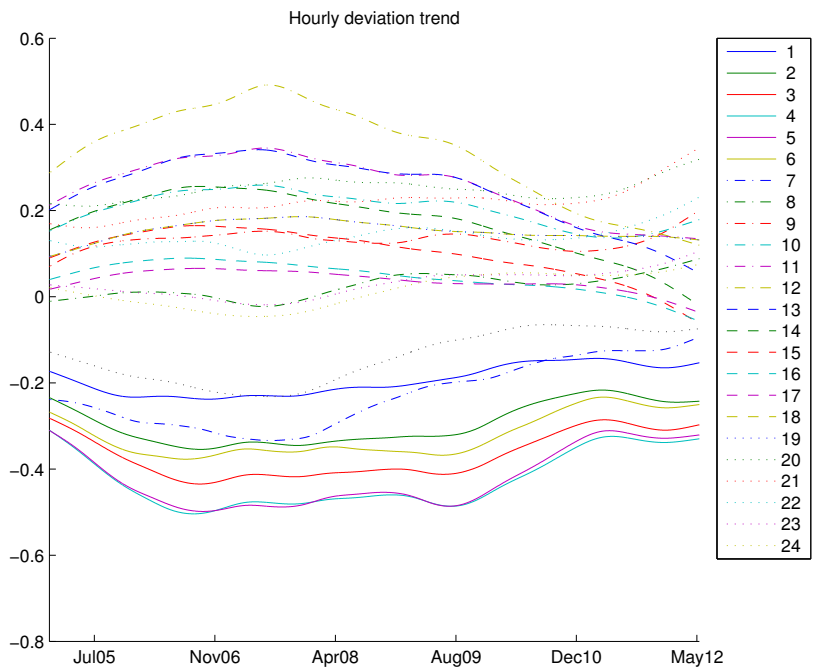

FIGURE 6. Function $trend_h(t)$ estimated for each hour $h = 1, \ldots, 24$.

sample period, the higher intra-day trend prices were in the middle of the peak hours (10:00–11:00, 11:00–12:00, and 12:00–13:00). However, in recent years the price of energy during evening bands has greatly increased, in some cases to even higher than during peak hours. This increase is the result of the entry of renewable energy into the electricity market, namely, wind power and photovoltaics. When these operate at full capacity, mainly during daylight hours, they take over all other forms of energy. Consequently, other energy sources, such as gas-fired power plants, have been gradually confined to the peripheral hours of the day and are activated less frequently. When the sun sets, however, the supplies of renewable energy suddenly disappear and the energy system must cope with the not negligible rising consumption of the evening. Other energy sources, such as gas-fired plants, are switched on to cover this energy demand, but this continuous "stop and go" has a fixed cost and companies are well aware that they have just few hours in the day to gain the margins needed to compensate at least for the fuel used. This explains the trends displayed in Figure 6.

Once the trends are removed, periodic components are estimated on the residuals:

$$Z_h(t) = \frac{S_h(t) - S(t)}{S(t)} - trend_h\,(t)\,.$$

Although each market shows a different seasonality pattern, the analysis conducted on the residual $Z_h(t)$ generally shows marked recurrences during mid-day and evening hours. Switching from a legal to a solar hour count mainly affects consumption in the evening hours, from 18:00 to 21:00. We therefore model each time series $\{Z_h(t)\}$ using 12 monthly dummy variables for the working

days and 12 more for the non-working days, for a total of 24 dummy variables for each of the 24 hours. These variables are included in the matrix $\mathbf{X}$. For every hour in the day, we estimate a corresponding seasonal component using a weighted linear regression. This amounts to solving the optimization problem

$$\min_{\mathbf{g}_h} \|\mathbf{W}^{1/2}(Z_h(t) - \mathbf{X}\mathbf{g}_h)\|_2^2, \quad h = 1, \ldots, 24, \tag{13}$$

where the weighting matrix $\mathbf{W}$ is diagonal with $w_{i,i} = e^{-\alpha(t_{end}-t)}$, with $\mathbf{g}_h \in \mathbb{R}^{24}$ for $h = 1, \ldots, 24$. Thereafter, the hourly seasonal component is shifted by a fixed amount so that the sum of the differences is zero over the day. Some calibration results are displayed in Figure 7. We use $\alpha = 0.4$ to give enough weight to the recent years of analysis. The behavior of the seasonality during mid-day hours has changed significantly in recent years due to the energy market changes described.

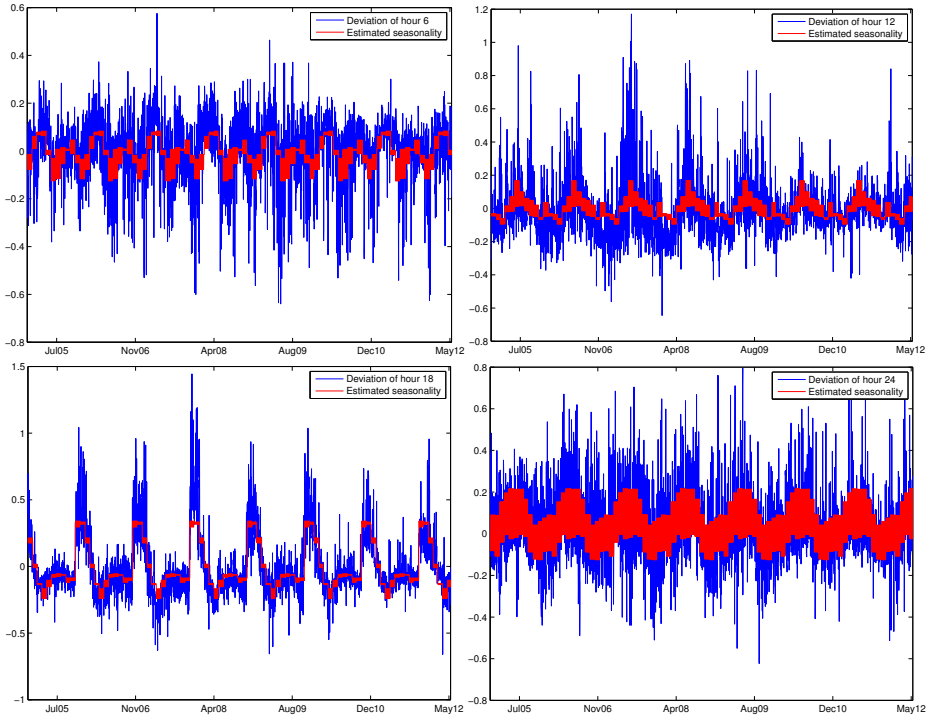

FIGURE 7. Normalized hourly deviation (blue) and fitted seasonality (red) for the price of hours 6 (upper left), 12 (upper right), 18 (bottom left), and 24 (bottom right).

5. Hourly shaping of the forward curve

This section describes how to construct an hourly forward curve from a daily forward curve and the estimated hourly seasonality. We begin by defining the component of forward price quotes stemming from spot trends. From the previous section, $trend_h(t)$ is defined by the Hodrick–Prescott filter for

any time prior to the evaluation date t_0 for which a spot quote is available and for any hour h in the day. Assume that the last portion of this trend, namely, $\{trend_h(t_0), h = 1, ..., 24\}$, is the sole contributor to the time t_0 quoted forward price curve. Since $\sum_{h=1}^{24} trend_h(t_0) =: l$ may not vanish, we define $l_h := trend_h(t_0) - \frac{l}{24}$, which implies that $\sum_{h=1}^{24} l_h = 0$ by construction.

Our first estimate of the hourly quoted forward curve is made on a historical basis and is given by

$$\bar{f}(t_0 + i, h) := \hat{f}(t_0 + i) \times \left(1 + l_h + \mathbf{g_h^*}^\top \mathbf{1}_m(i)\right) \quad i = 1, \ldots, N, \tag{14}$$

where

- t_0 is the estimation date;
- $t_0 + i$ denotes the time corresponding to a day i in the future, measured in days;
- h represents an hour in day i, that is, $h = 1, \ldots, 24$;
- $\hat{f}(t_0 + i)$ is the forward price computed at time t_0 for delivery over day i as defined in formula (12);
- $l_h = trend_h(t_0) - \frac{l}{24}$, as defined at the beginning of this section;
- $\mathbf{g}_h^*$ solves problem (13) stated in the previous section;
- $\mathbf{1}_m(i)$ is a 24-component vector with all zero elements except one: If day i is a working day in month k, then the kth component of $\mathbf{1}_m(i)$ is set equal to one; if day i is a non-working day in month k, then the $(12 + k)$th component of $\mathbf{1}_m(i)$ is set equal to one.

Concerning formula (14), first, we note that hourly prices are obtained by incrementing or decrementing each daily price by a percentage, represented by the quantity $l_h + \mathbf{g_h^*}^\top \mathbf{1}_m(i)$. Figure 8 shows such quantities computed for the German market example. We note a higher increment during the second intra-day peak for many days of the year. The first intra-day peak still shows a higher increment only during spring and summer business days, probably because of air conditioning. The choice to model the relative distance between the daily price and the hourly price guarantees the positivity of the hourly price. This is a decision commonly used in the literature. However, in recent years the Renewable Energy Act has substantially impacted the dynamics of intra-day electricity prices by increasing the likelihood of negative prices. Negative prices are still rare and related only to few markets, although a slight modification of the methodology could be a possible development to allow negative prices. For a detailed description of negative price phenomena in German energy market, see Fanone et al. (2011).

Second, we consider some practical solutions in the construction of the curve. To ensure that hourly deviations from the daily mean price sum to zero, we shift trends and seasonality estimations. We introduce this solution because we consider each hourly deviation a unidimensional time series. Describing hourly deviation as a multidimensional time series could be a possible theoretical improvement in the methodology, allowing for the joint estimation of such elements.

Finally, we use n base load quotations and historical information to construct a curve with a time horizon of N days such that $t_n = t_0 + N$. We assume that a broker provides a number n of peak load quotes to the user, but the estimated forward prices need not be compatible with these quotes. Therefore we modify our estimate to allow the constructed price to match market quotes.

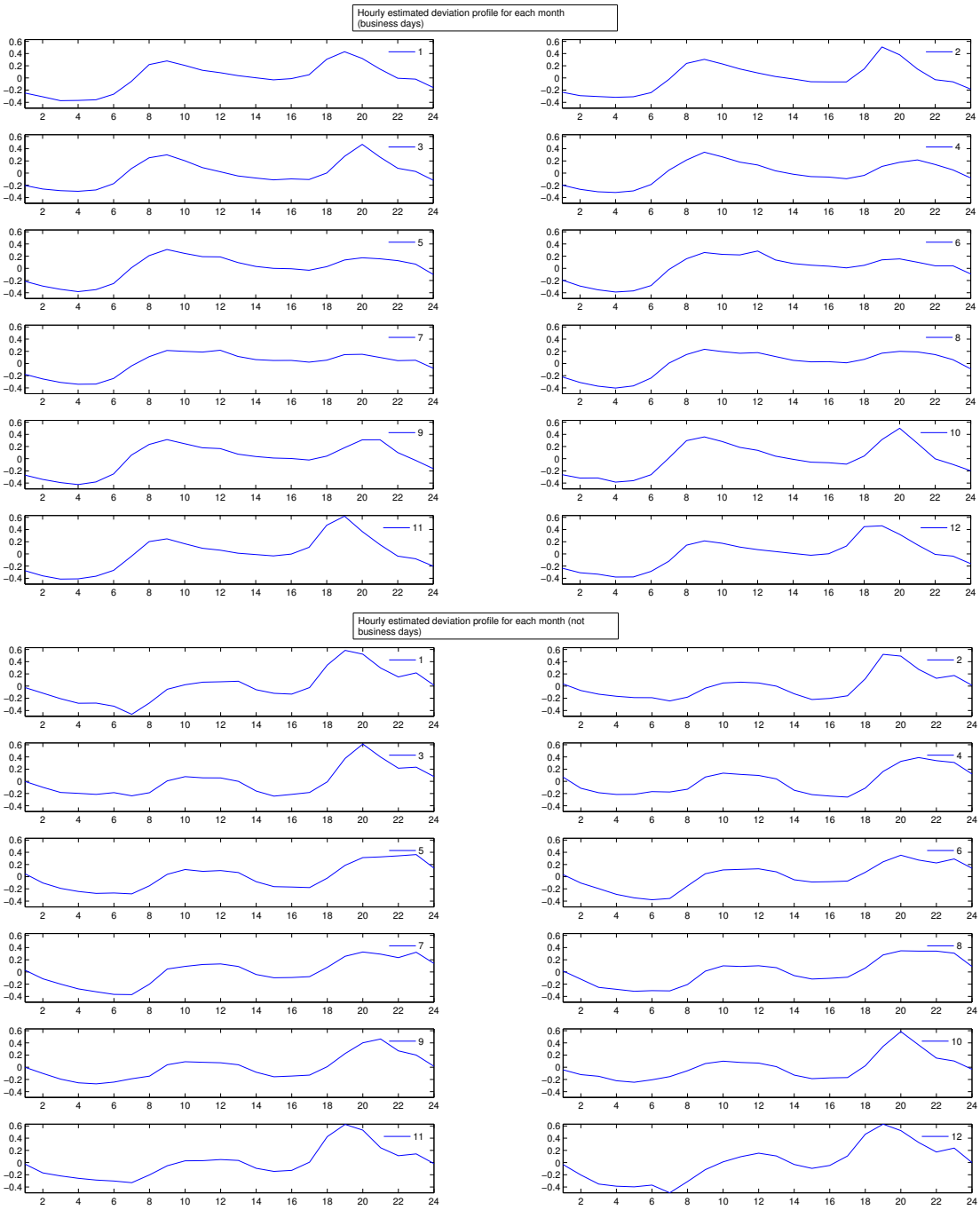

FIGURE 8. Computed percentage increments and decrements of the 24 hours of the day. The upper panel denotes business days and the lower panel non-working days. We plot a different profile for each month. The months are numbered from one (January) to twelve (December).

We now describe how to align the hourly curve to forward market quotations. To begin with, we note that market quotes can refer to overlapping time periods in the future. For base load contracts, the methodology of Benth et al. (2007b) easily manages overlapping contracts but, unfortunately, we cannot use the same method in the peak load case. However, we can define some rules to split quotations over non-overlapping periods. Without loss of generality, consider a simple example with only two peak load quotations F_1^{peak} and F_2^{peak} with settlement periods $[\tau_1^b, \tau_1^e]$ and $[\tau_2^b, \tau_2^e]$, respectively. We indicate with $BD[a,b]$ the number of business days in the interval [a,b]. We consider only the two most popular kinds of overlap in energy markets:

- $\tau_1^b = \tau_2^b < \tau_1^e < \tau_2^e$. We set $t_1 = \tau_1^b = \tau_2^b$, $t_2 = \tau_1^e$, and $t_3 = \tau_2^e$. We define $\hat{F}_1^{Peak} = F_1^{peak}$ on the settlement period $[t_1, t_2]$ and $\hat{F}_2^{Peak} = \frac{F_2^{peak} BD[t_1,t_3] - F_1^{peak} BD[t_1,t_2]}{BD[t_2,t_3]}$ on the settlement period $[t_2, t_3]$.
- $\tau_1^b < \tau_2^b < \tau_1^e < \tau_2^e$. Since in this case two quotations define three intervals, we introduce the rule $\hat{F}_1^{Peak} = \hat{F}_2^{Peak} = F_1^{Peak}$ to obtain a unique solution for $\hat{F}_3^{Peak}$. We set $t_1 = \tau_1^b$, $t_2 = \tau_2^b$, $t_3 = \tau_1^e$, and $t_4 = \tau_2^e$. We define $\hat{F}_1^{Peak} = F_1^{peak}$ on the settlement period $[t_1, t_2]$, $\hat{F}_2^{Peak} = F_1^{peak}$ on the settlement period $[t_2, t_3]$, and $\hat{F}_3^{Peak} = \frac{F_2^{peak} BD[t_2,t_4] - F_1^{peak} BD[t_2,t_3]}{BD[t_3,t_4]}$ on the settlement period $[t_3, t_4]$.

Hence, we compute n implied peak load prices referring to non-overlapping time periods and denote them $\hat{F}_j^{Peak}$, for $j = 1, \ldots, n$. In each period, we look for a coefficient $\hat{l}_h^j$ such that the historical curve is perfectly reproduced. The simple idea here is that the information in peak load contracts should affect only the economic trend of prices, without describing the impact of seasonality on price movements. The hourly forward price curve is then defined as

$$\hat{f}(t_0 + i, h) = \hat{f}(t_0 + i) \times \left(1 + \hat{l}_h^j + \mathbf{g}_h^{*\top} \mathbf{1}_m(i)\right), \tag{15}$$

$j = 1, \ldots, n$, $h = 1, \ldots, 24$, and $i \in [0, \ldots, N]$. To compute $\hat{l}_h^j$, let SP_j be the settlement period corresponding to the jth implied forward peak load and BD_j be the subset of SP_j comprising only working days. We solve the optimization problem of minimizing the discrepancy between the historical forward curve and the target function $\hat{f}(t_0 + i, h)$:

$$\min_{\hat{l}_h^j} \sum_{h=1}^{24} \sum_{i \in SP_j} \left(\bar{f}(t_0 + i, h) - \hat{f}(t_0 + i, h)\right)^2, \qquad j = 1, \ldots, n,$$

under the constraints

$$\frac{1}{24} \sum_{h=1}^{24} \hat{f}(t_0 + i, h) = \hat{f}(t_0 + i), \qquad \forall i \in SP_j, \quad j = 1, \ldots, n,$$

$$\frac{1}{12 \# BD_j} \sum_{i \in BD_j} \sum_{h=9}^{20} \hat{f}(t_0 + i, h) = \hat{F}_j^{Peak}, \qquad j = 1, \ldots, n.$$

This approach can be cast as a quadratic optimization problem with respect to the variables $\hat{l}_h^j$:

$$\min_{\hat{l}_h^j} \sum_{h=1}^{24} (\hat{l}_h^j)^2 - 2\hat{l}_h^j l_h, \qquad j, \ldots, n,$$

under constraints, for $j = 1, \ldots, n$,

$$\sum_{h=1}^{24} \hat{l}_h^j = 0,$$

$$\sum_{h=9}^{20} \hat{l}_h^j = \frac{\#BD_j F_j^{Peak} 12 - \sum_{i \in BD_j} \hat{f}(t_0 + i) \sum_{h=9}^{20} \left(1 + \mathbf{g}_h^{*\top} \mathbf{1}_m(i)\right)}{\sum_{i \in BD_j} \hat{f}(t_0 + i)}.$$

The resulting hourly forward price curve compatible with peak load quotes is as in (15), where $\hat{l}_h^j$ is computed by solving the quadratic optimization problem above. Figure 9 shows the final result of our computation. Because of the large amount of data and the difficulty of displaying them all simultaneously, we plot only the first month of the EEX hourly forward price curve generated.

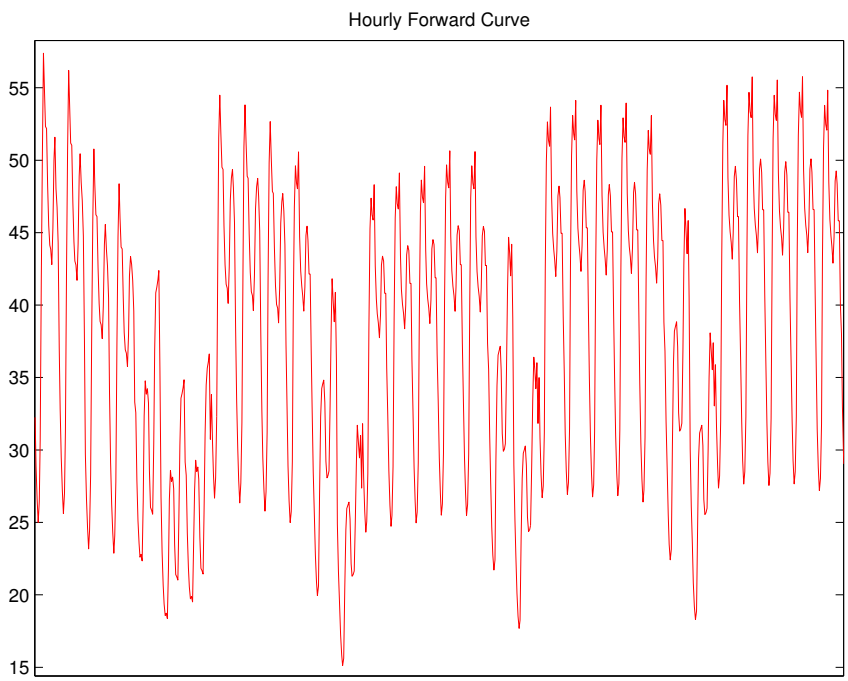

FIGURE 9. First month of the hourly forward price curve generated.

6. Backtesting and selecting α

This section describes a backtesting method to measure our curve's goodness-of-fit technique and presents the backtesting results of applying the hourly forward curve to several European markets, in Table 2. We consider day-ahead prices for five European energy spot market starting on different dates:

- Italy (MGP), data since January 1, 2005;

- Germany (EEX), data since January 1, 2005;
- France (PNXT), data since January 1, 2006;
- Switzerland (SWISSIX), data since December 12, 2006;
- Czech Republic (CZ), data since January 1, 2008.

Backtesting is implemented as follows. We define an evaluation date in the past and use historical spot data before the evaluation date to calibrate the model. Data after the evaluation date are used to extrapolate forward quotations and to measure the quality of fit. Our experiments consider three evaluation dates: December 31, 2009; June 30, 2010; and December 31, 2010. We calibrate the model for each country considering a time period spanning from its respective start date to each evaluation date. We consider four different values for the parameter α used in formulas (4) and (13): $0.2, 0.4, 0.6$ and 0.8. Forward contract quotations are obtained from spot prices delivered after each evaluation date, averaged over base load and peak load hours. Our tests consider two different settings of forward quotations. The first setting is comprised of monthly prices and is denoted M. The second setting tries to reproduce the market structure: We compute monthly average prices for three months. Then we compute the average prices over three-month periods, trying to reproduce the information of quarterly contracts. We call this setting the monthly/quarterly setting and it is denoted M/Q in Table 2. Curves evaluated December 31, 2009, and December 31, 2010, cover one year. Curves evaluated June 30, 2010, cover six months. The same spot data that we averaged to compute the forward quotations are used to check the curve fit. The distance between delivered spot prices and forecasts is measured by the Euclidean norm of the hourly price difference.

The results of backtesting are displayed in Table 2. First, we see that the fit does not seem highly dependent on the α parameter chosen. However, a comparative analysis, such as that in Table 2, could suggest the best parameter to use, depending on the market and the evaluation date. Second, curves obtained from monthly quotations are likely to perform better than those obtained from monthly and quarterly quotations. Although this is due to the use of more information about market prices, in many case the relative distance between the monthly curve and the monthly/quarterly curve is negligible, showing the quality of the fitting procedure. Third, the curves generated for the year 2010 have higher discrepancies with the spot data than those generated for 2011. This is the case for every market except for the German one, where performance seems to be stabler.

TABLE 2. Backtesting results.

Market	Eval. Date	Forward	Length	$\alpha = 0.2$	$\alpha = 0.4$	$\alpha = 0.6$	$\alpha = 0.8$
MGP	12/31/09	M	1y	1175	1118	1091	1080
	12/31/09	MQ	1y	1176	1119	1094	1087
	6/30/10	M	6m	783	742	728	725
	6/30/10	MQ	6m	788	745	731	728
	12/31/10	M	1y	879	853	821	811
	12/31/10	MQ	1y	991	924	899	890
EEX	12/31/09	M	1y	823	798	781	773
	12/31/09	MQ	1y	863	857	844	845
	6/30/10	M	6m	565	536	516	493
	6/30/10	MQ	6m	579	555	542	526
	12/31/10	M	1y	745	728	723	723
	12/31/10	MQ	1y	991	924	899	890
PNXT	12/31/09	M	1y	1134	1113	1102	1098
	12/31/09	MQ	1y	1166	1158	1148	1149
	6/30/10	M	6m	741	718	711	711
	6/30/10	MQ	6m	751	729	724	728
	12/31/10	M	1y	979	967	963	963
	12/31/10	MQ	1y	1022	1012	1013	1017
SWISSX	12/31/09	M	1y	954	949	948	948
	12/31/09	MQ	1y	908	893	893	894
	6/30/10	M	6m	628	621	616	620
	6/30/10	MQ	6m	539	539	548	562
	12/31/10	M	1y	720	715	714	717
	12/31/10	MQ	1y	828	830	834	839
CZ	12/31/09	M	1y	698	1073	1062	1057
	12/31/09	MQ	1y	1409	1385	1374	1369
	6/30/10	M	6m	882	871	864	860
	6/30/10	MQ	6m	673	675	673	675
	12/31/10	M	1y	752	746	746	749
	12/31/10	MQ	1y	829	823	826	832

CHAPTER 2

A general semi-closed form spread option pricing formula

Although this may seem a paradox,
all exact science is dominated by
the idea of approximation.

Bertrand Russell (1872–1970)

A spread option is a contract written on the price difference of two underlying assets whose values at time t are denoted by $S_1(t)$ and $S_2(t)$. We consider European-type options for which the buyer has the right to be paid, at the maturity date T, the difference $S_2(T) - S_1(T)$, known as the spread. To exercise the option, the buyer must pay at maturity a price K, known as the option's strike price. However, some financial spreads are not defined as the difference between just two prices; they are defined, more generally, as a linear combination of financial variables, that is, a basket of financial variables. The mathematical modeling we discuss in the following sections of this chapter pertains only to the case of an option written on the difference of two prices. See Chapter 3 for the basket option case.

The use of spread options is widespread despite the fact that pricing and hedging techniques are still underdeveloped, because, depending on the stock model we consider, the pricing problem is or is not solvable in closed form. In the Bachelier stock model, the price vector is assumed to evolve according to a bivariate Brownian motion and the option price is easily computable in closed form. If, instead, we consider price as a bivariate geometric Brownian motion and a zero option strike, we obtain the celebrated Margrabe (1978) formula. The important case in which the strike is not equal to zero does not have an explicit solution and few approximation methods have been developed. The most popular approximation is given by the formula of Kirk (1995), which is the current market standard. Carmona and Durrelman (2003a) obtain an analytical approximation formula using a family of lower bounds and determine un upper bound. The two bounds return a price range that is very tight for certain parameter values. Deng et al. (2008) approximate spread option price and Greeks as a sum of one-dimensional integrals following the method developed by Pearson (1995). Venkatramana and Alexander (2011) propose a closed-form approximation expressing the price of a spread option as the sum of the prices of two compound options. Deelstra et al. (2010) develop approximation formulas based on comonotonicity theory and moment matching methods. Finally, Bjerksund and Stensland (2011) propose a lower bound, showing that their formula is more accurate than Kirk's approximation.

Very little is discussed in the literature about the pricing of spread options in a non-Gaussian setup. Some asset classes, for example, energy price, require models with mean reversions and jumps and the spread options pricing in such situations can be challenging. A Fourier transform was originally introduced by Dempster and Hong (2002), who implement a valuation method based on the fast

Fourier transform (FFT), applying the idea of Carr and Madan (2000). An FFT technique is also applied by Hurd and Zhou (2009), who propose a pricing method based on an explicit formula for the Fourier transform of the spread option payoff in terms of the gamma function. Their formula requires a bivariate Fourier inversion. Cheang and Chiarella (2011) generalize Margrabe's formula to jump diffusion dynamics of the type originally introduced by Merton (1976) but do not discuss the non-zero strike case or provide a numerical example. Closed form distribution free bounds and optimal hedging strategies for spread options are derived in Laurence and Wang (2008).

The main contribution of the present work is the derivation of a lower bound, as in Bjerksund and Stensland (2011), but for general processes. The only quantity we need to know explicitly is the joint characteristic function of the log-returns of the two assets. In addition, the computation of our lower bound requires a univariate Fourier inversion, as opposed to the bivariate inversion required by Hurd and Zhou (2009). Finally, our bound turns out to be extremely accurate and easily computable. To this regard we apply it to different non-Gaussian models, such as jump diffusion models with different distributions of jump size, multivariate stochastic volatility models, mixtures of variance gamma (VG), and a VG time changed model. Mean-reverting models are also considered. Numerical examples are discussed for all these cases and benchmarked against Monte Carlo simulations. The second contribution of this work is the derivation of a tight upper bound based on the price of a new contract, the quadratic spread option. As for the lower bound, it can be provided for very general processes, provided that the bivariate characteristic function is known in closed form. The chapter outline is as follows. Section 1 describes spread in financial markets. Section 2 describes the state of the art in spread option pricing. Section 3 generalizes the lower bound of Bjerksund and Stensland (2011) for non-Gaussian models. Section 4 derives a new general upper bound. Section 5 examines in more detail the bivariate geometric Brownian motion model, discussing two additional bounds. The new lower bound improves the Bjerksund–Stensland bound, but from a practical point of view the improvement is negligible. Section 6 briefly reviews several non-Gaussian stochastic dynamic models used in financial applications. Section 7 presents some numerical experiments.

1. Spread in financial markets

Spread is a popular financial quantity in money and foreign exchange markets, where certain spreads are actively tracked. In the U.S. fixed income market, one of the most liquid spread instruments is the note over bond spread, a spread between maturities. It is a yield curve spread created by selling the 10-year U.S. Treasury note futures contract and buying the 30-year bond contract on the Chicago Board of Trade (CBOT). Alternately, an equivalent position can be created in the cash/repo market. An investor expecting inversion of a flat yield curve buys the bond contract and sells the note contract in an appropriate ratio. An investor expecting a steepening yield curve purchases the note contract and sells the bond contract in some proportion. Interest rate spreads are also important when they involve the yield curves of different countries or different entities. Interest rates (and, more importantly, the market's perception of future interest rates) have a direct impact on currency exchange rates. A currency offering a high interest rate often attracts purchases of that currency, strengthening it against other currencies. Currencies offering low interest rates often suffer from low demand and weaken as a result. Spreads between spot rates for different currencies affect forward exchange rates and can indicate relative strength or weakness in currencies. Another example is the bond spreads between the entities of an economic system where the same currency

is used. This spread is interesting to monitor the distribution of wealth in the economic system. In this sense, an important spread in the U.S. fixed income market is the municipal over bonds spread. The municipal over bonds spread is the difference in price between the municipal bond futures contract listed on the CBOT and the Treasury bond futures contract listed on the same exchange. Comparing the credit quality of an American city or another local government with the credit quality of the U.S. government, the municipal over bonds spread is sometimes used for determining tax strategies. We find another example in the European Union, where bond spreads between Germany and other European Union countries are used. Germany has the strongest economy of the European Union and is used as a benchmark by financial actors. When the spread between Germany's bond rates and a peripheral country's bond rates increases, that market's actors are losing trust in the peripheral country's financial system.

In fixed income markets, the yields or spot rates at which instruments trade are modeled as comprising a benchmark yield or interest rate plus spreads attributed to factors such as credit risk, liquidity, embedded options, and tax advantages. We discuss spreads concerning credit risk and liquidity. The TED spread is an example of spread between credit quality levels in the U.S. fixed income market. The TED spread is the difference between the interest rates on interbank loans and those on short-term U.S. government debt; TED is an acronym formed from T-bill and ED, the ticker symbol for Eurodollar futures contracts. Being a spread between a "risk-free" Treasury rate and a comparable commercial rate, the TED spread offers an indication of market-wide credit concern. More generally, it is useful for credit investors to have a measure to determine how much they are being paid to compensate them for assuming the credit risk embedded within a specific security. There is, in fact, a multiplicity of such measures. Most are called credit spreads since they attempt to capture the difference in credit quality by measuring the return of the credit risk security as a spread to some higher credit quality benchmark, typically either the government curve or the same maturity London Inter-Bank Overnight Rate (Libor) swap rate (linked to the funding rate of the AA-rated commercial banking sector). In the fixed rate bond market, the most widely used credit spread measure is the yield spread, the difference between the yield to maturity of the credit risky bond and the yield to maturity of an on-the-run Treasury benchmark bond with similar but not necessarily identical maturity. A slight modification of this measure is the interpolated spread, or I-spread, which is the difference between the bond's yield to maturity and the linearly interpolated yield for the same maturity on an appropriate reference curve. The option adjusted spread is the parallel shift to the Libor zero rate curve required so that the adjusted curve reprices the bond. It was originally conceived as a measure of the amount of optionality priced into a callable or puttable bond. The last credit spread concerning a fixed rate bond is the asset swap spread, the spread over Libor paid on the floating leg in a par asset swap package. It is important because it is a traded spread rather than an artificial measure such as the credit spreads listed above. A floating rate note market has two important measures of credit risk: the discount margin and the zero discount margin. The discount margin is a fixed add-on to the current Libor rate that is required to reprice the bond. The zero discount margin is the parallel shift to the forward Libor curve that is required to reprice the floating rate note. The last and probably the most important credit spread is the credit default swap spread. The credit default swap spread is the contractual spread that determines the cash flows paid on the premium leg of a credit default swap. Regarding the liquidity task, the bid–ask spread is sometimes used as a market liquidity measure. Narrow bid–ask spreads indicate greater liquidity. Indeed, in any market in equilibrium, there is generally a difference between the best quoted ask price and the best quoted bid price, called the bid–ask spread (or bid–offer spread). Depending upon the market, quotes can be expressed as actual prices,

yields, implied volatilities, and so on. Bid–ask spreads are measured in similar units. The average of the bid and ask prices is called the mid-offer price.

Spreads are popular even in several commodity markets. A temporal spread is a spread between the same variable at two points in time. A temporal spread for the price of an agricultural product prior to and after a harvest can be of interest, as can be the calendar spread between the prices of natural gas in summer and winter. In commodity markets, spread options can even be based on the differences between the prices of the same commodity at two different locations (locational spreads) or between the prices of inputs to and outputs from a production process (processing spreads), as well as between the prices of different grades of the same commodity (quality spreads). An important example of spread frequently traded in agricultural futures markets is the so-called crush spread, also known as the soybean complex spread, traded on the CBOT. The underlying indexes comprise futures contracts of soybean, soybean oil, and soybean meal. The unrefined product is the soybean and the derivative products are meal and oil. The spread is known as the crush spread because soybeans are processed by crushing. The crush spread is quoted as the difference between the combined sales value of soybean meal and soybean oil and the price of soybeans. Soybean futures are traded in cents per bushel, soybean meal futures in dollars per short ton, and soybean oil futures in cents per pound. As a result of these differences in units, conversion of meal and oil prices to cents per bushel is necessary to determine the relations of the three commodities and potential trading opportunities. The value $[CS]_t$ at time t of the crush spread in dollars per bushel is defined as

$$[CS]_t = 48[SM]_t/2000 + 11[SO]_t/100 - [S]_t,$$

where $[S]_t$ is the futures price at time t of a soybean contract in dollars per bushel, $[SO]_t$ is the futures price at time t of a contract of soy oil in dollars per 100 pounds, and $[SM]_t$ is the price at time t of a soy meal contract in dollars per ton. If we think of the crushing cost as a real constant, then crushing soybeans is profitable when the spread $[CS]_t$ is greater than that real constant. The crush spread gives market participants an indication of the average gross processing margin. It is used by processors to hedge cash positions and by market participants for pure speculation. Notice that the computation of the spread requires three prices, as well as the yield of oil and meal per bushel. An option written on the crush spread is not a proper spread option but, rather, a basket option. For an analysis of the crush spread market, see Johnson et al. (1991).

Regarding energy markets, the most frequently quoted spread options are the crack spread options and the spark spread options. A crack spread is the simultaneous purchase (sale) of crude oil futures and sale (purchase) of petroleum products futures (i.e., heating oil and/or gasoline). The magnitude of this spread reflects the cost of refining crude oil into petroleum products. Crude oil prices are usually quoted in dollars per barrel, while unleaded gasoline and heating oil prices are quoted in dollars per gallon. A simple conversion of 42 gallons to the barrel needs to be applied to the data. We indicate with $[UG]_t$, $[HO]_t$, and $[CO]_t$ the prices at time t of a futures contract of unleaded gasoline, heating oil, and crude oil, respectively. Many popular crack spread contracts exist. The 3:2:1 crack spread involves three contracts of crude oil: two contracts of unleaded gasoline and one contract of heating oil. The formula for such a spread is

$$[CS]t = 2[UG]_t + 1[HO]_t - [CO]_t.$$

Note that the computation of the 3:2:1 crack spread requires three prices, so an option written on such a spread is a basket option. The 1:1:0 gasoline crack spread involves one contract of crude oil

and one contract of unleaded gasoline. Its value is given by the formula

$$[GCS]_t = [UG]_t - [CO]_t.$$

The 1:0:1 heating oil crack spread involves one contract of crude oil and one contract of heating oil. It is defined by the formula

$$[HOCS]_t = [HO]_t - [CO]_t.$$

A spark spread is a proxy for the cost of converting a specific fuel (usually natural gas) into electricity at a specific facility. It is the primary cross-commodity transaction in the electricity markets. Mathematically, it can be defined as the difference between the price of electricity sold by a generator and the price of the fuel used to generate it, provided these prices are expressed in appropriate units. The most commonly traded contracts include the 4:3 spark spread and the 5:3 spark spread. The 4:3 spark spread involves four electric contracts and three contracts of natural gas and its value is given by

$$[SS]_t^{4,3} = 4[E]_t - 3[NG]_t.$$

The 5:3 spark spread involves five electric contracts and three contracts of natural gas and its value is given by

$$[SS]_t^{5,3} = 5[E]_t - 3[NG]_t.$$

Since spreads between indexes and financial variables are popular across different markets, options written on these spreads are also popular. They are used to speculate, mitigate basis risk, and even evaluate real assets:

- Consider, for example, certain commodity future contracts traded in the NYMEX and IPE. We observe WTI and Brent futures prices are cointegrated, which means the spread between the two is stationary. Thus this spread can be used as an indicator for buy and sell trading strategy in several ways, for example, using technical trading rules or forecasting the spread with econometric techniques. A financial market actor using such a strategy to take a position in a spread option contract in expectation of a future gain, despite significant risk of losing the initial outlay, is speculating. See Girma and Paulson (1998, 1999) for papers on the profitability of spread-based trading strategies in petroleum markets.

- Spread options can be used to mitigate the adverse movements of several indexes. Consider the crack spread. The magnitude of this spread reflects the cost of refining crude oil into petroleum products. A refinery's output varies according to the plant design, its crude slate, and its operational and maintenance program, which can be related to seasonal product demand and changing market conditions. Therefore refineries take positions in crack spread futures strategies according to their physical and operational requirements and hedge against price fluctuations to mitigate risk or secure a profit margin on the production output. A recent empirical analysis on the crack spread is that of Dempster et al. (2008).

- Spread options are also relevant in investment valuation problems. For example, in the energy industry a power generation unit can be priced using a real options approach. The spark spread measures the difference between the costs of operating a gas-powered generation unit, determined by the natural gas price, and the revenues from selling power at the market price. Thus it determines the economic value of power plants that are used to transform gas into electricity. In day-to-day operations, the plant operator generally

consumes a particular gas unit only if the electricity spot price is greater than the cost of generating that unit. If the generation profit is negative, it would be unreasonable to burn a valuable commodity such as gas to obtain a low-valued product such as electricity. One would instead sell gas in the market, buy power, and stop running the plant. The flexibility of turning the plant on and off, based on market prices, represents a real option for the asset owner and the power plant can be evaluated as a strip of European spark spread options. For an example of investment valuation using spark spread options, see Fusai and Roncoroni (2008).

- Eventually, the spread between the hourly day-ahead electricity prices of different countries is another important spread in energy markets and a crucial quantity when evaluating an interconnector capacity contract. An interconnector is an asset that gives the owner the option to transmit electricity between two locations. In financial terms, the value of an interconnector is the same as a strip of real options written on the spread between power prices in two markets. The application of spread options in the modeling and valuation of interconnector capacity contracts is discussed in Chapter 4.

2. Spread option pricing: A literature review

Let $S_1(t)$ and $S_2(t)$ be two stock price processes. An European spread option pays at the maturity date T the amount

$$C_K(T) = (S_1(T) - S_2(T) - K)^+.$$

The time 0 no-arbitrage fair price of the spread option is

$$C_K(0) = e^{-rT}\mathbb{E}\Big[(S_1(T) - S_2(T) - K)^+\Big], \tag{16}$$

where the expectation is with respect to a risk-neutral measure and r is the riskless interest rate. Here, we have used the usual notation x^+ for the positive part of x, that is, $x^+ = \max\{x, 0\}$. The use of spread options is widespread, despite the fact that pricing and hedging techniques are still underdeveloped. The pricing problem is or is not solvable in closed form, depending on the stock model considered. In the simple case of the Bachelier stock model, the price vector is assumed to evolve according to a bivariate Brownian motion and the option price is easily computed in closed form. In the more interesting case of the bivariate Black–Scholes model (see Black and Scholes (1973)), the stock price vector $\mathbf{S}(t)$ has components

$$S_j(t) = S_j(t)\exp[(r - \delta_j - \sigma_j^2/2)t + \sigma_j W_j(t)], \quad j = 1, 2 \tag{17}$$

where $\sigma_1, \sigma_2 > 0$, and W_1, W_2 are risk-neutral Brownian motions with instantaneous correlation $\rho, |\rho| < 1$, r is the risk-free rate, and δ_j is the dividend yield or the instantaneous convenience yield, depending on the nature of the underlying asset. If we consider spread options on futures, we have to set $\delta_1 = \delta_2 = r$. With both $S_1(t)$ and $S_2(t)$ being log-normal, there is no known general formula for the spread option value. However, a closed-form solution is available for the limiting case in which $K = 0$, where the spread option collapses into an option to exchange one asset for another. The option value in this case is given by the formula of Margrabe (1978). In the general case, however, we must rely on either approximation formulas or extensive numerical methods. Approximation formulas allow quick calculations and facilitate analytical tractability, whereas numerical methods typically produce more accurate results. Practitioners are very focused on simple calculations and

real-time solutions; hence a closed-form approximation formula is typically the preferred alternative. In this modeling framework the standard market practice is given by Kirk's formula

$$C_K^{Kirk}(0) = e^{-rT}\left(S_1(0)e^{(r-\delta_1)T}N(d_1) - S_2(0)e^{(r-\delta_2)T}N(d_2)\right), \tag{18}$$

where

$$\begin{aligned} d_1 &= \frac{\ln(S_1(0)e^{(r-\delta_1)T}/a) + \frac{\sigma_K^2}{2}T}{\sigma_K\sqrt{T}}, \quad d_2 = d_1 - \sigma_K\sqrt{T}, \\ \sigma_K &= \sqrt{\sigma_1^2 - 2b\rho\sigma_1\sigma_2 + b^2\sigma_2^2}, \end{aligned}$$

$a = S_2(0)e^{(r-\delta_2)T} + K$ and $b = \frac{S_2(0)e^{(r-\delta_2)T}}{S_2(0)e^{(r-\delta_2)T}+K}$.

Bjerksund and Stensland (2011) propose a lower bound, showing their approximation is more accurate than (18). The Bjerksund–Stensland approximation is

$$C_K^{BS}(0) = e^{-rT}\left(S_1(0)e^{(r-\delta_1)T}N(d_1) - S_2(0)e^{(r-\delta_2)T}N(d_2) - KN(d_3)\right)^+, \tag{19}$$

where quantity d_1 is defined as in Kirk's formula and

$$d_2 = \frac{\ln(S_1(0)e^{(r-\delta_1)T}/a) + T(b^2\sigma_2^2 - 2b\sigma_2^2 - \sigma_1^2 + 2\rho\sigma_1\sigma_2)/2}{\sigma_K\sqrt{T}},$$

$$d_3 = \frac{\ln(S_1(0)e^{(r-\delta_1)T}/a) + T(b^2\sigma_2^2 - \sigma_1^2)/2}{\sigma_K\sqrt{T}}.$$

We note that in the case $K = 0$, both formulas collapse in Margrabe's formula, providing the exact result. Formula (19) is equivalent to the classical Black–Scholes formula when $S_1(t) = 0$ or $S_2(t) = 0$. We modified Bjerksund and Stensland's formula by introducing the positive part operator to avoid negative prices for deeply out of the money options. To obtain a stricter lower bound, one could optimize the spread call value (19) above with respect to a and b, even if the authors show that, with their initial choice a and b, there is very little to gain from implementing such an optimization procedure. Before generalizing this formula to general stock dynamics (Section 3), we briefly describe other kinds of approximation for the spread option value.

A popular lower approximation formula is proposed by Carmona and Durrelman (2003a) and Carmona and Durrelman (2003b). The authors represent spot prices by two independent state variables and model the correlation using trigonometric functions. They propose the formula

$$\begin{aligned} C_K^{CD}(0) &= S_2(0)e^{-\delta_2 T}N(d^* + \sigma_2\cos(\theta^* + \phi)\sqrt{T}) \\ &\quad - S_1(0)e^{-\delta_1 T}N(d^* + \sigma_1\sin(\theta^* + \phi)\sqrt{T}) - Ke^{-rT}N(d^*), \end{aligned} \tag{20}$$

where

$$\cos\phi = \rho, \quad \cos\psi = \frac{\sigma_1 - \rho\sigma_2}{\sigma}, \quad \sigma = \sqrt{\sigma_1^2 + \sigma_2^2 - 2\rho\sigma_1\sigma_2}$$

and

$$d^* = \frac{1}{\sigma\cos(\theta^* - \psi)\sqrt{T}}\ln\left(\frac{S_2(0)e^{-\delta_2 T}\sigma_2\sin(\theta^* + \psi)}{S_1(0)e^{-\delta_1 T}\sigma_1\sin(\theta^*)}\right) - \frac{1}{2}(\sigma_2\cos(\theta^* + \phi) + \sigma_1\cos\theta^*).$$

The parameter θ^* is computed as the solution of the equation

$$\frac{1}{\delta\cos\theta}\ln\left(-\frac{\beta\kappa\sin(\theta+\phi)}{\gamma[\beta\sin(\theta+\phi)-\delta\sin\theta]}\right)-\frac{\delta\cos\theta}{2}=$$
$$\frac{1}{\delta\cos(\theta+\phi)}\ln\left(-\frac{\delta\kappa\sin\theta}{\alpha[\beta\sin(\theta+\phi)-\delta\sin\theta]}\right)-\frac{\beta\cos(\theta+\phi)}{2}$$

and

$$\alpha=S_2(0)e^{-\delta_2 T},\quad \gamma=S_1(0)e^{-\delta_1 T},\quad \beta=\sigma_2\sqrt{T},\quad \delta=\sigma_1\sqrt{T},\quad \text{and}\quad \kappa=Ke^{-rT}.$$

The approximation (20) is a lower bound and is equal to the true option price when $K=0$, or $S_1(t)=0$, or $S_2(t)=0$, or $\rho=\pm1$. In particular, (20) reduces to Margrabe's formula when $K=0$ and to the classical Black–Scholes formula when $S_1(t)=0$, or $S_2(t)=0$. The formula of Carmona and Durrelman (2003a) not only works in the geometric Brownian motion framework, but also can be rewritten for general log-normal processes, allowing the introduction of mean reversion and jumps. Carmona and Durrelman (2003a) provide a rather accurate upper bound; however, it does not reflect the extreme accuracy of their lower bound. Bjerksund and Stensland (2011) show that optimizing formula (19) with respect to a and b is equivalent to solving formula (20).

Another general approximation formula in the log-normal setup is suggested by Deng et al. (2008), who rewrite the spread option value as the sum of one-dimensional integrals, following the method of Pearson (1995). Integrals I_1, I_2, and I_3 are then approximated by a second-order expansion, yielding the approximation

$$C_K^{DLZ}(0)=e^{\nu_1^2/2+\mu_1-rT}I_1-e^{\nu_2^2/2+\mu_2-rT}I_2-Ke^{-rT}I_3, \tag{21}$$

where

$$I_i\approx J_0(C^i,D^i)+J_1(C^i,D^i)\epsilon+\frac{1}{2}J_2(C^i,D^i)\epsilon^2$$

and

$$\begin{aligned}
J_0(u,v) &= N\left(\frac{u}{\sqrt{1+v^2}}\right),\\
J_1(u,v) &= \frac{1+(1+u^2)v^2}{(1+v^2)^{5/2}}n\left(\frac{u}{\sqrt{1+v^2}}\right),\\
J_1(u,v) &= \frac{(6-6u^2)v^2+(21-2u^2-u^4)v^4+4(3+u^2)v^6-3}{(1+v^2)^{11/2}}u\cdot n\left(\frac{u}{\sqrt{1+v^2}}\right).
\end{aligned}$$

The arguments C^i, D^i, and ϵ are given by

$$\begin{aligned}
C^1 &= C^3 + D^3\varrho\nu_1 + \epsilon\varrho^2\nu_1^2 + \sqrt{1-\varrho^2}\nu_1, \\
D^1 &= D^3 + 2\varrho\nu_1\epsilon, \\
C^2 &= C^3 + D^3\nu_2 + \epsilon\nu_2^2, \\
D^2 &= D^3 + 2\nu_2\epsilon, \\
C^3 &= \frac{1}{\nu_1\sqrt{1-\varrho^2}}\left(\mu_1 - \ln(R+K) + \frac{\nu_2 R}{R+K}y_0 - \frac{\nu_2^2 RK}{2(R+K)^2}y_0^2\right), \\
D^3 &= \frac{1}{\nu_1\sqrt{1-\varrho^2}}\left(\varrho\nu_1 - \frac{\nu_2 R}{R+K} + \frac{\nu_2^2 RK}{(R+K)^2}y_0\right), \\
\epsilon &= -\frac{1}{2\nu_1\sqrt{1-\varrho^2}}\frac{\nu_2^2 RK}{(R+K)^2},
\end{aligned}$$

where $R = e^{\nu_2 y_0 + \mu_2}$ and y_0 is any real number close to zero. The quantities μ_j and ν_j appearing in formula (21) are the mean and variance of price returns, respectively. The parameter ϱ is the instant correlation of the standardized log-prices, which, in the geometric Brownian motion framework, become

$$\mu_i = \ln S_i(0) + (r - \delta_i - \sigma_i^2/2)T, \quad \nu_i = \sigma_i\sqrt{T} \quad \text{and} \quad \varrho = \rho.$$

The boundary conditions for $K = 0$, $S_1(0) = 0$, and $S_2(0) = 0$ are satisfied. The parameter y_0 can be freely chosen as a real number close to zero because formula (21) is based on a second-order integral approximation. The method has been proven to be extremely fast and accurate. With the same integral approximation technique, Deng et al. (2008) obtain a closed formula for the spread option's Greeks.

The last approximation formula we describe in the geometric Brownian motion setting is based on an idea of Venkatramana and Alexander (2011). These authors express the price of a spread option as the sum of the prices of two compound options. One compound option is to exchange vanilla call options on the two underlying assets and the second is to exchange the corresponding put options. Let $U_i(0)$ and $V_i(0)$ be the Black–Scholes option prices at time 0 for the calls and put options, respectively. Let $K_1 = mK$ be the strike of U_1 and V_1 and let $K_2 = (m-1)K$ be the strike of U_2 and V_2 for some real number $m \geq 1$. Choosing m such that single-asset call options are deep in the money, the risk-neutral price at time 0 of a European spread option can be expressed as

$$C_K^{VA}(0) = e^{-rT}\left(U_1(0)N(d_{1U}) - U_2(0)N(d_{2U}) - (V_1(0)N(-d_{1V}) - V_2(0)N(-d_{2V}))\right), \tag{22}$$

where

$$d_{1A} = \frac{\ln(A_1(0)/A_2(0)) + (\delta_2 - \delta_1 + \sigma_A^2/2)T}{\sigma_A\sqrt{T}}, \quad d_{2A} = d_{1A} - \sigma_A\sqrt{T}$$

and

$$\begin{aligned}
\sigma_U &= \sqrt{\xi_1^2 + \xi_2^2 - 2\rho\xi_1\xi_2}, \\
\sigma_V &= \sqrt{\eta_1^2 + \eta_2^2 - 2\rho\eta_1\eta_2}, \\
\xi_i &= \sigma_i \frac{S_i(0)}{U_i(0)} \left(\frac{\partial U_i(t)}{\partial S_i(t)} \right)_{t=0}, \\
\eta_i &= \sigma_i \frac{S_i(0)}{V_i(0)} \left| \frac{\partial V_i(t)}{\partial S_i(t)} \right|_{t=0}.
\end{aligned}$$

The authors show that formula (22) is a better approximation than Kirk's formula and allows one to properly quantify the correlation risk of the spread option.

There is very little literature about pricing spread options in a non-Gaussian setup. A Fourier transform was originally introduced by Dempster and Hong (2002), who implement an FFT-based valuation method, applying the idea of Carr and Madan (2000). The most advanced FFT-based spread option pricing method is that proposed by Hurd and Zhou (2009). These authors introduce a formula for general spread option pricing based on Fourier analysis of the spread option payoff function. The method is applicable to models in which the joint characteristic function of the underlying assets forming the spread is known analytically. This enables the authors to incorporate stochasticity in the volatility and correlation structure by introducing, for example, additional factors within an affine jump diffusion framework. Without loss of generality, the authors describe the payoff as $(e^{x_1} - e^{x_2} - 1)^+$. Let $\mathbf{u} = (u_1, u_2)^\intercal$ and $\mathbf{X}(t) = (\ln S_1(t), \ln S_2(t))^\intercal$ and consider the joint characteristic function

$$\Phi_T(\mathbf{u}) = \Phi_T(u_1, u_2) = \mathbb{E}\Big[e^{iu_1 \ln S_1(T) + iu_2 \ln S_2(T)}\Big] = \mathbb{E}\Big[e^{i\mathbf{u}^\intercal \mathbf{X}(T)}\Big].$$

The value of this spread option can be computed as

$$C_K^{HZ} = \frac{1}{(2\pi)^2} e^{-rT} \int\int_{\mathrm{R}^2 + i\epsilon} e^{i\mathbf{u}^\intercal \mathbf{X}(0)} \Phi_T(\mathbf{u}) \hat{P}(\mathbf{u}) d^2\mathbf{u}, \tag{23}$$

where

$$\hat{P}(\mathbf{u}) = \frac{\Gamma(i(u_1 + u_2) - 1)\Gamma(-iu_2)}{\Gamma(iu_1 + 1)}.$$

Authors describe how to solve the double Fourier integrals in formula (23) using a two-dimensional FFT approximation. Such approximations involve both a truncation and discretization of the integral and the two properties that determine their accuracy are the decay of the integrand of (23) in u-space and the decay of the function C_K^{HZ} in x-space.

3. The lower bound

Consider the problem (16). If $K = 0$ and $S_1(t), S_2(t)$ are jointly log-normal, we have the so-called Margrabe exchange option formula. Very little regarding non-zero strikes and non-Gaussian processes is discussed in the literature, despite the relevance of a closed pricing formula in a number of financial applications, such as those previously described.

Let us define the event A

$$A = \left\{\omega : \frac{S_1(T)}{S_2^{\alpha}(T)} > \frac{e^k}{E\left(S_2^{\alpha}(T)\right)}\right\} \tag{24}$$

and let us consider the following lower bound to the spread option payoff:

$$\left(S_1(T) - S_2(T) - K\right)^+ \geq \left(S_1(T) - S_2(T) - K\right) 1_{(A)}. \tag{25}$$

Bjerksund and Stensland (2011) are able to explicitly compute

$$C_K^{k,\alpha}(0) = e^{-rT}\mathbb{E}\Big[\left(S_1(T) - S_2(T) - K\right) 1_{(A)}\Big] \tag{26}$$

in the log-normal case. They also show that $C_K^{k,\alpha}(0)$ is a very good approximation to the exact spread option price $C_K(0)$ for suitable choices of the parameters α and k. In particular, they show that their formula in the log-normal setup is more accurate than Kirk's approximation.

We now generalize their result to a general bivariate stock price dynamic, provided that the joint characteristic function of $(\ln S_1(T), \ln S_2(T))^{\intercal}$ is available in closed form. Let $\mathbf{u} = (u_1, u_2)^{\intercal}$ and $\mathbf{X}(t) = (\ln S_1(t), \ln S_2(t))^{\intercal}$ and consider the joint characteristic function

$$\Phi_T(\mathbf{u}) = \Phi_T(u_1, u_2) = \mathbb{E}\Big[e^{iu_1 \ln S_1(T) + iu_2 \ln S_2(T)}\Big] = \mathbb{E}\Big[e^{i\mathbf{u}^{\intercal}\mathbf{X}(T)}\Big].$$

Our main result is stated in the following proposition.

Proposition 1. *The approximate spread option value $C_K^{k,\alpha}(0)$ is given in terms of a Fourier inversion formula as*

$$C_K^{k,\alpha}(0) = \left(e^{-\delta k - rT}\frac{1}{\pi}\int_0^{+\infty} e^{-i\gamma k}\Psi(\gamma;\delta,\alpha)d\gamma\right)^+, \tag{27}$$

where

$$\begin{aligned}\Psi(\gamma;\delta,\alpha) = {} & \frac{e^{i(\gamma - i\delta)\ln(\Phi_T(0,-i\alpha))}}{i(\gamma - i\delta)}\Big[\Phi_T((\gamma - i\delta) - i, -\alpha(\gamma - i\delta)) - \\ & \Phi_T(\gamma - i\delta, -\alpha(\gamma - i\delta) - i) - K\Phi_T(\gamma - i\delta, -\alpha(\gamma - i\delta))\Big]\end{aligned}$$

and

$$\alpha = \frac{F_2(0,T)}{F_2(0,T) + K}, \tag{28}$$

$$k = \ln\big(F_2(0,T) + K\big). \tag{29}$$

Proof: See Appendix B, Section 1.

The quantity $F_2(0,T) = \mathbb{E}[S_2(T)]$ in formulas (28) and (29) is the forward price of the second asset at time 0 for delivery at future date T. Using the characteristic function properties, we can also write $F_2(0,T) = \Phi_T(0,-i)$. The parameter δ tunes an exponentially decaying term introduced to allow the integration, as in Carr and Madan (2000) and Dempster and Hong (2002).

A few remarks can be made about the above formula. First, if the characteristic function $\Phi_T(\mathbf{u})$ is known analytically, then the Fourier transform of the lower bound can be expressed in closed form, as well in terms of the complex function $\Psi(\gamma;\delta,\alpha)$. The integral in (27) can be easily computed using standard numerical quadratures (`NIntegrate` in Mathematica or `quadgk` in Matlab) or via

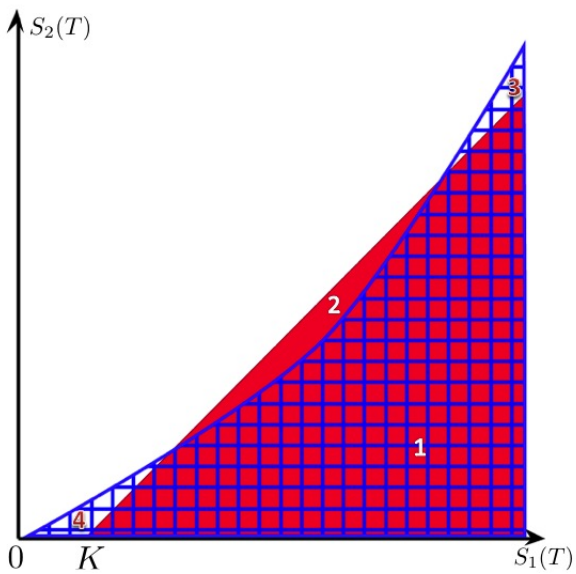

FIGURE 1. The true exercise region B (red) and its approximation A (blue grid).

the FFT algorithm. The main point concerning the above formula is that the approximated option price is obtained through a univariate Fourier inversion, while, for example, Hurd and Zhou (2009) propose an analytical formula requiring a bivariate Fourier inversion. Although our formula is supposed to be a lower bound to the exact price, the bound turns out to be so tight that in practice it provides an estimate that is indistinguishable from the true price. A third point relates to the free parameters, α and k. In theory, we could maximize the lower bound with respect to these parameters. Again, in practice, this is not necessary because the educated guesses proposed by Bjerksund and Stensland (2011) and described here and generalized to the expressions (28) and (29) turn out to be very effective, in the non-Gaussian case as well. The fourth remark relates to the positive part in formula (27). The positive part function is necessary because the original Bjerksund and Stensland (2011) formulation can give negative prices for deeply out-of-the-money options. In this case, we adopt a practical approach and set the value of the spread option to zero.

For a better understanding of the approximation, see Figure 1. If we define the true exercise set

$$B = \{\omega : S_1(T) \geq S_2(T) + K\},$$

the approximation replaces the set B by the set A defined in (24). In particular, the set A can be rewritten as

$$A = \left\{ \omega : S_1(T) \geq e^k \frac{S_2^\alpha(T)}{\mathbb{E}\left[S_2^\alpha(T)\right]} \right\}.$$

We can identify four regions in Figure 1. In region 1, sets A and B overlap and the true and approximate payoffs are equal. In region 2, the true payoff is positive but small—indeed, $S_1(T)$ is only slightly greater than $S_2(T) + K$—while the approximated payoff is zero. In regions 3 and

4, the option payoff is zero while the approximated payoff is slightly negative. In the remaining, white region, both payoffs are zero. The role of the free parameters k is to control the slope of the frontier of the approximating exercise region A, while the parameter α controls both slope and curvature. Finally, if $K = 0$, it follows that $\alpha = 1$ and $k = \ln(\Phi_T(0, -i))$, so that $A \equiv B$ and the approximated formula (27) gives the exact fair value of the exchange option.

4. The upper bound

To control the error of the approximation in (27), we provide an estimate of an upper bound of the spread option price. Consider the quadratic spread option payoff

$$Q(T) = \frac{1}{2}(S_1(T) - S_2(T) - L)^2 1_{(S_1(T) \geq S_2(T))}.$$

Notice that the exercise region is the same as for an exchange option, that is, a spread option with zero strike. The price of this new contract is given in the following proposition.

Proposition 2. *The no-arbitrage price $Q(0)$ of the quadratic spread option is given by the formula*

$$Q(0) = \frac{e^{-rT}}{2}\mathbb{E}\big[(S_1(T) - S_2(T) - L)^2 1_{(S_1(T) \geq S_2(T))}\big] \tag{30}$$

$$= e^{-\delta k - rT}\frac{1}{2\pi}\int_0^{+\infty} e^{-i\gamma k}\Xi(\gamma; \delta, \alpha)d\gamma, \tag{31}$$

where

$$\begin{aligned}\Xi(\gamma; \delta, \alpha) = {} & \frac{e^{i(\gamma - i\delta)\ln(\Phi_T(0, -i\alpha))}}{i(\gamma - i\delta)}\Big[\Phi_T((\gamma - i\delta) - 2i, -\alpha(\gamma - i\delta)) + \\ & \Phi_T(\gamma - i\delta, -\alpha(\gamma - i\delta) - 2i) + L^2\Phi_T(\gamma - i\delta, -\alpha(\gamma - i\delta)) - \\ & 2L\Phi_T(\gamma - i\delta - i, -\alpha(\gamma - i\delta)) + 2L\Phi_T(\gamma - i\delta, -\alpha(\gamma - i\delta) - i) - \\ & 2\Phi_T(\gamma - i\delta - i, -\alpha(\gamma - i\delta) - i)\Big]\end{aligned}$$

and $\alpha = 1$ and $k = \ln(F_2(0, T))$.

Proof: See Appendix B, Section 2.

Consider now the function

$$\pi(x) = \Delta K \sum_{j=1}^{N} \max(x - \Delta K(j - 0.5) + L, 0),$$

where $\Delta K > 0$ and $N \in \mathbb{N}^+$. We observe that the function $\pi(x)$ and the payoff $q(x) = \frac{1}{2}(x - L)^2 1_{(x \geq 0)}$ are tangent in N points, exactly in $x_j = L + j\Delta K$, and moreover $q(x) \geq \pi(x)$. This is shown in Figure 2. If we set $x = S_1(T) - S_2(T)$, $\pi(x)$ is nothing more than a portfolio of spread options with varying strikes $K_j = \Delta K(j - 0.5) - L$ and each option is held for an amount equal to ΔK. Therefore the fair value of this portfolio is

$$\Pi(0) = \Delta K \sum_{j=1}^{N} C_{K_j}(0)$$

and clearly $Q(0) \geq \Pi(0)$, $Q(0)$ being the fair value of the payoff $q(S_1(T) - S_2(T))$.

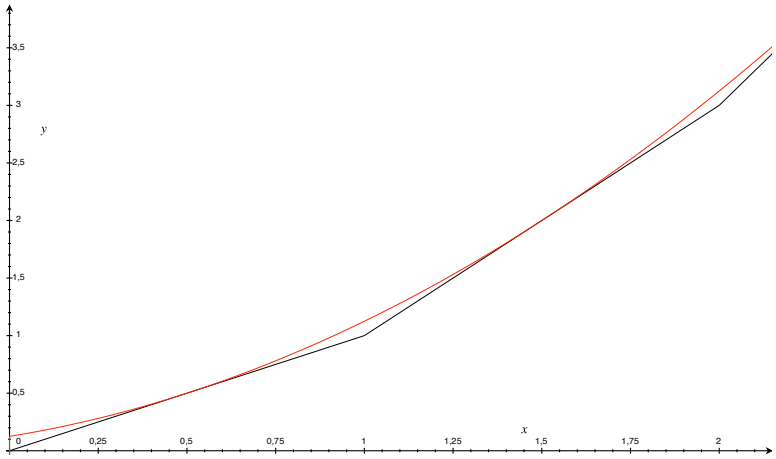

FIGURE 2. Comparison of the payoff $Q(T)$ (red line) and the sub-replicating strategy (black line). Here $x = S_1(T) - S_2(T)$.

Suppose we are interested in pricing a spread option having strike $K_{\bar{j}}$, with $K_{\bar{j}} \in K_1, \cdots, K_N$. We can write

$$Q(0) \geq \Pi(0) = \Delta K \left(\sum_{j \neq \bar{j}} C_{K_j}(0) + C_{K_{\bar{j}}}(0) \right) \geq \Delta K \left(\sum_{j \neq \bar{j}} C_{K_j}^{\alpha_j, k_j}(0) + C_{K_{\bar{j}}}(0) \right),$$

where the true prices $C_{K_j}(0)$ of the spread options in the first sum are replaced by our lower bound $C_{K_j}^{\alpha_j, k_j}(0)$ in the second sum and where $\alpha_j = \frac{\Phi_T(0,-i)}{\Phi_T(0,-i)+K_j}$ and $k_j = \ln(\Phi_T(0,-i)+K_j)$. Rearranging terms, it follows that an upper bound for the spread option is given by

$$C_{K_{\bar{j}}}(0) \leq \frac{Q(0)}{\Delta K} - \sum_{j \neq \bar{j}} C_{K_j}^{\alpha_j, k_j}(0) := U_{K_{\bar{j}}}^{N, \Delta K}(0).$$

The computation of the upper bound $U_K^{N,\Delta K}(0)$ requires the value of the deal $Q(0)$, given in formula (30), and the pricing of N spread option contracts via the lower bound approximation in formula (27). The choice of the parameter L is arbitrary, except for the fact that we must guarantee that $K_{\bar{j}} \in \{K_1, \cdots, K_N\}$.

Numerical examples show that this upper bound is extremely accurate.

5. The geometric Brownian motion case

This section discusses in more detail the geometric Brownian motion and presents a different argument to obtain Bjerksund and Stensland's lower bound via the conditional expected value. In addition, it explicitly computes the quantity $Q(T)$ in the upper bound given in the previous section. Finally, this section proposes an improved lower bound and a second upper bound, following Rogers and Shi (1995) for Asian options.

We consider the dynamics in (17) and provide a different derivation of Bjerksund and Stensland's lower bound via conditional expected value theory. Define

$$R(t) = \frac{S_1(t)}{S_2(t)^\alpha} = \frac{S_1(0)}{S_2(0)^\alpha} e^{t(r-\delta_1-\sigma_1^2/2-\alpha(r-\delta_2-\sigma_2^2/2))+\sigma_1 W_1(t)-\alpha\sigma_2 W_2(t)}$$

and set

$$\sqrt{t}\sigma_R Z = \sigma_1 W_1(t) - \alpha\sigma_2 W_2(t), \quad \sigma_R^2 = \sigma_1^2 - 2\rho\alpha\sigma_1\sigma_2 + \alpha^2\sigma_2^2, \quad Z \sim \mathcal{N}(0,1).$$

We can rewrite the set A as

$$\begin{aligned} A &= \left\{\omega : R(T) > \frac{e^k}{\mathbb{E}[S_2^\alpha(T)]}\right\} \\ &= \left\{\omega : Z \geq d = \frac{k - \ln(R(0)\mathbb{E}[S_2^\alpha(T)]) - T(r-\delta_1-\sigma_1^2/2-\alpha(r-\delta_2-\sigma_2^2/2))}{\sqrt{T}\sigma_R}\right\}. \end{aligned} \tag{32}$$

If we set $U = S_1(T) - S_2(T) - K$, the Bjerksund–Stensland lower bound can be equivalently rewritten as

$$\mathbb{E}\big[U^+\big] \geq \mathbb{E}\big[U 1_{(A)}\big]^+ = \mathbb{E}\big[\mathbb{E}\big[U|Z\big]1_{(Z\geq d)}\big]^+.$$

We observe that $(W_1(T), W_2(T)|Z)^\intercal \sim \mathcal{MN}(\mu, \Sigma)$, where

$$\mu = \sqrt{T}Z\begin{pmatrix} a_1 \\ a_2 \end{pmatrix}, \quad \Sigma = T\begin{pmatrix} 1-a_1^2 & \rho - a_1a_2 \\ \rho - a_1a_2 & 1-a_2^2 \end{pmatrix}, \quad a_1 = \frac{\sigma_1 - \rho\alpha\sigma_2}{\sigma_R}, \quad a_2 = \frac{\sigma_1\rho - \alpha\sigma_2}{\sigma_R},$$

and therefore it follows that $(S_1(T), S_2(T)|Z)^\intercal \sim \mathcal{MLN}(\hat{\mu}, \hat{\Sigma})$, where

$$\hat{\mu} = \begin{pmatrix} \ln S_1(0) + (r-\delta_1-\sigma_1^2/2)T + \sigma_1 a_1\sqrt{T}Z \\ \ln S_2(0) + (r-\delta_2-\sigma_2^2/2)T + \sigma_2 a_2\sqrt{T}Z \end{pmatrix}, \hat{\Sigma} = T\begin{pmatrix} \sigma_1^2(1-a_1^2) & \sigma_1\sigma_2(\rho - a_1a_2) \\ \sigma_1\sigma_2(\rho - a_1a_2) & \sigma_2^2(1-a_2^2) \end{pmatrix}.$$

We can now compute the approximated payoff expectation

$$\begin{aligned} & \mathbb{E}\big[\mathbb{E}\big[U|Z\big]1_{(Z\geq d)}\big]^+ \\ = \; & \mathbb{E}\big[\big(e^{\ln S_1(0)+(r-\delta_1-\sigma_1^2a_1^2/2)T+\sigma_1a_1\sqrt{T}Z} - e^{\ln S_2(0)+(r-\delta_2-\sigma_2^2a_2^2/2)T+\sigma_2a_2\sqrt{T}Z} - K\big)1_{(Z\geq d)}\big]^+. \end{aligned}$$

By using the partial expectation property of the log-normal distribution and discounting, the above expectation gives us Bjerksund and Stensland's lower bound

$$C_K^{\alpha,k}(0) = e^{-rT}\big(S_1(0)e^{(r-\delta_1)T}N(\sigma_1a_1\sqrt{T}-d) - S_2(0)e^{(r-\delta_2)T}N(\sigma_2a_2\sqrt{T}-d) - KN(-d)\big)^+, \tag{33}$$

where α and k, in the definition of a_1, a_2, and d, can be chosen to maximize the above formula or can be set according to the guess of Bjerksund and Stensland.

We now show how to improve the lower bound. We note that

$$\underbrace{\mathbb{E}\big[U^+\big]}_{\text{True price}} \geq \underbrace{\mathbb{E}\big[\mathbb{E}\big[U|Z\big]^+1_{(Z\geq d)}\big]}_{\text{Improved lower bound}} \geq \underbrace{\mathbb{E}\big[\mathbb{E}\big[U|Z\big]1_{(Z\geq d)}\big]^+}_{\text{Bjerksund and Stensland's lower bound}}$$

so a strengthened lower bound turns out to be

$$\begin{aligned} & \mathbb{E}\big[\mathbb{E}\big[U|Z\big]^+1_{(Z\geq d)}\big] \\ = \; & \mathbb{E}\big[\big(e^{\ln S_1(0)+(r-\delta_1-\sigma_1^2a_1^2/2)T+\sigma_1a_1\sqrt{T}Z} - e^{\ln S_2(0)+(r-\delta_2-\sigma_2^2a_2^2/2)T+\sigma_2a_2\sqrt{T}Z} - K\big)^+1_{(Z\geq d)}\big] \\ = \; & \mathbb{E}\big[\big(e^{\ln S_1(0)+(r-\delta_1-\sigma_1^2a_1^2/2)T+\sigma_1a_1\sqrt{T}Z} - e^{\ln S_2(0)+(r-\delta_2-\sigma_2^2a_2^2/2)T+\sigma_2a_2\sqrt{T}Z} - K\big)1_{(D)}\big], \end{aligned}$$

where the set D is defined as

$$D \equiv \big\{z : e^{\ln S_1(0)+(r-\delta_1-\sigma_1^2 a_1^2/2)T+\sigma_1 a_1\sqrt{T}Z} - e^{\ln S_2(0)+(r-\delta_2-\sigma_2^2 a_2^2/2)T+\sigma_2 a_2\sqrt{T}Z} - K \geq 0\big\} \cap \big\{z \geq d\big\}.$$

The function appearing in the definition of the set D can have at most two real roots[1] that can be numerically calculated. One of the following three situations can occur:

(a) $D = \emptyset$;

(b) $D = [d_1, d_2]$, where $d_1 \leq d_2$ and $d_1, d_2 \in \mathbb{R}^*$;

(c) $D = [d_1, d_2] \cup [d_3, d_4]$, where $d_1 \leq d_2 < d_3 \leq d_4$ and $d_1, d_2, d_3, d_4 \in \mathbb{R}^*$.

Let us define a function F such that $\forall d_1 \leq d_2$ and $d_1, d_2 \in \mathbb{R}^*$, we have, $\forall x \in \mathbb{R}$,

$$F(\emptyset; x) = 0, \qquad F([d_1, d_2]; x) = N(x - d_1) - N(x - d_2),$$

and, $\forall d_1 \leq d_2 < d_3 \leq d_4$ and $d_1, d_2, d_3, d_4 \in \mathbb{R}^*, \forall x \in \mathbb{R}$,

$$F([d_1, d_2] \cup [d_3, d_4]; x) = F([d_1, d_2]; x) + F([d_3, d_4]; x).$$

We can write the following improved lower bound in terms of F as

$$\hat{C}_K^{\alpha,k}(0) = e^{-rT}\big(S_1(0)e^{(r-\delta_1)T}F(D; \sigma_1 a_1\sqrt{T}) - S_2(0)e^{(r-\delta_2)T}F(D; \sigma_2 a_2\sqrt{T}) - KF(D; 0)\big).$$

Note that $C_K^{\alpha,k}(0) = \hat{C}_K^{\alpha,k}(0)$ when $D = [d_1, d_2]$ and $d_1 = d$ and $d_2 = +\infty$. From a practical perspective, this is often, but not always, the case. So in general we expect only a small improvement from adopting $\hat{C}_K^{\alpha,k}(0)$ rather than $C_K^{\alpha,k}(0)$. Numerical experiments confirm this.

Let us discuss now how to explicitly compute an upper bound that we call $U^{RS}(0)$, because it exploits ideas first proposed by Rogers and Shi (1995). Define the sets

$$B = \{\omega : S_1(T) \geq S_2(T) + K\}$$

and the set A^{RS}:

$$A^{RS} = \left\{\omega : \frac{S_1(T)}{S_2^\alpha(T)} > \frac{e^k}{\mathbb{E}[S_2^\alpha(T)]}, B \subseteq A\right\}.$$

The shape of the set A^{RS} is shown in Figure 3. Here A^{RS} is constructed requiring tangency between the function describing the exercise frontier of B, that is, $b(x) = x - K$, and the function describing the exercise frontier of A^{RS}, that is, $a(x) = (x\frac{\mathbb{E}[S_2(T)^\alpha]}{e^k})^{1/\alpha}$. We thus have $U^+ = U^+ 1_{(A^{RS})}$ and the following equality is satisfied:

$$\mathbb{E}\big[U^+\big] - \mathbb{E}\big[\mathbb{E}\big[U 1_{(A^{RS})}|A^{RS}\big]^+\big] = \mathbb{E}\big[U^+ 1_{(A^{RS})}\big] - \mathbb{E}\big[\mathbb{E}\big[U 1_{(A^{RS})}|A^{RS}\big]^+\big].$$

Therefore, following Nielsen and Sandmann (2003), the error on the lower bound can be expressed as

$$0 \leq \mathbb{E}\Big[\mathbb{E}\big[U^+ 1_{(A^{RS})}|A^{RS}\big] - \mathbb{E}\big[U 1_{(A^{RS})}|A^{RS}\big]^+\Big] \leq \frac{1}{2}\mathbb{E}[\mathrm{var}(U|Z)1_{(Z>d)}]^{1/2}\mathbb{E}[1_{(Z>d)}]^{1/2},$$

where d is defined in (32). The conditional variance of U is

$$\mathrm{var}(U|Z) = \mathrm{var}(S_1(T)|Z) + \mathrm{var}(S_2(T)|Z) - 2\mathrm{cov}(S_1(T), S_2(T)|Z).$$

[1]An exponential polynomial with $N+1$ nonzero terms, i.e. $A(z) = \sum_{j=1}^{N+1} \alpha_j e^{\lambda_j z}$ with distinct $\lambda_j \in \mathbb{R}$ and each $\alpha_j \in \mathbb{R}^*$, can have at most N real roots.

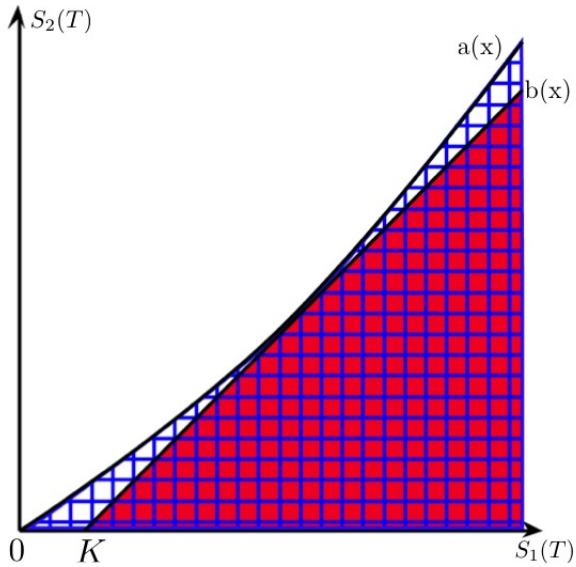

FIGURE 3. The true exercise region B (red) and its approximation A^{RS} (blue grid).

The conditional covariance matrix between $S_1(T)$ and $S_2(T)$ is given from properties of the log-normal distribution so that

$$\begin{aligned}\operatorname{cov}(S_i(T), S_j(T)|Z) &= (e^{T\sigma_i\sigma_j(\varrho_{ij}-a_ia_j)}-1)\exp\{\ln S_i(0)+\ln S_j(0)+\\ &\quad T(2r-\delta_i-\delta_j-\sigma_i^2a_i^2/2-\sigma_j^2a_j^2/2)+\sqrt{T}(\sigma_ia_i+\sigma_ja_j)Z)\},\end{aligned}$$

where ϱ_{ij} stands for the elements of the matrix

$$\varrho = \begin{pmatrix} 1 & \rho \\ \rho & 1 \end{pmatrix}.$$

The formula for the error ϵ is obtained by once again applying the partial expectation property of the log-normal distribution and discounting. The upper bound is therefore

$$U^{RS}(0) := \hat{C}_K^{\alpha,k}(0) + \epsilon^{\alpha,k},$$

where

$$\begin{aligned}\epsilon^{\alpha,k} &= \frac{e^{-rT}}{2}N(-d)^{1/2}\Bigg(\sum_{i=1}^{2}\sum_{j=1}^{2}(-1)^{i+j}\big(e^{T\sigma_i\sigma_j(\varrho_{ij}-a_ia_j)}-1\big)\times\\ &\quad e^{\ln S_i(0)+\ln S_j(0)+T(2r-\delta_i-\delta_j+a_ia_j\sigma_i\sigma_j)}N\big(-d+\sqrt{T}(\sigma_ia_i+\sigma_ja_j)\big)\Bigg)^{1/2}.\end{aligned}$$

This upper bound $U^{RS}(0)$ depends on the parameters α and k appearing in the definition of d, a_1, and a_2 and can be minimized under the constraint $B \subseteq A^{RS}$. In practice, we see that, numerically, this upper bound is less tight than that obtained using the quadratic spread option argument.

In this regard, in the bivariate geometric Brownian motion case, the quantity $Q(0)$ in the upper bound $U_K^{N,\Delta K}$ is equal to

$$\begin{aligned} Q(0) &= \frac{e^{-rT}}{2}\Big(S_1(0)^2 e^{(2r-2\delta_1+\sigma_1^2)T} N(2\sigma_1 a_1\sqrt{T}-d) - 2LS_1(0)e^{(r-\delta_1)T}N(\sigma_1 a_1\sqrt{T}-d) \\ &\quad + S_2(0)^2 e^{(2r-2\delta_2+\sigma_2^2)T} N(2\sigma_2 a_2\sqrt{T}-d) + 2LS_2(0)e^{(r-\delta_2)T}N(\sigma_2 a_2\sqrt{T}-d) + L^2 N(-d) \\ &\quad - 2S_1(0)S_2(0)e^{(2r-\delta_1-\delta_2-\sigma_1 a_1/2-\sigma_2 a_2/2+\sigma_1\sigma_2(\rho-a_1a_2))T} N((\sigma_1 a_1+\sigma_2 a_2)\sqrt{T}-d)\Big). \end{aligned}$$

In this case, we set $\alpha = 1$ and $k = \ln(\Phi_T(0,-i))$.

6. Non-Gaussian stock price models

The following presents several stock price models for which we analyze the performance of our lower and upper bounds. The numerical results show that bounds $C_K^{\alpha,k}(0)$ and $U_K^{N,\Delta K}(0)$ are very accurate and that, from a practical point of view, the lower bound is indistinguishable from the true price, estimated using Monte Carlo simulation.

Let $\mathbf{S}(t) = (S_1(t), S_2(t))^\intercal$ be the stock price vector and assume that the joint characteristic function of $\mathbf{X}(t) = (\ln S_1(t), \ln S_2(t))^\intercal$ has the functional form $\Phi_T(\mathbf{u}) = e^{i\mathbf{u}^\intercal \mathbf{X}(0)}\varphi_T(\mathbf{u})$. In the following, we set $\mathbf{e} = (1,1)^\intercal$. We recall the expression of the characteristic function in the case of geometric Brownian motion.

6.1. Geometric Brownian motion. In the well-known two-asset Black–Scholes model, the vector $\mathbf{S}(t)$ has components

$$S_j(t) = S_j(t)\exp[(r-\delta_j-\sigma_j^2/2)t + \sigma_j W_j(t)], \quad j = 1,2,$$

where $\sigma_1, \sigma_2 > 0$, and W_1, W_2 are risk-neutral Brownian motions with instantaneous correlation $\rho, |\rho| < 1$, r is the risk-free rate, and δ_j is the continuous dividend yield paid by asset j. We have

$$\varphi_T(\mathbf{u}) = \exp[iT\mathbf{u}^\intercal(r-\delta)\mathbf{e} - \sigma^2/2) - \mathbf{u}^\intercal\Sigma\mathbf{u}T/2],$$

where $\Sigma = [\sigma_1^2, \rho\sigma_1\sigma_2; \rho\sigma_1\sigma_2, \sigma_2^2]$ and $\sigma^2 = \operatorname{diag}(\Sigma)$.

6.2. Jump diffusion model I (normally distributed jump size). The second model is the bidimensional jump diffusion model introduced by Cheang and Chiarella (2011). It generalizes the above bidimensional geometric Brownian motion by adding two jump components. The components of the stock price vector have the following functional form:

$$S_j(t) = S_j(0)\exp\left[\left(r-\delta_j-\frac{\sigma_j^2}{2}-\lambda\kappa_j-\lambda_j\kappa_{Z_j}\right)t + \sigma_j W_j(t) + \sum_{m=1}^{N_j(t)} Z_j(m) + \sum_{n=1}^{N(t)} Y_j(n)\right], \tag{34}$$

where $\sigma_1, \sigma_2 > 0$, and W_1, W_2 are risk-neutral Brownian motions with instantaneous correlation $\rho, |\rho| < 1$. In addition, $\sum_{m=1}^{N_1(t)} Z_1(m)$ and $\sum_{m=1}^{N_2(t)} Z_2(m)$ are univariate compound Poisson processes, driven, respectively, by the Poisson processes N_1 and N_2 with intensity rates λ_1 and λ_2. This jump component is unique to each stock and describes the idiosyncratic shocks for that particular asset only. The idiosyncratic jump sizes Z_1 and Z_2 are independently and identically distributed

according to a Gaussian distribution $\mathcal{N}(\alpha_{jj}, \xi_{jj}^2)$. The model also allows for macroeconomic shocks in the expression

$$\sum_{n=1}^{N(t)} \mathbf{Y}(n) = \left(\sum_{n=1}^{N(t)} Y_1(n), \sum_{n=1}^{N(t)} Y_2(n) \right)^{\intercal},$$

which is a bivariate compound Poisson process with intensity rate λ. Under the risk-neutral measure $\mathbb{Q}$, the jump sizes $\mathbf{Y}$ are assumed to be independently and identically distributed according to a multivariate normal $\mathcal{MN}(\alpha, \Sigma_Y)$, where $\alpha = (\alpha_1, \alpha_2)^{\intercal}$ and

$$\Sigma_{\mathbf{Y}} = \begin{pmatrix} \xi_1^2 & \rho_Y \xi_1 \xi_2 \\ \rho_Y \xi_1 \xi_2 & \xi_2^2 \end{pmatrix}.$$

Finally, the quantities κ_j and $\kappa_{Z_j}, j = 1, 2$ in (34) are, respectively,

$$\kappa_j = \int_{\mathbb{R}^2} [e^{y_j} - 1] m_{\mathbb{Q}}(dy) = \int_{\mathbb{R}} [e^{y_j} - 1] m_{\mathbb{Q}}(dy_j) = \exp(\alpha_j + \xi_j^2/2) - 1,$$

$$\kappa_{Z_j} = \int_{\mathbb{R}} [e^{z_j} - 1] m_{\mathbb{Q}}(dz_j) = \exp(\alpha_{jj} + \xi_{jj}^2/2) - 1.$$

The joint characteristic function is $\Phi_T(\mathbf{u}) = e^{i\mathbf{u}^{\intercal}\mathbf{X}(0)} \varphi_T(\mathbf{u})$, where

$$\begin{aligned} \varphi_T(\mathbf{u}) &= \exp\big[T\big(i\mathbf{u}^{\intercal}\gamma - \mathbf{u}^{\intercal}\Sigma\mathbf{u}/2 + \lambda_1(e^{iu_1\alpha_{11} - u_1^2\xi_{11}^2/2} - 1) + \lambda_2(e^{iu_2\alpha_{22} - u_2^2\xi_{22}^2/2} - 1) + \\ &\quad \lambda(e^{i\mathbf{u}^{\intercal}\alpha - \mathbf{u}^{\intercal}\Sigma_{\mathbf{Y}}\mathbf{u}/2} - 1)\big)\big] \end{aligned} \tag{35}$$

and $\Sigma = [\sigma_1^2, \rho\sigma_1\sigma_2; \rho\sigma_1\sigma_2, \sigma_2^2]$, $\gamma_j := r - \delta_j - \sigma_j^2/2 - \lambda\kappa_j - \lambda_j\kappa_{Z_j}, j = 1, 2$. Formula (35) is obtained by using a conditioning argument, whose details are provided in Appendix B, Section 3.

6.3. Jump diffusion model II (asymmetric Laplace distributed jump size). The third model is the bidimensional jump diffusion model studied by Huang and Kou (2006). The difference from the previous jump diffusion model in (34) is that idiosyncratic jump sizes Z_1 and Z_2 are independently and identically distributed according to an asymmetric Laplace distribution $\mathcal{AL}(\alpha_{jj}, \xi_{jj}^2)$ instead of being Gaussian. Macroeconomic shocks N follow a compound Poisson process with intensity λ. Jump sizes $\mathbf{Y}$ are independently and identically distributed as a multivariate asymmetric Laplace distribution $\mathcal{MAL}(\alpha, \Sigma_Y)$, where $\alpha = (\alpha_1, \alpha_2)^{\intercal}$ and

$$\Sigma_{\mathbf{Y}} = \begin{pmatrix} \xi_1^2 & \rho_Y \xi_1 \xi_2 \\ \rho_Y \xi_1 \xi_2 & \xi_2^2 \end{pmatrix}.$$

For a detailed description of the asymmetric Laplace distribution and its properties, see Kotz et al. (2001). In this model the quantities κ_j and $\kappa_{Z_j}, j = 1, 2$ are, respectively,

$$\kappa_j = \frac{1}{1 - \alpha_j - \xi_j^2/2} - 1, \qquad \kappa_{Z_j} = \frac{1}{1 - \alpha_{jj} - \xi_{jj}^2/2} - 1.$$

As discussed by Huang and Kou (2006), the joint characteristic function is $\Phi_T(\mathbf{u}) = e^{i\mathbf{u}^{\intercal}\mathbf{X}(0)} \varphi_T(\mathbf{u})$, where

$$\begin{aligned} \varphi_T(\mathbf{u}) &= \exp\big[T\big(i\mathbf{u}^{\intercal}\gamma - \mathbf{u}^{\intercal}\Sigma\mathbf{u}/2 + \lambda_1/(1 - iu_1\alpha_{11} + u_1^2\xi_{11}^2/2) + \lambda_2/(1 - iu_2\alpha_{22} + u_2^2\xi_{22}^2/2) + \\ &\quad \lambda/(1 - i\mathbf{u}^{\intercal}\alpha + \mathbf{u}^{\intercal}\Sigma_{\mathbf{Y}}\mathbf{u}/2) - \lambda_1 - \lambda_2 - \lambda\big)\big] \end{aligned} \tag{36}$$

and $\Sigma = [\sigma_1^2, \rho\sigma_1\sigma_2; \rho\sigma_1\sigma_2, \sigma_2^2]$, $\gamma_j := r - \delta_j - \sigma_j^2/2 - \lambda\kappa_j - \lambda_j\kappa_{Z_j}, j = 1, 2$.

6.4. Mean-reverting jump diffusion model. The fourth model is a mean-reverting jump diffusion model that generalizes the model proposed by Hambly et al. (2009). For $j = 1, 2$, the spot price process $S_j(t)$ is defined as the exponential of the sum of three components: a deterministic function $f_j(t)$, a Gaussian Ornstein–Uhlenbeck process $X_j(t)$, and a mean-reverting process with a jump component $Y_j(t)$:

$$\begin{aligned} S_j(t) &= \exp\left(f_j(t) + X_j(t) + Y_j(t)\right), \\ dX_j &= -\alpha_j X_j(t)dt + \sigma_j dW_j, \\ dY_j &= -\alpha_j Y_j(t-)dt + J_j^+ dN_j^+ - J_j^- dN_j^-. \end{aligned}$$

The parameter σ_j is strictly positive and W_j is a risk-neutral Brownian motion. We assume a speed of mean reversion $\alpha_j > 0$ for both the diffusion process $X_j(t)$ and the jump process $Y_j(t)$. The two Brownian motions have instantaneous correlation $\rho, |\rho| < 1$ and N_j^+ and N_j^- are Poisson processes with intensity λ_j^+ and λ_j^-, respectively, and describe the positive and negative jump arrivals separately. The terms J_j^+ and J_j^- are independent identically distributed random variables representing the jump size and we assume they are exponentially distributed with parameters $0 < \mu_j^+ < 1$ and $\mu_j^- > 0$, respectively. Assuming independence between the jump processes, we obtain the joint characteristic function

$$\begin{aligned} \Phi_T(\mathbf{u}) \;=\; & \exp\Big[iu_1\left((X_1(0)+Y_1(0))\,e^{-\alpha_1 T} + f_1(T)\right) + iu_2\left((X_2(0)+Y_2(0))\,e^{-\alpha_2 T} + f_2(T)\right) - \\ & \frac{u_1^2\sigma_1^2}{4\alpha_1}\left(1-e^{-2\alpha_1 T}\right) - \frac{u_2^2\sigma_2^2}{4\alpha_2}\left(1-e^{-2\alpha_2 T}\right) - \rho\frac{u_1u_2\sigma_1\sigma_2}{\alpha_1+\alpha_2}\left(1-e^{-(\alpha_1+\alpha_2)T}\right) + \\ & \frac{\lambda_1^+}{\alpha_1}\ln\left(\frac{1-i\mu_1^+u_1e^{-\alpha_1 T}}{1-i\mu_1^+u_1}\right) + \frac{\lambda_2^+}{\alpha_2}\ln\left(\frac{1-i\mu_2^+u_2e^{-\alpha_2 T}}{1-i\mu_2^+u_2}\right) + \\ & \frac{\lambda_1^-}{\alpha_1}\ln\left(\frac{1+i\mu_1^-u_1e^{-\alpha_1 T}}{1+i\mu_1^-u_1}\right) + \frac{\lambda_2^-}{\alpha_2}\ln\left(\frac{1+i\mu_2^-u_2e^{-\alpha_2 T}}{1+i\mu_2^-u_2}\right)\Big]. \end{aligned}$$

6.5. Three-factor stochastic volatility model. The fifth model is the stochastic volatility model discussed by Dempster and Hong (2002) and Hurd and Zhou (2009). The risk-neutral dynamics of the log-price vector $\mathbf{X}(t) = (\ln S_1(t), \ln S_2(t))^\intercal$ are given by

$$\begin{aligned} dX_1 &= (r - \delta_1 - \sigma_1^2/2)dt + \sigma_1\sqrt{v}dW_1, \\ dX_2 &= (r - \delta_2 - \sigma_2^2/2)dt + \sigma_2\sqrt{v}dW_2, \\ dv &= \kappa(\mu - v)dt + \sigma_v\sqrt{v}dW_v, \end{aligned}$$

where

$$\begin{aligned} \mathbb{E}[dW_1dW_2] &= \rho dt, \\ \mathbb{E}[dW_1dW_v] &= \rho_1 dt, \\ \mathbb{E}[dW_2dW_v] &= \rho_2 dt. \end{aligned}$$

The characteristic function is $\Phi_T(\mathbf{u}) = e^{i\mathbf{u}^\intercal\mathbf{X}(0)}\varphi_T(\mathbf{u})$, where

$$\begin{aligned} \varphi_T(\mathbf{u}) \;=\; & \exp\Bigg[\left(\frac{2\zeta(1-e^{-\theta T})}{2\theta-(\theta-\gamma)(1-e^{-\theta T})}\right)v(0) + \\ & i\mathbf{u}^\intercal(r\mathbf{e}-\delta)T - \frac{\kappa\mu}{\sigma_v^2}\left[2\ln\left(\frac{2\theta-(\theta-\gamma)(1-e^{-\theta T})}{2\theta}\right) + (\theta-\gamma)T\right]\Bigg] \end{aligned}$$

and

$$\begin{aligned}\zeta &:= -\frac{1}{2}\big[(\sigma_1^2u_1^2+\sigma_2^2u_2^2+2\rho\sigma_1\sigma_2u_1u_2)+i(\sigma_1^2u_1+\sigma_2^2u_2)\big],\\ \gamma &:= \kappa - i(\rho_1\sigma_1u_1+\rho_2\sigma_2u_2)\sigma_v,\\ \theta &:= \sqrt{\gamma^2-2\sigma_v^2\zeta}.\end{aligned}$$

6.6. VG mixture model. The sixth model is the exponential Lévy model described by Hurd and Zhou (2009). A univariate VG process is a Lévy process with a Lévy characteristic triplet $(0,0,\nu)$, where the Lévy measure is $\nu=\lambda[e^{-a_+x}\mathbf{1}_x>0+e^{-a_-x}\mathbf{1}_x<0]/|x|$ for $\lambda, a_\pm>0$. Here we consider a bivariate VG model driven by three independent univariate VG processes Y_1, Y_2, Y with parameters $\lambda_1,\lambda_2,\lambda_Y$. Choosing $\lambda_1=\lambda_2=(1-\alpha)\lambda, \lambda_Y=\alpha\lambda$, the bivariate log return process $\mathbf{X}(t)=(\ln S_1(t),\ln S_2(t))^\intercal$ is given by the mixture

$$X_1(t)=X_1(0)+Y_1(t)+Y(t),\quad X_2(t)=X_2(0)+Y_2(t)+Y(t).$$

As discussed by Hurd and Zhou (2009), the joint characteristic function is given by $\Phi_T(\mathbf{u})=e^{i\mathbf{u}^\intercal\mathbf{X}(0)}\varphi_T(\mathbf{u})$, where

$$\begin{aligned}\varphi_T(\mathbf{u}) &= \left[1+i\left(\frac{1}{a_-}-\frac{1}{a_+}\right)(u_1+u_2)+\frac{(u_1+u_2)^2}{a_-a_+}\right]^{-\alpha\lambda T}\times\\ &\quad\left[1+i\left(\frac{1}{a_-}-\frac{1}{a_+}\right)u_1+\frac{u_1^2}{a_-a_+}\right]^{-(1-\alpha)\lambda T}\left[1+i\left(\frac{1}{a_-}-\frac{1}{a_+}\right)u_2+\frac{u_2^2}{a_-a_+}\right]^{-(1-\alpha)\lambda T}.\end{aligned}$$

6.7. VG time changed model. The last model we consider is a bivariate VG process with a time change by an independent integrated CIR process. This model was introduced by Ballotta and Bonfiglioli (2012). The parameterization of the Lévy measure used by Ballotta and Bonfiglioli (2012) is

$$\nu(x)=\frac{1}{\kappa|x|}\exp\left[\frac{\theta}{\sigma^2}-|x|\,\frac{\sqrt{\theta^2+2\sigma^2/\kappa}}{\sigma^2}\right].$$

Given the parameterization above, the characteristic function of a VG process is

$$\phi(u)=-\frac{1}{\kappa}\ln\Big(1-iu\theta\kappa+u^2\frac{\sigma^2}{2}\kappa\Big). \tag{37}$$

If $Y_j(t)$, for $j=1,2$ are two independent VG processes with parameters $\sigma_j,\theta_j,\kappa_j$ and $Z(t)$ a third independent VG process with parameters σ_Z,θ_Z, and κ_Z, the authors introduce asset correlations considering the dynamics $G_j(t)=Y_j(t)+a_jZ(t)$, where $a_j\in\mathbb{R}$. The rate of time change of asset j is modeled by a CIR process $v_j(s)=b_jv(t)$, where $b_j>0$ and

$$dv(t)=k(\eta-v(t))dt+\lambda\sqrt{v(t)}dW(t)$$

and $W(t)$ is a Brownian motion common to the whole vector of time changes but independent of the base process $\mathbf{G}(t)=(G_1(t),G_2(t))^\intercal$. The clock of asset j is assumed to be the integrated variance process $V_j(t)=b_jV(t)$, that is,

$$V_j(t)=\int_0^t v_j(s)ds.$$

Considering $B_j(t) = G_j(V_j(t))$, we define the stock price risk-neutral dynamics as

$$S_j(t) = S_j(0)e^{(r-\delta_j)t}\frac{e^{B_j(t)}}{\mathbb{E}[e^{B_j(t)}]}.$$

Assuming that $b_1 < b_2$, we give the joint characteristic function by $\Phi_T(\mathbf{u}) = e^{i\mathbf{u}^\intercal \mathbf{X}(0)}\varphi_T(\mathbf{u})$, where

$$\varphi_T(\mathbf{u}) \quad = \quad \phi_T^V(-ig(u_1,u_2;a_1,a_2,b_1,b_2))e^{i\mathbf{u}^\intercal((r\mathbf{e}-\delta)T-\mathbf{p}_T)},$$

with

$$g(u_1,u_2;a_1,a_2,b_1,b_2) = b_1\phi^{Y_1}(u_1) + b_2\phi^{Y_2}(u_2) + b_1\phi^Z(u_1a_1+u_2a_2) + (b_2-b_1)\phi^Z(u_2a_2),$$

$$\mathbf{p}_T = (\phi_T^V(-ig(-i,0;a_1,a_2,b_1,b_2)), \phi_T^V(-ig(0,-i;a_1,a_2,b_1,b_2)))^\intercal.$$

In the above expression ϕ_T^V is the characteristic function of the integrated CIR process V that we recall below for completeness, while the characteristic functions of Y_1, Y_2, and Z are, respectively, indicated by ϕ^{Y_1}, ϕ^{Y_2}, and ϕ^Z and have the form in equation (37). The characteristic function of the integrated CIR process $V(t)$ is

$$\begin{aligned}
\phi_t^V(u) &= e^{A(u,t)+B(u,t)v(0)} \\
A(u,t) &= \frac{2k\eta}{\lambda^2}\ln\left(\frac{2\zeta(u)e^{\frac{\zeta(u)+k}{2}t}}{(\zeta(u)+k)(e^{\zeta(u)t}-1)+2\zeta(u)}\right) \\
B(u,t) &= \frac{2iu(e^{\zeta(u)t}-1)}{(\zeta(u)+k)(e^{\zeta(u)t}-1)+2\zeta(u)} \\
\zeta(u) &= \sqrt{k^2-2\lambda^2 iu}.
\end{aligned}$$

7. Numerical results

This section discusses numerical results with reference to the models presented. We compute the fair value of spread option contracts, spanning different strike prices, for each model presented in Section 6. Numerical results are reported in Tables 1 to 7. Prices obtained via Monte Carlo simulation are used as a benchmark. To reduce the simulation error, we use the lower bound as a control variate.[2] The number of simulations is chosen depending on the model, as indicated for each table. The columns labeled *C.I. length* gives the length of the 95% mean-centered Monte Carlo confidence interval. In all cases the confidence interval is so small that it allows us to appreciate the accuracy of our lower bound. The lower bound is computed using the formula (27) and is displayed in the column labeled $C_K^{\alpha,k}$. The integral is solved by a Gauss–Kronrod quadrature rule using Matlab's built-in function `quadgk`. Values obtained maximizing the lower bound with respect to α and k are presented in the column labeled $C_K^{\alpha^*,k^*}$. However, we can see that the optimized lower bound does not significantly improve the approximation provided by formula $C_K^{\alpha,k}$.

[2]We rewrite equation (16) as

$$C_K(0) = C_K^{k,\alpha}(0) + e^{-rT}\mathbb{E}\Big[(S_1(T)-S_2(T)-K)^+\Big] - e^{-rT}\mathbb{E}\Big[(S_1(T)-S_2(T)-K)1_{(A)}\Big]^+.$$

We calculate $C_K^{k,\alpha}(0)$ with formula (27) and use Monte Carlo simulation to compute the two expected values, which are highly correlated. The simulation error is thus reduced.

The upper bound is shown in the column labeled $U_K^{N,\Delta K}(0)$ and is computed by setting N and ΔK as indicated for each table. Our numerical experiments show that the upper bound is quite good in all cases, even though it does not achieve the same tightness as the lower bound, even when minimized with respect to N and ΔK. When available, we show the numbers C_K^{HZ} computed by Hurd and Zhou (2009).

For the geometric Brownian motion case, in Table 1, we also present Kirk's approximation formula, the improved lower bound $\hat{C}_K^{\alpha^*,k^*}(0)$, and the Rogers–Shi-type upper bound $U^{RS}(0)$. As noted in the previous section, the lower bound $\hat{C}_K^{\alpha^*,k^*}(0)$ does not significantly improve with respect to the approximation $C_K^{k,\alpha}(0)$. In addition, the upper bound $U^{RS}(0)$, although developed ad hoc for the geometric Brownian motion case, seems to work worse than the more general upper bound $U_K^{N,\Delta K}(0)$.

TABLE 1. Prices for the geometric Brownian motion model for different choices of K. The parameter values are $S_1(0) = 100$, $S_2(0) = 96$, $\rho = 0.5$, $\sigma_1 = 0.2$, $\sigma_2 = 0.1$, $\delta_1 = 0.05$, $\delta_2 = 0.05$, $r = 0.1$, $T = 1.0$, $M = 10^6$, $N = 1000$, and $\Delta K = 0.5$.

K	$C_K^{\alpha,k}$	$C_K^{\alpha^*,k^*}$	$\hat{C}_K^{\alpha^*,k^*}$	$C_K^{Kirk}(0)$	C_K^{HZ}	MC	C.I. length	$U_K^{N,\Delta K}(0)$	$U^{RS}(0)$
0.4	8.312461	8.312461	8.312461	8.312461	8.312461	8.312461	3.128×10^{-8}	8.330379	8.867626
0.8	8.114993	8.114993	8.114993	8.114993	8.114994	8.114994	7.059×10^{-8}	8.132623	8.633288
1.2	7.920819	7.920819	7.920819	7.920819	7.920820	7.920820	1.158×10^{-7}	7.938902	8.410323
1.6	7.729931	7.729931	7.729931	7.729931	7.729932	7.729933	1.896×10^{-7}	7.748035	8.195125
2.0	7.542322	7.542322	7.542322	7.542322	7.542324	7.542324	2.564×10^{-7}	7.560385	7.986151
2.4	7.357982	7.357982	7.357982	7.357982	7.357984	7.357984	3.283×10^{-7}	7.375900	7.782577
2.8	7.176899	7.176899	7.176899	7.176899	7.176902	7.176902	4.081×10^{-7}	7.194528	7.583903
3.2	6.999060	6.999060	6.999060	6.999060	6.999065	6.999065	5.155×10^{-7}	7.017144	7.389794
3.6	6.824452	6.824452	6.824452	6.824452	6.824458	6.824458	6.291×10^{-7}	6.842556	7.200013
4.0	6.653058	6.653058	6.653058	6.653058	6.653065	6.653065	7.217×10^{-7}	6.671121	7.014377

TABLE 2. Prices for jump diffusion model I for different choices of K. The parameter values are $S_1(0) = 100$, $S_2(0) = 96$, $\delta_1 = 0.03$, $\delta_2 = 0.05$, $\sigma_1 = 0.15$, $\sigma_2 = 0.1$, $\rho = 0.5$, $r = 0.1$, $\lambda = 0.2$, $\alpha_1 = 0.06$, $\alpha_2 = 0.03$, $\xi_1 = 0.03$, $\xi_2 = 0.09$, $\rho_y = -0.8$, $\lambda_1 = 0.2$, $\alpha_{11} = 0.02$, $\xi_{11} = 0.06$, $\lambda_2 = 0.1$, $\alpha_{22} = -0.07$, $\xi_{22} = 0.01$, $M = 10^6$, $N = 1000$, and $\Delta K = 0.5$.

K	$C_K^{\alpha,k}$	$C_K^{\alpha^*,k^*}$	MC	C.I. length	$U_K^{N,\Delta K}(0)$
0.4	8.561005	8.561005	8.561006	2.215×10^{-7}	8.584905
0.8	8.333472	8.333472	8.333473	3.514×10^{-7}	8.357044
1.2	8.109743	8.109743	8.109745	6.414×10^{-7}	8.133830
1.6	7.889839	7.889839	7.889841	9.603×10^{-7}	7.913949
2.0	7.673778	7.673778	7.673781	1.135×10^{-6}	7.697841
2.4	7.461575	7.461575	7.461580	1.338×10^{-6}	7.485474
2.8	7.253242	7.253242	7.253249	1.701×10^{-6}	7.276814
3.2	7.048788	7.048788	7.048797	2.468×10^{-6}	7.072875
3.6	6.848219	6.848219	6.848228	2.289×10^{-6}	6.872329
4.0	6.651536	6.651536	6.651548	3.089×10^{-6}	6.675600

TABLE 3. Prices for jump diffusion model II for different choices of K. The parameter values are $S_1(0) = 100$, $S_2(0) = 96$, $\delta_1 = 0.03$, $\delta_2 = 0.05$, $\sigma_1 = 0.15$, $\sigma_2 = 0.1$, $\rho = 0.5$, $r = 0.1$, $\lambda = 0.2$, $\alpha_1 = 0.06$, $\alpha_2 = 0.03$, $\xi_1 = 0.03$, $\xi_2 = 0.09$, $\rho_y = -0.8$, $\lambda_1 = 0.2$, $\alpha_{11} = 0.02$, $\xi_{11} = 0.06$, $\lambda_2 = 0.1$, $\alpha_{22} = -0.07$, $\xi_{22} = 0.01$, $M = 10^6$, $N = 1000$, and $\Delta K = 0.5$.

K	$C_K^{\alpha,k}$	$C_K^{\alpha^*,k^*}$	MC	C.I. length	$U_K^{N,\Delta K}(0)$
0.4	8.585660	8.585660	8.591228	1.591×10^{-4}	8.622334
0.8	8.359561	8.359561	8.365381	1.630×10^{-4}	8.395902
1.2	8.137301	8.137301	8.143190	1.634×10^{-4}	8.174164
1.6	7.918901	7.918901	7.924987	1.665×10^{-4}	7.955787
2.0	7.704377	7.704377	7.710662	1.692×10^{-4}	7.741216
2.4	7.493741	7.493741	7.500078	1.698×10^{-4}	7.530414
2.8	7.287004	7.287004	7.293383	1.704×10^{-4}	7.323346
3.2	7.084171	7.084172	7.090606	1.712×10^{-4}	7.121034
3.6	6.885247	6.885247	6.891644	1.710×10^{-4}	6.922133
4.0	6.690231	6.690231	6.696675	1.713×10^{-4}	6.727070

TABLE 4. Prices for the mean-reverting jump diffusion process for different choices of K. The parameter values are $f_1(T) = \ln(30)$, $f_2(T) = \ln(26)$, $X_1(0) = 0$, $X_2(0) = 0$, $Y_1(0) = 0$, $Y_2(0) = 0$, $\sigma_1 = 0.1$, $\sigma_2 = 0.08$, $\rho = 0.5$, $r = 0.1$, $\alpha_1 = 0.6$, $\alpha_2 = 0.6$, $\lambda_1^+ = 0.025$, $\lambda_1^- = 0.02$, $\lambda_2^+ = 0.03$, $\lambda_2^- = 0.025$, $\mu_1^+ = 0.3$, $\mu_1^- = 0.35$, $\mu_2^+ = 0.3$, $\mu_2^- = 0.37$, $M = 10^6$, $N = 1500$, and $\Delta K = 1$.

K	$C_K^{\alpha,k}$	$C_K^{\alpha^*,k^*}$	MC	C.I. length	$U_K^{N,\Delta K}(0)$
2.0	2.230264	2.230267	2.230267	5.035×10^{-7}	2.295558
2.2	2.083929	2.083933	2.083933	1.166×10^{-6}	2.149442
2.4	1.942230	1.942235	1.942235	1.273×10^{-6}	2.007675
2.6	1.805556	1.805562	1.805562	9.500×10^{-7}	1.869047
2.8	1.674271	1.674278	1.674278	1.442×10^{-6}	1.738926
3.0	1.548706	1.548715	1.548716	2.176×10^{-6}	1.614000
3.2	1.429154	1.429164	1.429164	1.233×10^{-6}	1.494667
3.4	1.315855	1.315867	1.315867	1.292×10^{-6}	1.381300
3.6	1.208999	1.209012	1.209013	2.071×10^{-6}	1.272490
3.8	1.108713	1.108727	1.108728	2.842×10^{-6}	1.173368
4.0	1.015062	1.015077	1.015078	2.570×10^{-6}	1.080355

TABLE 5. Prices for the three-factor stochastic volatility model for different choices of K. The parameter values are $S_1(0) = 100$, $S_2(0) = 96$, $\rho = 0.5$, $\sigma_1 = 1.0$, $\sigma_2 = 0.5$, $\rho_1 = -0.5$, $\rho_2 = 0.25$, $\delta_1 = 0.05$, $\delta_2 = 0.05$, $v_0 = 0.04$, $\kappa = 1.0$, $\mu = 0.04$, $\sigma_v = 0.05$, $r = 0.1$, $T = 1.0$. $M = 10^6$, $N = 1000$, and $\Delta K = 0.5$.

K	$C_K^{\alpha,k}$	$C_K^{\alpha^*,k^*}$	C_K^{HZ}	MC	C.I. length	$U_K^{N,\Delta K}(0)$
2.0	7.548500	7.548500	7.548502	7.548503	1.304×10^{-6}	7.565996
2.2	7.453534	7.453534	7.453536	7.453537	1.246×10^{-6}	7.471050
2.4	7.359379	7.359379	7.359381	7.359382	1.467×10^{-6}	7.376733
2.6	7.266033	7.266033	7.266036	7.266038	1.728×10^{-6}	7.283569
2.8	7.173498	7.173498	7.173501	7.173503	1.836×10^{-6}	7.190568
3.0	7.081771	7.081771	7.081775	7.081776	2.037×10^{-6}	7.099266
3.2	6.990852	6.990852	6.990856	6.990857	1.823×10^{-6}	7.008368
3.4	6.900740	6.900740	6.900745	6.900746	2.261×10^{-6}	6.918094
3.6	6.811434	6.811434	6.811439	6.811441	2.423×10^{-6}	6.828970
3.8	6.722932	6.722932	6.722939	6.722939	2.516×10^{-6}	6.740003
4.0	6.635234	6.635234	6.635241	6.635244	2.980×10^{-6}	6.652730

TABLE 6. Prices for the VG mixture model for different choices of K. The parameter values are $S_1(0) = 100$, $S_2(0) = 96$, $\rho = 0.5$, $a_+ = 20.4499$, $a_- = 24.4499$, $\alpha = 0.4$, $\lambda = 10$, $r = 0.1$, $T = 1.0$. $M = 10^7$, $N = 1000$, and $\Delta K = 0.5$.

K	$C_K^{\alpha,k}$	$C_K^{\alpha^*,k^*}$	C_K^{HZ}	MC	C.I. length	$U_K^{N,\Delta K}(0)$
2.0	9.727443	9.727444	9.727458	9.727496	7.343×10^{-6}	9.913274
2.2	9.629988	9.629990	9.630006	9.630018	5.596×10^{-6}	9.815834
2.4	9.533178	9.533180	9.533200	9.533196	4.294×10^{-6}	9.718898
2.6	9.437015	9.437017	9.437040	9.437025	3.306×10^{-6}	9.622878
2.8	9.341499	9.341501	9.341527	9.341505	2.540×10^{-6}	9.526996
3.0	9.246629	9.246632	9.246662	9.246633	1.946×10^{-6}	9.432460
3.2	9.152407	9.152410	9.152445	9.152409	1.496×10^{-6}	9.338254
3.4	9.058833	9.058837	9.058875	9.058834	1.159×10^{-6}	9.244552
3.6	8.965907	8.965911	8.965954	8.965907	8.913×10^{-7}	9.151769
3.8	8.873628	8.873633	8.873681	8.873629	6.752×10^{-7}	9.059125
4.0	8.781998	8.782003	8.782057	8.781999	5.093×10^{-7}	8.967829

TABLE 7. Prices for the VG time changed model for different choices of K. The parameter values are $S1 = 51$, $S2 = 47$, $M = 10^6$, $T = 1.0$, $v0 = 1.0$, $rf = 0.1$, $a_1 = 0.5971$, $a_2 = 0.7801$ $\sigma_1 = 0.2824$, $\sigma_2 = 0.1849$, $\sigma_Z = 0.3497$, $\delta_1 = 0.018$, $\delta_2 = 0.03$, $\nu_1 = 0.1726$, $\nu_2 = 2.2360$, $\nu_Z = 0.2$, $\theta_1 = -0.1144$, $\theta_2 = 0.0962$, $\theta_Z = -1.0417$, $\lambda = 0.8332$, $k = 1.0992$, $\eta = 1.1275$, $b_1 = 0.2219$, $b_2 = 0.2351$, , $N = 1000$, and $\Delta K = 0.5$.

K	$C_K^{\alpha,k}$	$C_K^{\alpha^*,k^*}$	MC	C.I. length	$U_K^{N,\Delta K}(0)$
2.0	4.946084	4.946121	4.946232	1.647×10^{-5}	5.157113
2.2	4.818943	4.818990	4.819121	1.937×10^{-5}	5.032578
2.4	4.693307	4.693365	4.693515	2.205×10^{-5}	4.906663
2.6	4.569215	4.569286	4.569475	2.621×10^{-5}	4.778981
2.8	4.446705	4.446791	4.446996	2.927×10^{-5}	4.659943
3.0	4.325819	4.325922	4.326171	3.418×10^{-5}	4.536848
3.2	4.206597	4.206720	4.207014	3.890×10^{-5}	4.420232
3.4	4.089081	4.089225	4.089553	4.298×10^{-5}	4.302436
3.6	3.973312	3.973481	3.973867	4.914×10^{-5}	4.183078
3.8	3.859334	3.859530	3.859974	5.530×10^{-5}	4.072572
4.0	3.747190	3.747416	3.747923	6.227×10^{-5}	3.958219

CHAPTER 3

A general semi-closed form basket option pricing formula

One should always generalize.
Carl Jacobi (1804–1851)

Basket options are popular in all kind of financial markets and are becoming increasingly widespread in commodity and energy markets. Basket options are options whose payoff depends on the value of a basket, that is, a portfolio of n assets of financial variables whose values at time t are denoted $S_1(t), \ldots, S_n(t)$. A basket call option gives the holder the right, but not the obligation, to purchase a portfolio of assets at a fixed price K, known as the option's strike price. We consider options of the European type, for which the buyer has the right to exercise the option at the maturity date T. An important subclass of basket options is spread options, where the underlying value is the spread (i.e., the difference) between the prices of two or more financial variables. Spread options are discussed in Chapter 2, which proposes a valuation method for the special case of options on the difference between two asset prices.

Basket options are difficult to price and hedge because the underlying value is a weighted sum of individual asset prices. The problem is similar to the Asian option valuation problem, where the payoff is determined by the average underlying price over some predetermined period of time. Almost all the literature on Asian or basket options pricing assumes the underlying asset prices follow log-normal processes. The famous Black–Scholes formula cannot be applied directly, since the sum of the log-normal random variables is not log-normal. Several approaches have been proposed in the literature to solve the problem, including Monte Carlo simulations, tree-based methods, partial differential equations, and analytical approximations. The last category is the most appealing because most of the other methods are very complex and slow due to the large number of possible state variables. However, we identify two weak points in the existing approximation method literature:

(1) Many methods have limited scope because they require a basket value that is always positive and cannot be applied in the basket spread option valuation.

(2) Few works study a non-Gaussian setting and almost all discuss specific non-Gaussian dynamics. The study of general pricing methods is still underdeveloped.

This chapter presents a lower bound for general processes for the basket option value. The only quantity we need to know explicitly is the joint characteristic function of the log-returns of the assets. Moreover, the basket value is not required to always be positive. The lower bound computation requires optimization of a univariate Fourier inversion and we test the bound on different models in Gaussian and non-Gaussian settings. Numerical examples are discussed and benchmarked against Monte Carlo simulations. In addition, we show an upper bound for general processes. The chapter

outline is as follows: Section 1 reviews the literature on basket option pricing methods. Section 2 discusses a general lower approximation and Section 3 considers a general upper bound. The geometric Brownian motion case is discussed in Section 4 and a non-Gaussian model is shown in Section 5. Finally, Section 6 presents numerical experiments.

1. Basket option pricing: Literature review

Given a vector of weights $\mathbf{w} \in \mathbb{R}^n$, the arithmetic average of the stock prices at time T is

$$A_n(T) = \sum_{k=1}^{n} w_k S_k(T).$$

We assume (but it is not necessary) that $\sum_{k=1}^{n} w_k = 1$. The payoff of a fixed-strike arithmetic basket option depends on the arithmetic average of the prices observed on a given date. The payoff at time T is $(A_n(T) - K)^+$. Here, we use the usual notation x^+ for the positive part of x, that is, $x^+ = \max\{x, 0\}$. The time t no-arbitrage fair price of the basket option is

$$C_K^{\mathbf{w}}(t) = e^{-r(T-t)}\mathbb{E}\left[(A_n(T) - K)^+\right],$$

where the expectation is with respect to a risk-neutral measure and r is the riskless interest rate.

If we assume that the dynamic of the underlying follows a multivariate geometric Brownian motion, several results are available. Curran (1994) proposes a method based on conditioning on the geometric mean, introducing the idea of a conditioning variable and conditional moment matching. Assuming Λ is a random variable correlated with A_n and satisfying $A_n \geq K$, whenever $\Lambda \geq \kappa$ for some constant κ the option price is decomposed into two parts:

$$\mathbb{E}\left[(A_n(T) - K)^+\right] = \mathbb{E}\left[(A_n(T) - K)\, I(\Lambda > \kappa)\right] + \mathbb{E}\left[(A_n(T) - K)^+ I(\Lambda < \kappa)\right].$$

With Λ as the geometric average, the first part can be calculated exactly. The second part can be computed approximately by conditional moment matching method. Rogers and Shi (1995) derive lower and upper bounds for pricing Asian options through conditioning. The lower bound is obtained using a conditioning variable Λ and Jensen's inequality. Since the approach for Asian options can be easily adapted to basket options and vice versa, Thompson (1999) and Beisser (2001) extend to the basket option valuation the idea of Rogers and Shi (1995) and study the bound

$$\mathbb{E}\left[(A_n(T) - K)^+\right] \geq \mathbb{E}\left[(\mathbb{E}\left[A_n(T)\,|\Lambda\right] - K)^+\right]. \tag{38}$$

The approximation in formula (38) is analytically computable under our assumptions. It is a lower bound but it turns out to be very close to the true option value in many practical situations. Rogers and Shi (1995) also give an upper bound to the true option value, which was later improved by Nielsen and Sandmann (2003) as

$$\mathbb{E}\left[(A_n(T) - K)^+\right] \leq \mathbb{E}\left[(\mathbb{E}\left[A_n(T)\,|\Lambda\right] - K)^+\right] + \frac{1}{2}\mathbb{E}\left[\mathrm{var}(A_n(T)\,|\Lambda) I(\Lambda < \kappa)\right]^{1/2} \mathbb{E}\left[I(\Lambda < \kappa)\right]^{1/2}.$$

Other bounds to the true option price are proposed in the literature using comonotonicity theory. Dhaene et al. (2002a) and Dhaene et al. (2002b) introduced the concept of comonotonicity and discuss comonotonic lower and upper bounds. Vyncke et al. (2004) propose a two-moment matching approximation with a convex combination of the comonotonic lower and upper bounds for Asian

options while Vanmaele et al. (2004) suggest a similar approximation for basket options. Deelstra et al. (2004) develop a general framework for pricing baskets and Asian options via conditioning and derive lower and upper bounds based on comonotonic risks. Further extensions and applications are discussed by Lord (2006).

Other authors have tried to approximate the basket using the moment matching method. The idea is to approximate the payoff as

$$\mathbb{E}\left[\left(A_n\left(T\right)-K\right)^+\right] \approx \mathbb{E}\left[\left(\hat{A}_n\left(T\right)-K\right)^+\right],$$

where $\hat{A}_n\left(T\right)$ is a random variable with a suitable distribution, chosen to be "close" to the distribution of $A_n\left(T\right)$. For example, Gentle (1993) approximates the arithmetic average in the basket payoff by a geometric average. The fact that a geometric average of log-normal random variables is again log-normally distributed allows for a Black–Scholes-type valuation formula for pricing the approximating payoff. Levy (1992) approximates the distribution of the basket by a log-normal distribution such that its first two moments coincide with those of the original distribution of the weighted sum of the stock prices. Huynh (1993) applies the Edgeworth expansion method proposed by Turnbull and Wakeman (1991) to basket option valuation for Asian options. Milevsky and Posner (1998a) use the reciprocal gamma distribution as an approximation for the distribution of the basket. The motivation is the fact that the distribution of correlated log-normally distributed random variables converges to a reciprocal gamma distribution as the dimension of the basket increases. Milevsky and Posner (1998b) use distributions from the Johnson (1949) family as state–price densities to match the higher moments of distribution of the arithmetic mean. Ju (2002) considers a Taylor expansion of the ratio of the characteristic function of the arithmetic average with that of the approximating log-normal random variable around zero volatility. Krekel et al. (2004) compare the performance of certain pricing methods, concluding that the approximations of Ju (2002) and Beisser (2001) are the most accurate in the geometric Brownian motion setting when $w_k > 0$ for $k = 1, \ldots, n$, although the methods tend to slightly overprice and underprice, respectively.

Many of the methods listed above have limited validity or scope. They may require a basket value that is always positive so they cannot be applied in the spread option valuation. Moreover, they may not identify the effect of each individual volatility or pairwise correlation on the multi-asset option price or its hedge ratios. To overcome these issues, Alexander and Venkatramanan (2011) derive a general analytic approximation for pricing basket options expressing each option's price as a sum of the prices of various compound exchange options, each with different pairs of subordinate multi- or single-asset options. The underlying asset prices are assumed to follow log-normal processes, although their results can be extended to certain other price processes. The case of a basket where not all the assets have a positive weight ($w_k < 0$ for some k) is discussed by Borovkova et al. (2007) and Deelstra et al. (2010) in a geometric Brownian motion setting. Borovkova et al. (2007) approximates the basket distribution using a generalized family of log-normal distributions. This approximation copes with negative basket values as well as the negative skewness of the basket distribution and provides closed formulas for the option price and Greeks. Deelstra et al. (2010) develop approximations formulae based on comonotonicity theory and moment matching methods for spread options, basket spread options, and Asian basket spread options. In addition, they compare the relative performances of several methods and explain how to choose the best approximation technique as a function of spread characteristics. The authors conclude that the shifted log-normal moment matching method of Borovkova et al. (2007) and their hybrid

moment matching method based on the so-called improved comonotonic upper bound (ICUB) are the two best-performing methods for basket spread option pricing. The ICUB-based moment matching method seems to be the best method in the more general case of Asian basket spread options.

Few results are available in the non-Gaussian setting. Flamouris and Giamouridis (2007) propose the use of a simplified jump process, namely, Bernoulli jump process, to develop approximate basket option valuation formulas. Xu and Zheng (2009) show that a lower bound similar to that of Rogers and Shi (1995) can also be calculated exactly in a special jump diffusion model with constant volatility and two types of Poisson jumps (systematic and idiosyncratic jumps). An asymptotic expansion approximation and a lower bound to basket option values for local volatility jump diffusion models are studied by Xu and Zheng (2010a,b), respectively. However, it would be useful to have a general enough pricing method. One could thus change the price dynamic without changing the pricing method. Lower and upper bounds based on comonotonicity theory are theoretically applicable to general dynamics, but research of such methods outside the geometric Brownian motion setting is still in its early stage. Hurd and Zhou (2009) propose a general pricing method applicable to all stochastic dynamics, provided the joint characteristic function of the log-underlying is known. Their pricing method is based on an explicit formula for the Fourier transform of the spread option payoff in terms of the gamma function. Hurd and Zhou (2009) propose their method for a two-dimensional spread option and describe how to generalize their method to following multidimensional payoff

$$(S_0(T) - S_1(T) - \cdots - S_n(T) - K)^+.$$

The main drawback of this method is that it needs an n-dimensional fast Fourier transform (FFT) to price an n-dimensional spread option. The next section derives a lower bound for the arithmetic basket option value for general dynamics, provided the joint characteristic function of the log-underlying and geometric average are known. Our method is very simple and requires optimization of a one-dimensional Fourier inversion formula, as opposed to the n-dimensional FFT of Hurd and Zhou (2009), regardless of basket dimension.

2. The lower bound

This section derives a lower bound formula for the arithmetic basket option in terms of its Fourier transform. If we define $\mathcal{A} = \{\omega \in \Omega : A_n(T) > K\}$, the value of the fixed-strike basket option is

$$C_K^{\mathbf{w}}(t) = e^{-r(T-t)}\mathbb{E}_t\left[(A_n(T) - K)^+\right] = e^{-rT}\mathbb{E}\left[(A_n(T) - K)\, I(\mathcal{A})\right] \tag{39}$$

$$\geq e^{-rT}\mathbb{E}\left[(A_n(T) - K)\, I(\mathcal{G})\right]^+ = \hat{C}_K^{\mathbf{w}}(t) \tag{40}$$

for any event set $\mathcal{G} \in \Omega$, since $A_n(T) \leq K$ for $\omega \in \mathcal{G} - \mathcal{A}$. Thus, the choice of an event set $\mathcal{G}$ gives us a lower bound for the option price. We choose the set $\mathcal{G}$ depending on the geometric average of the underlying prices,

$$G_n(T) = (\Pi_{k=1}^n S_k(T)^{w_k})^{\frac{1}{\Sigma_{k=1}^n w_k}} = \Pi_{k=1}^n S_k(T)^{w_k}.$$

Define $Y_n(T) = \ln G_n(T)$. We choose $\mathcal{G} = \{\omega : Y_n(T) > \kappa\}$. This choice, which is intuitive and technically convenient, also turns out to be very accurate. We address how to choose the parameter κ shortly. Note that we introduced the positive part operator in (40); otherwise the lower bound

to the option price could be negative. The term $X_k(T)$ is denoted the log-return over the period $[t,T]$:

$$X_k(T) = \ln\left(\frac{S_k(T)}{S_k(t)}\right).$$

We assume that the risk-neutral joint characteristic function of the n stock returns is exponential affine:

$$\mathbb{E}\left[e^{i\sum_{k=1}^{n}\gamma_k X_k(T)}\right] = e^{\langle \mathbf{A}(\boldsymbol{\gamma},\Delta),\mathbf{X}(t)\rangle + B(\boldsymbol{\gamma},\Delta)},$$

where $\boldsymbol{\gamma} = [\gamma_1, \gamma_2, ..., \gamma_n]'$ and $\mathbf{A}$ and $\mathbf{X}$ are n-dimensional vectors, B is a scalar, $\Delta = T - t$, and $\langle .,. \rangle$ stands for the inner product. As seen shortly, we are interested in finding the joint characteristic function of the log-underlying and log-geometric average. Simple algebra shows that

$$Y_n(T) = \sum_{k=1}^{n} w_k X_k(T) + Y_n(t),$$

so the joint characteristic function of the log-returns and the log-geometric average is

$$\begin{aligned} \Phi_T(\gamma_0, \boldsymbol{\gamma}, \mathbf{w}) &= \mathbb{E}_t\left[e^{i\sum_{k=1}^{n}\gamma_k X_k(T) + i\gamma_0 Y_n(T)}\right] \\ &= \mathbb{E}_t\left[e^{i\sum_{k=1}^{n}(\gamma_k + w_k\gamma_0) X_k(T) + i\gamma_0 Y_n(t)}\right] \\ &= e^{\langle \mathbf{A}(\boldsymbol{\gamma}+\gamma_0\mathbf{w},\Delta),\mathbf{X}(t)\rangle + B(\boldsymbol{\gamma}+\gamma_0\mathbf{w},\Delta) + i\gamma_0 Y_n(t)} \end{aligned} \tag{41}$$

and $\boldsymbol{\gamma} + \gamma_0\mathbf{w}$ is the vector with components $\gamma_k + \gamma_0 w_k$. In particular, the characteristic function of the log-geometric average is given by $\Phi_T(\gamma_0, \mathbf{0}, \mathbf{w})$. We now proceed to calculate the Fourier transform of (40) with respect to κ.

Proposition 3. *The lower bound of the basket option value $\hat{C}_K^{\mathbf{w}}(t)$ is given in terms of a Fourier inversion formula as*

$$\hat{C}_K^{\mathbf{w}}(t) = \max_{\kappa}\left(e^{-\delta\kappa - r(T-t)}\frac{1}{\pi}\int_0^{+\infty} e^{-i\gamma\kappa}\Psi(\gamma;\delta)d\gamma\right)^+, \tag{42}$$

where

$$\Psi(\gamma;\delta) = \frac{1}{i\gamma+\delta}\left[\sum_{k=1}^{n} w_k S_k(t)\,\Phi_T(\gamma - i\delta, -i\mathbf{e}_k, \mathbf{w}) - K\Phi_T(\gamma - i\delta, \mathbf{0}, \mathbf{w})\right]. \tag{43}$$

Proof: See Appendix C, Section 1.

Note that the dumping factor $\exp(\delta\kappa)$ is introduced in (42) to ensure the existence of the Fourier transform, as Carr and Madan (2000) does. Formula (43) indicates with $\mathbf{e}_k$ the vector $(0,\ldots,0,1,0,\ldots,0)^\intercal$, with 1 in the kth position. If the characteristic function $\Phi_T(\mathbf{u})$ is known analytically, then the Fourier transform of the lower bound can be expressed in closed form as well in terms of the complex function $\Psi(\gamma;\delta)$. The integral in (42) can be easily computed using standard numerical quadratures (`NIntegrate` in Mathematica or `quadgk` in Matlab) or via an FFT algorithm and the target lower bound is obtained by maximization.

To determine the optimal value of κ, we differentiate the argument of the positive part in (42) with respect to κ and then search for a critical point equating it with zero. The maximum is obtained for $\kappa = \kappa^*$ such that

$$\int_0^{+\infty} (i\gamma + \delta) e^{-i\gamma\kappa^*} \Psi(\gamma; \delta) d\gamma = 0$$

and can be computed with a numerical search. Alternatively, we can use the FFT algorithm proposed by Carr and Madan (2000). The FFT output is a finite number of option prices at equally spaced values for the parameter κ. Given (42), we compute the Fourier inverse with respect to k via the FFT and we choose the maximum value as a lower bound to the price of the basket.

3. The upper bound

To control the error of the approximation in (42), we provide here an estimate of an upper bound of the basket option price. Consider the quadratic payoff

$$Q(T) = \frac{1}{2} \left(A_n(T) - L \right)^2 .$$

Given the moments and the mixed moments of the asset price vector $\mathbf{S}(T)$, the no-arbitrage price $Q(t)$ of the quadratic payoff is easy to compute:

$$\begin{aligned} Q(t) \quad = \quad & \frac{e^{-r(T-t)}}{2} \left(\sum_{k=1}^{n} w_k^2 \mathbb{E}[S_k^2(T)] + 2 \sum_{k=1}^{n} \sum_{j<k}^{n} w_k w_j \mathbb{E}[S_k(T) S_j(T)] - \right. \\ & \left. 2L \sum_{k=1}^{n} w_k \mathbb{E}[S_k(T)] + L^2 \right) . \end{aligned} \tag{44}$$

Consider now the functions

$$\pi(x) = \Delta K \sum_{j=1}^{N_c} (x - \Delta K(j - 0.5) + L)^+ + \Delta K \sum_{j=1}^{N_p} (-x - \Delta K(j + 0.5) + L)^+,$$

where $\Delta K > 0$ and $N_c, N_p \in \mathbb{N}^+$. We observe that the function $\pi(x)$ and the function $q(x) = \frac{1}{2}(x - L)^2$ are tangent in $N_c + N_p + 1$ points, exactly in $x_j = L + j\Delta K$ for $j = -N_p, \ldots, N_c$, and moreover $q(x) \geq \pi(x)$. This is shown in Figure 1. If we set $x = A_n(T)$, $\pi(x)$ is nothing more than a portfolio of call and put options on the basket. Strikes vary and equal $K_j^c = \Delta K(j - 0.5) - L$ for call options and $K_j^p = L - \Delta K(j - 0.5)$ for put options. Each option is held for an amount equal to ΔK. A put option on a basket with weights $\mathbf{w}$ and strike K is equal to a call option on a basket with weights $-\mathbf{w}$ and strike $-K$. So, if we indicate with $C_K^{\mathbf{w}}(t)$ the value of a call option on a basket with weights $\mathbf{w}$ and strike K, the fair value of portfolio $\Pi(t)$ is

$$\Pi(t) = \Delta K \left(\sum_{j=1}^{N_c} C_{K_j^c}^{\mathbf{w}}(t) + \sum_{j=1}^{N_p} C_{-K_j^p}^{-\mathbf{w}}(t) \right)$$

and clearly we must have $Q(t) \geq \Pi(t)$, $Q(t)$ being the fair value of the payoff $q(\sum_{k=1}^{n} w_k S_k(T))$. Suppose we are interested in pricing a basket option having strike $K_{\bar{j}}$, with $K_{\bar{j}} \in K_1^c, \cdots, K_N^c$. We

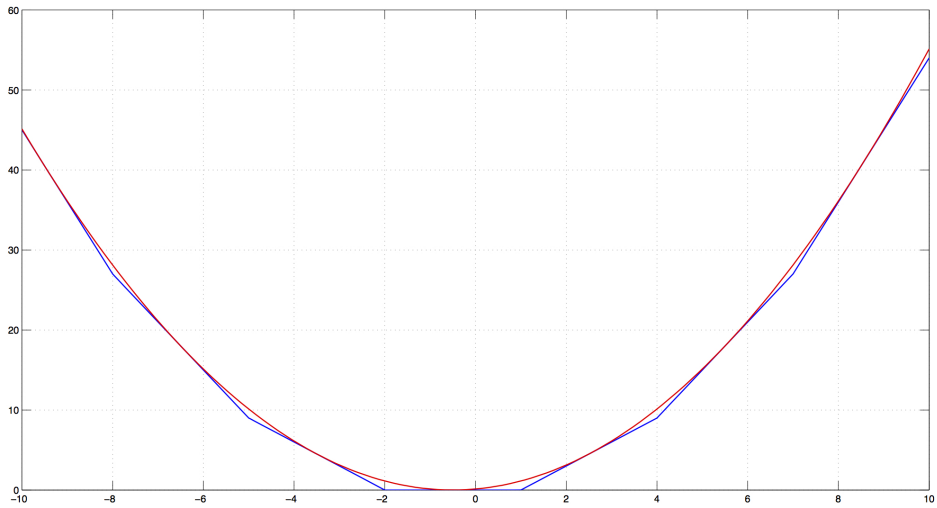

FIGURE 1. Comparison of the payoff $Q(T)$ (red line) and a sub-replicating strategy (blue line). Here $x = A_n(T)$.

can write

$$Q(t) \geq \Pi(t) = \Delta K \left(\sum_{j \neq \bar{j}, j=1}^{N_c} C^{\mathbf{w}}_{K^c_j}(t) + \sum_{j=1}^{N_p} C^{-\mathbf{w}}_{-K^p_j}(t) + C^{\mathbf{w}}_{K_{\bar{j}}}(t) \right).$$

Rearranging terms, it follows that an upper bound for the basket option is given by

$$C^{\mathbf{w}}_{K_{\bar{j}}}(t) \leq U_{K_{\bar{j}}}(t) := \frac{Q(t)}{\Delta K} - \sum_{j \neq \bar{j}, j=1}^{N_c} C^{\mathbf{w}}_{K^c_j}(t) - \sum_{j=1}^{N_p} C^{-\mathbf{w}}_{-K^p_j}(t).$$

The computation of the upper bound $U_K(t)$ requires the value of the deal $Q(t)$, given in formula (44), and the pricing of $N_c + N_p - 1$ basket option contracts, which can be easily accomplished by the lower bound approximation in formula (42). The choice of the parameter L is arbitrary, except for the fact that we must guarantee $K_{\bar{j}} \in K^c_1, \cdots, K^c_{N_c}$.

4. The geometric Brownian motion case

This section discusses in more detail the geometric Brownian motion case. It shows the joint characteristic function involved in formula (42), explicitly computes formula (40), and suggests a starting point for the maximization procedure.

We consider a multivariate Black–Scholes model. The dynamics are given by

$$d \begin{pmatrix} S_1(t) \\ \vdots \\ S_n(t) \end{pmatrix} = Diag(\mathbf{S}(t)) \left((r\mathbf{1} - \mathbf{q})dt + \sqrt{\Sigma} d\mathbf{W}(t) \right), \tag{45}$$

where r is the risk-free rate, $\mathbf{q}$ is the vector of dividend yields for each asset, $\mathbf{1}$ is a vector whose entries are all equal to one, Σ is the variance–covariance matrix, and $\mathbf{W}$ is an n-dimensional Brownian motion. The risk-neutral joint characteristic function of the n stock returns in the geometric Brownian motion case is

$$\mathbb{E}\left[e^{i\langle\boldsymbol{\gamma},\mathbf{X}(T)\rangle}\right] = e^{i\boldsymbol{\gamma}^\intercal\mathbf{m}-\frac{1}{2}\boldsymbol{\gamma}^\intercal\Sigma\boldsymbol{\gamma}(T-t)}, \tag{46}$$

where

$$\mathbf{m} = \left(r\mathbf{1} - \mathbf{q} - \frac{1}{2}Vec(\Sigma_{ii})\right)(T-t). \tag{47}$$

We are interested in the computation of the joint characteristic function of the log-returns and the log-geometric average, as in formula (41),

$$\mathbb{E}\left[e^{i\langle\boldsymbol{\gamma},\mathbf{X}(T)\rangle+i\gamma_0 Y_n(T)}\right] = \mathbb{E}\left[e^{i\langle\boldsymbol{\gamma},\mathbf{X}(T)\rangle+i\gamma_0(\langle\mathbf{w},\mathbf{X}(T)\rangle+Y_n(t))}\right] = e^{i\gamma_0 Y_n(t)}\mathbb{E}\left[e^{i(\boldsymbol{\gamma}^\intercal+\gamma_0\mathbf{w}^\intercal)\mathbf{X}(T)}\right].$$

Thus, in the geometric Brownian motion case, the solution is

$$\Phi_T(\gamma_0,\boldsymbol{\gamma},\mathbf{w}) = e^{i\gamma_0 Y_n(t)+i(\boldsymbol{\gamma}^\intercal+\gamma_0\mathbf{w}^\intercal)\mathbf{m}-\frac{1}{2}(\boldsymbol{\gamma}^\intercal+\gamma_0\mathbf{w}^\intercal)\Sigma(\boldsymbol{\gamma}+\gamma_0\mathbf{w})(T-t)}. \tag{48}$$

Formula (48) can be used to compute the lower bound as in Proposition 3; however, in the geometric Brownian motion setting, the formula (40) can be explicitly computed as a function of the parameter κ. We now show this result.

Let us introduce the notation

$$\ln(\mathbf{S}(t)) = \begin{pmatrix} \log S_1(t) \\ \vdots \\ \log S_n(t) \end{pmatrix}.$$

We consider the set

$$\begin{aligned} \mathcal{G} &= \{\omega : Y_n(T) > \kappa\} \\ &= \left\{\omega : \mathbf{w}^\intercal\left(\ln(\mathbf{S}(t)) + \left(r\mathbf{1} - \mathbf{q} - \frac{1}{2}Vec(\Sigma_{ii})\right)(T-t) + \sqrt{\Sigma}\mathbf{W}(T-t)\right) > \kappa\right\}. \end{aligned}$$

We see that $w^\intercal\sqrt{\Sigma}\mathbf{W}(T-t)$ has the same distribution as a univariate Brownian motion $\sigma^* W^*(T-t)$, where $\sigma^* = \sqrt{\mathbf{w}^\intercal\Sigma\mathbf{w}}$. Considering $\mathbf{m}$ as in formula (47), we can write the set $\mathcal{G}$ as

$$\mathcal{G} = \left\{\omega : Z > d = \frac{\kappa - \mathbf{w}^\intercal(\ln(\mathbf{S}(t)) + \mathbf{m})}{\sigma^*\sqrt{T-t}}\right\},$$

where Z is a standard normal random variable. We can write the expectation in (40) as

$$\begin{aligned} \mathbb{E}\left[(A_n(T) - K)I(\mathcal{G})\right]^+ &= \mathbb{E}\left[\mathbb{E}\left[A_n(T) - K|\mathcal{G}\right]|(\mathcal{G})\right]^+ \\ &= \mathbb{E}\left[\mathbb{E}\left[A_n(T) - K|Z\right]I(Z > d)\right]^+. \end{aligned}$$

Conditionally to the random variable Z, the vector $\mathbf{W}$ is distributed like a multivariate normal with mean $\boldsymbol{\mu}$ and variance V, with their elements defined for $k, j = 1, \ldots, n$ as

$$\mu_k = Za_k\sqrt{T-t}, \quad V_{kj} = (T-t)(\rho_{kj} - a_k a_j), \quad a_k = \frac{\sum_{j=1}^n w_j\rho_{kj}\sqrt{\Sigma_{jj}}}{\sigma^*}, \quad \rho_{kj} = \frac{\Sigma_{kj}}{\sqrt{\Sigma_{kk}\Sigma_{jj}}}$$

and we indicate with Σ_{kj} the element of Σ in position (k,j). Due to this fact, $\mathbf{S}(T)|Z$ follows a multivariate log-normal $\mathcal{MLN}(\hat{\boldsymbol{\mu}},\hat{V})$, where, for $k,j=1,\ldots,n$,

$$\hat{\mu}_k = \ln S_k(t) + (r - q_k - \Sigma_{kk}/2)(T-t) + a_k\sqrt{\Sigma_{kk}(T-t)}Z,$$
$$\hat{V}_{kj} = (T-t)\sqrt{\Sigma_{kk}\Sigma_{jj}}(\rho_{kj} - a_k a_j).$$

We can now compute the inner expectation of the payoff, using the log-normal distribution properties

$$\begin{aligned} & \mathbb{E}\left[\mathbb{E}\left[A_n(T) - K|Z\right]1_{(Z\geq d)}\right]^+ \\ = \quad & \mathbb{E}\left[\left(\sum_{k=1}^n w_k e^{\ln S_k(t)+(r-q_k 1-\Sigma_{kk}a_k^2/2)(T-t)+a_k\sqrt{\Sigma_{kk}(T-t)}Z} - K\right) I\left(Z\geq d\right)\right]^+ . \end{aligned}$$

We solve the above expectation by using the partial expectation property of the log-normal distribution. Discounting and maximizing with respect to κ, we obtain the lower bound

$$\hat{C}_K^{\mathbf{w}}(t) = \max_{\kappa} e^{-r(T-t)}\left(\sum_{k=1}^n w_k S_k(t) e^{(r-q_k)(T-t)}\mathcal{N}(a_k\sqrt{\Sigma_{kk}(T-t)} - d) - K\mathcal{N}(-d)\right)^+ . \tag{49}$$

We indicate with $\mathcal{N}(\cdot)$ the standard normal distribution function. The formula above still depends on maximization with respect to the parameter κ, involved in the definition of d. Maximization must be carried out by a numerical search, equating to zero the first derivative with respect to κ. We need to solve the equation

$$\sum_{k=1}^n w_k S_k(t) e^{(r-q_k)(T-t)}\phi(a_k\sqrt{\Sigma_{kk}(T-t)} - d) - K\phi(-d) = 0, \tag{50}$$

where we indicate with $\phi(\cdot)$ the standard normal density function. Using a linearization argument, we can provide the starting point κ^{start} of the numerical search. We approximate the term $\phi(a_k\sqrt{\Sigma_{kk}(T-t)} - d)$ in formula (50) with a first-order Taylor expansion centered at $-d$,

$$\phi(a_k\sqrt{\Sigma_{kk}(T-t)} - d) = \phi(-d) + a_k\sqrt{\Sigma_{kk}(T-t)}\phi'(-d) = \phi(-d) + da_k\sqrt{\Sigma_{kk}(T-t)}\phi(-d),$$

obtaining

$$\sum_{k=1}^n w_k S_k(t) e^{(r-q_k)(T-t)}\left(1 + da_k\sqrt{\Sigma_{kk}(T-t)}\right) - K = 0.$$

Substituting the definition of d and rearranging terms, it is easy to obtain the following approximation for the value of κ in which the option price is maximum:

$$\kappa^{start} = \sigma^* \frac{\sum_{k=1}^n w_k S_k(t) e^{(r-q_k)(T-t)} - K}{\sum_{k=1}^n w_k a_k\sqrt{\Sigma_{kk}} S_k(t) e^{(r-q_k)(T-t)}} + \sum_{k=1}^n w_k\left(\ln S_k(t) + \left(r - q_k - \frac{\Sigma_{kk}}{2}\right)(T-t)\right).$$

5. A non-Gaussian stock price model

This section presents an example of a non-Gaussian multidimensional stock price model. We generalize the jump diffusion process with an asymmetric Laplace distributed jump size (discussed in Chapter 2, Section 6) to the multidimensional case.

The components of the stock price vector, for $k = 1, \ldots, n$, have the form

$$S_k(t) = S_k(0) \exp\left[\left(r - q_k - \frac{\sigma_k^2}{2} - \lambda\kappa_k - \lambda_k\kappa_{Z_k}\right)t + \sigma_k W_k(t) + \sum_{m_Z=1}^{N_k(t)} Z_k(m_Z) + \sum_{m_Y=1}^{N(t)} Y_k(m_Y)\right], \tag{51}$$

where $\sigma_k > 0$, for $k = 1, \ldots, n$, and W_k, W_j are risk-neutral Brownian motions with instantaneous correlation $\rho_{kj}, |\rho| < 1$, for $k, j = 1, \ldots, n$. In addition, $\sum_{m_Z=1}^{N_k(t)} Z_k(m_Z)$, for $k = 1, \ldots, n$, are n univariate compound Poisson processes driven by the Poisson processes N_k with intensity rate λ_k. This jump component is unique to each stock and describes the idiosyncratic shocks for that particular asset only. The idiosyncratic jump sizes Z_k are independently and identically distributed according to an asymmetric Laplace distribution $\mathcal{AL}(\alpha_{kk}, \xi_{kk}^2)$. The model also allows for macroeconomic shocks in the expression

$$\sum_{m_Y=1}^{N(t)} \mathbf{Y}(m_Y) = \left(\sum_{m_Y=1}^{N(t)} Y_1(m_Y), \ldots, \sum_{m_Y=1}^{N(t)} Y_n(m_Y)\right)^{\intercal},$$

which is a n-dimensional compound Poisson process with intensity rate λ. Under the risk-neutral measure $\mathbb{Q}$ the jump sizes $\mathbf{Y}$ are assumed to be independently and identically distributed according to a multivariate asymmetric Laplace distribution $\mathcal{MAL}(\alpha, \Sigma_Y)$, where $\alpha = (\alpha_1, \ldots, \alpha_n)^{\intercal}$ and $\Sigma_{\mathbf{Y}}$ is an $n \times n$ matrix whose elements are defined as

$$(\Sigma_{\mathbf{Y}})_{k,j} = \xi_k \xi_j \rho_{kj}^Y, \qquad kj = 1, \ldots, n.$$

Finally, the quantities κ_k and $\kappa_{Z_k}, k = 1, \ldots, n$, in (51) are, respectively,

$$\kappa_k = \int_{\mathbb{R}^2} [e^{y_k} - 1] m_{\mathbb{Q}}(dy) = \int_{\mathbb{R}} [e^{y_k} - 1] m_{\mathbb{Q}}(dy_k) = \frac{1}{1 - \alpha_k - \xi_k^2/2} - 1,$$

$$\kappa_{Z_k} = \int_{\mathbb{R}} [e^{z_k} - 1] m_{\mathbb{Q}}(dz_k) = \frac{1}{1 - \alpha_{kk} - \xi_{kk}^2/2} - 1.$$

The joint characteristic function of the log-returns is

$$\begin{aligned} \mathbb{E}\left[e^{i\langle \boldsymbol{\gamma}, \mathbf{X}(T)\rangle}\right] &= \exp\Bigg[(T-t)\Bigg(i\boldsymbol{\gamma}^{\intercal}\boldsymbol{\eta} - \boldsymbol{\gamma}^{\intercal}\Sigma\boldsymbol{\gamma}/2 + \frac{\lambda}{1 - i\boldsymbol{\gamma}^{\intercal}\alpha + \boldsymbol{\gamma}^{\intercal}\Sigma_{\mathbf{Y}}\boldsymbol{\gamma}/2} - \lambda + \\ &\qquad \sum_{k=1}^{n}\left(\frac{\lambda_k}{1 - i\gamma_k\alpha_{kk} + \gamma_k^2\xi_{kk}^2/2} - \lambda_k\right)\Bigg)\Bigg], \end{aligned} \tag{52}$$

where $(\Sigma)_{k,j} = \sigma_k\sigma_j\rho_{k,j}$ and $\eta_k := r - q_k - \sigma_k^2/2 - \lambda\kappa_k - \lambda_k\kappa_{Z_k}, k = 1, \ldots, n$.

We are interested in the computation of the joint characteristic function of the log-returns and the log-geometric average, as in formula (41):

$$\mathbb{E}\left[e^{i\langle \boldsymbol{\gamma}, \mathbf{X}(T)\rangle + i\gamma_0 Y_n(T)}\right] = \mathbb{E}\left[e^{i\langle \boldsymbol{\gamma}, \mathbf{X}(T)\rangle + i\gamma_0(\langle \mathbf{w}, \mathbf{X}(T)\rangle + Y_n(t))}\right] = e^{i\gamma_0 Y_n(t)}\mathbb{E}\left[e^{i(\boldsymbol{\gamma}^{\intercal} + \gamma_0\mathbf{w}^{\intercal})\mathbf{X}(T)}\right].$$

Thus the solution is

$$\begin{aligned}\Phi_T(\gamma_0,\boldsymbol{\gamma},\mathbf{w}) &= \exp\Bigg[i\gamma_0 Y_n(t)+(T-t)\Bigg(i\left(\boldsymbol{\gamma}^\intercal+\gamma_0\mathbf{w}^\intercal\right)\boldsymbol{\eta}-\left(\boldsymbol{\gamma}^\intercal+\gamma_0\mathbf{w}^\intercal\right)\Sigma\left(\boldsymbol{\gamma}+\gamma_0\mathbf{w}\right)/2+\\ &\quad \frac{\lambda}{1-i\left(\boldsymbol{\gamma}^\intercal+\gamma_0\mathbf{w}^\intercal\right)\alpha+\left(\boldsymbol{\gamma}^\intercal+\gamma_0\mathbf{w}^\intercal\right)\Sigma_{\mathbf{Y}}\left(\boldsymbol{\gamma}+\gamma_0\mathbf{w}\right)/2}-\lambda+\\ &\quad \sum_{k=1}^{n}\left(\frac{\lambda_k}{1-i\left(\gamma_k+\gamma_0 w_k\right)\alpha_{kk}+\left(\gamma_k+\gamma_0 w_k\right)^2\xi_{kk}^2/2}-\lambda_k\right)\Bigg)\Bigg]. \end{aligned} \tag{53}$$

6. Numerical results

In this section we discuss some numerical results with reference to the models presented. We first examine the geometric Brownian motion case, comparing the performance of our method to that of other methods in the literature. Krekel et al. (2004) compare the performance of the pricing methods proposed by Levy (1992), Gentle (1993), Milevsky and Posner (1998a,b), Beisser (2001), and Ju (2002). They conclude that the approximations of Ju (2002) and Beisser (2001) are the most accurate in the geometric Brownian motion setting when $w_k > 0$ for $k = 1, \ldots, n$, although they tend to slightly overprice and underprice, respectively. We reproduce experiments of Krekel et al. (2004) in Tables 1 to 5. Each table shows the values for $\hat{C}_K^{\mathbf{w}}(t)$ computed by using our pricing formula with the results obtained by Krekel et al. (2004) with the methods of Ju (2002) and Beisser (2001). We also compute a benchmark for the valuation using a Monte Carlo simulation with 10^6 simulation trials and show the length of the computed mean centered 95% confidence interval. Finally, we show the results for the upper bound $U_K(t)$ proposed in Section 3. The upper bound is obtained by setting $N_c = 100$ and $N_p = 0$ (the basket cannot take negative values in these experiments). The parameter ΔK is set to minimize the upper bound, using a numeric search. We denote the matrix Σ in formula (45) as $(\Sigma)_{kj} = \rho_{kj}\sigma_k\sigma_j$ and the default model parameters are

$$T-t=5.0, \quad r=0, \quad n=4, \quad K=100,$$
$$S_k(t)=100 \quad q_k=0 \quad \sigma_k=40\%, \quad w_k=0.25 \quad \text{for} \quad k=1,\ldots,n,$$
$$\rho_{kj}=0.5 \quad k\neq j.$$

The first group of test is performed as follows:

- Table 1 shows the effect of simultaneously changing all correlations from $\rho = \rho_{kj} = 0.1$ to $\rho = 0.95$.
- With all the other parameters set to the default values, the strike K is varied from 50 to 150 in Table 2.
- Table 3 shows the results of varying the same starting price $S_k(t) = S(t)$ between 50 and 150.
- Volatilities are changed simultaneously between 5% and 100%, yielding the results in Table 4.
- In Table 5 we change volatilities simultaneously between 5% and 100% but σ_1 is set to 100%.

Regarding the numerical results, we note two points. First, the values $\hat{C}_K^{\mathbf{w}}(t)$ obtained with our method produces results equal to those produced with the method of Beisser (2001). The lower approximation of Beisser (2001) is obtained, solving the problem of Rogers and Shi (1995) in formula (38), assuming a suitable conditioning variable. The basket call is estimated by the weighted sum of (artificial) European call prices. The setting of the valuation problem is slightly different and a different conditioning variable is chosen, but the computed values are the same in practice. Second,

TABLE 1. Varying the correlations simultaneously.

ρ	$\hat{C}_K^{\mathbf{w}}(t)$	Beisser	Ju	MC	IC length	$U_K(t)$
0.1	20.12	20.12	21.77	21.69	0.02976	27.49
0.3	24.21	24.21	25.05	25.04	0.01911	30.23
0.5	27.63	27.63	28.01	28.01	0.01064	33.36
0.7	30.62	30.62	30.74	30.74	0.004702	36.13
0.8	31.99	31.99	32.04	32.04	0.002481	38.04
0.95	33.92	33.92	33.92	33.92	0.0002894	41.5

TABLE 2. Varying the strike.

K	$\hat{C}_K^{\mathbf{w}}(t)$	Beisser	Ju	MC	IC length	$U_K(t)$
50	54.16	54.16	54.31	54.31	0.004699	59.86
60	47.27	47.27	47.48	47.48	0.006221	52.94
70	41.26	41.26	41.52	41.52	0.007375	47.09
80	36.04	36.04	36.36	36.35	0.00854	41.76
90	31.53	31.53	31.88	31.88	0.009609	37.33
100	27.63	27.63	28.01	28.01	0.01062	33.36
110	24.27	24.27	24.67	24.66	0.0115	29.93
120	21.36	21.36	21.77	21.76	0.01218	26.85
130	18.84	18.84	19.26	19.25	0.01262	24.53
140	16.65	16.65	17.07	17.06	0.01325	22.44
150	14.75	14.75	15.17	15.17	0.01412	20.51

TABLE 3. Varying the price.

$S_k(t)$	$\hat{C}_K^{\mathbf{w}}(t)$	Beisser	Ju	MC	IC length	$U_K(t)$
50	4.16	4.16	4.34	4.34	0.007479	6.86
60	7.27	7.27	7.51	7.509	0.008631	10.41
70	11.26	11.26	11.55	11.55	0.009727	15.18
80	16.04	16.04	16.37	16.37	0.009957	20.38
90	21.53	21.53	21.89	21.89	0.01043	26.54
100	27.63	27.63	28.01	28	0.0105	33.36
110	34.27	34.27	34.66	34.65	0.01056	40.74
120	41.36	41.36	41.75	41.74	0.01076	48.63
130	48.84	48.84	49.23	49.23	0.01079	56.96
140	56.65	56.65	57.04	57.04	0.01083	64.02
150	64.75	64.75	65.13	65.13	0.01051	72.78

TABLE 4. Varying the volatilities simultaneously.

σ	$\hat{C}_K^{\mathbf{w}}(t)$	Beisser	Ju	MC	IC length	$U_K(t)$
0.05	3.53	3.53	3.53	3.53	5.644×10^{-5}	3.59
0.1	7.04	7.04	7.05	7.05	0.0003358	7.27
0.15	10.55	10.55	10.57	10.57	0.0009116	11.07
0.2	14.03	14.03	14.08	14.08	0.001891	15.03
0.3	20.91	20.91	21.08	21.08	0.005237	23.47
0.4	27.63	27.63	28.01	28.01	0.01083	33.35
0.5	34.15	34.15	34.84	34.82	0.01813	43.89
0.6	40.41	40.41	41.52	41.49	0.02851	60.97
0.7	46.39	46.39	47.97	47.96	0.04283	86.33
0.8	52.05	52.05	54.09	54.13	0.05894	129.4
1	62.32	62.32	64.93	65.42	0.09682	321.6

TABLE 5. Varying the volatilities simultaneously with $\sigma_1 = 100\%$.

σ	$\hat{C}_K^{\mathbf{w}}(t)$	Beisser	Ju	MC	IC length	$U_K(t)$
0.05	19.45	19.45	35.59	19.46	0.0005861	152.2
0.1	20.84	20.84	36.19	20.97	0.004047	152.8
0.15	22.6	22.6	36.93	23.01	0.009306	148.2
0.2	24.69	24.69	37.8	25.38	0.01408	148.8
0.3	29.52	29.52	39.97	30.6	0.02125	151.3
0.4	34.72	34.72	42.66	36.06	0.02738	154.5
0.5	39.96	39.96	45.84	41.51	0.0342	158.8
0.6	45.05	45.05	49.39	46.82	0.04273	165.4
0.7	49.88	49.88	53.21	51.95	0.05364	176.5
0.8	54.39	54.39	57.17	56.78	0.0666	197.2
1	62.32	62.32	64.93	65.42	0.09654	321.6

the upper bound does not appear to be very tight, even if we try to minimize it with respect to the free parameter ΔK. In addition, it appears to be very sensitive to the volatility of the model. In only a few situations is the upper bound close to the true price, mainly for low volatility levels, as shown in Table 4. Given these poor results, we do not use it anymore in the remaining tests.

The second numerical experiment concerns the valuation of basket spread options. Deelstra et al. (2010) compare the relative performances of several methods and conclude that the shifted log-normal moment matching method of Borovkova et al. (2007) and their hybrid moment matching method based on the so-called ICUB are the two best-performing methods for basket spread option pricing. We reproduce their experiments in Tables 6 to 9. Each table shows the values $\hat{C}_K^{\mathbf{w}}(t)$ computed by using our pricing formula and the results of Deelstra et al. (2010). We also compute a benchmark via Monte Carlo simulation with 10^6 trials, also providing the length of a 95% confidence interval. These experiments use $T - t = 1$ and $r = 5\%$. The remaining model parameters are indicated for each table. Our results confirm that the shifted log-normal moment matching and ICUB-based hybrid moment matching methods are the best for basket spread option pricing in the

geometric Brownian motion case. They are better than the approximation $\hat{C}_K^{\mathbf{w}}(t)$ in almost all situations. Deelstra et al. (2010) also test a comonotonic lower bound, among others. They conclude that such a lower approximation does not perform as well as the shifted log-normal moment matching method or the ICUB-based hybrid moment matching. Since the idea behind their comonotonic lower bound is similar to our lower approximation, the computed results are not surprising.

The last test in the geometric Brownian motion framework concerns the implied volatility surface generated by the model. The test investigates whether the pricing method can be useful to calibrate the model to an implied volatility surface. Furthermore, recalling that options on indices are basket

TABLE 6. In this table $\mathbf{w} = [1; -1; -1]$, $\mathbf{S}(t) = [100; 24; 46]$, $\boldsymbol{\sigma} = [0.4; 0.22; 0.3]$, $\rho_{12} = 0.17$, $\rho 13 = 0.91$, $\rho_{23} = 0.41$.

K	$\hat{C}_K^{\mathbf{w}}(t)$	SLN	MMICUB	MC	IC length
15	17.2435	19.6925	19.5231	19.6796	0.0245036
20	13.4984	16.7345	16.5673	16.7033	0.0298483
25	10.1956	14.146	13.9944	14.1079	0.0348811
30	7.40244	11.9059	11.779	11.8447	0.0395552
35	5.14929	9.9851	9.8876	9.927	0.043695
40	3.42276	8.3506	8.2837	8.27783	0.0463941
45	2.16972	6.9683	6.9305	6.91537	0.0487735

TABLE 7. In this table $\mathbf{w} = [1; -1; -1; -1]$, $\mathbf{S}(t) = [100; 100; 50; 70]$, $\boldsymbol{\sigma} = [0.5; 0.15; 0.2; 0.17]$, $\rho_{kj} = 0.9$ for all k and j.

K	$\hat{C}_K^{\mathbf{w}}(t)$	SLN	MMICUB	MC	IC length
-90	0.0967632	2.4884	2.4043	2.41311	0.0478315
-100	0.41189	3.482	3.3098	3.31895	0.0506866
-110	1.39163	4.9521	4.6565	4.65662	0.0490433
-120	3.75078	7.1616	6.7643	6.77166	0.0424209
-130	8.18408	10.519	10.2529	10.2641	0.0319529
-140	14.8344	15.6048	15.8233	15.8428	0.0207096
-150	23.1375	22.9793	23.4623	23.4726	0.0109605

TABLE 8. In this table $\mathbf{w} = [1; -1; -1; -1]$, $\mathbf{S}(t) = [100; 60; 40; 30]$, $\boldsymbol{\sigma} = [0.16; 0.23; 0.32; 0.43]$, $\rho_{12} = 0.42$, $\rho_{13} = 0.5$, $\rho_{14} = 0.3$, $\rho_{23} = 0.24$, $\rho_{24} = 0.42$, $\rho_{34} = 0.35$.

K	$\hat{C}_K^{\mathbf{w}}(t)$	SLN	MMICUB	MC	IC length
-5	0.780148	1.3847	1.5248	1.43949	0.0105866
-10	1.49831	2.2538	2.378	2.28151	0.0114167
-20	4.0638	4.9936	5.0508	4.94776	0.0119248
-30	8.31642	9.2153	9.1939	9.13061	0.0113287
-40	14.1503	14.8764	14.8006	14.782	0.0099275
-50	21.247	21.7566	21.6606	21.685	0.00825845
-60	29.2471	29.5647	29.4747	29.5315	0.00668519

TABLE 9. In this table $\mathbf{w} = [1; -1; -1]$, $\mathbf{S}(t) = [100; 63; 12]$, $\boldsymbol{\sigma} = [0.21; 0.34; 0.63]$, $\rho_{12} = 0.87$, $\rho_{13} = 0.3$, $\rho_{23} = 0.43$.

K	$\hat{C}_K^{\mathbf{w}}(t)$	SLN	MMICUB	MC	IC length
2.5	23.3605	23.1681	23.5137	23.5944	0.00278116
10	16.7954	16.8591	17.1363	17.2054	0.00356326
17.5	10.7091	11.3394	11.3854	11.4126	0.00453313
25	5.50174	6.9203	6.6579	6.6013	0.00548593
32.5	1.79652	3.7629	3.3226	3.1898	0.00617322
40	0.16223	1.7925	1.395	1.25122	0.00574751
47.5	0	0.7369	0.4861	0.601204	0.00443468

options, we would like to investigate whether by assuming log-normality in the underlying, we can generate a smile effect when we price options on an index. Even if each asset has a constant volatility, the resulting basket implied volatility could be skewed by the fact that a weighted sum of log-normal random variables is not log-normal. The model parameters are set to $r = 0.01$, $S_k(t) = 100$, $q_k = 0$, $\sigma_k = 40\%$, and $w_k = 0.25$ for $k = 1, \ldots, n = 4$. The correlation parameter $\rho_{kj} = \rho = 0.5$ for $k \neq j$. Figure 2 plots the implied volatility surface of a single asset and that of the whole basket. We compute the surfaces for $T - t \in [0.3, 2]$ and $K \in [50, 150]$. The volatility of each component of the basket is flat and equal to 40%. The volatility of the basket shows a flat area equal to 30.98% for a large number of strikes and maturities. The surface is no longer flat for short maturities and small strike prices.

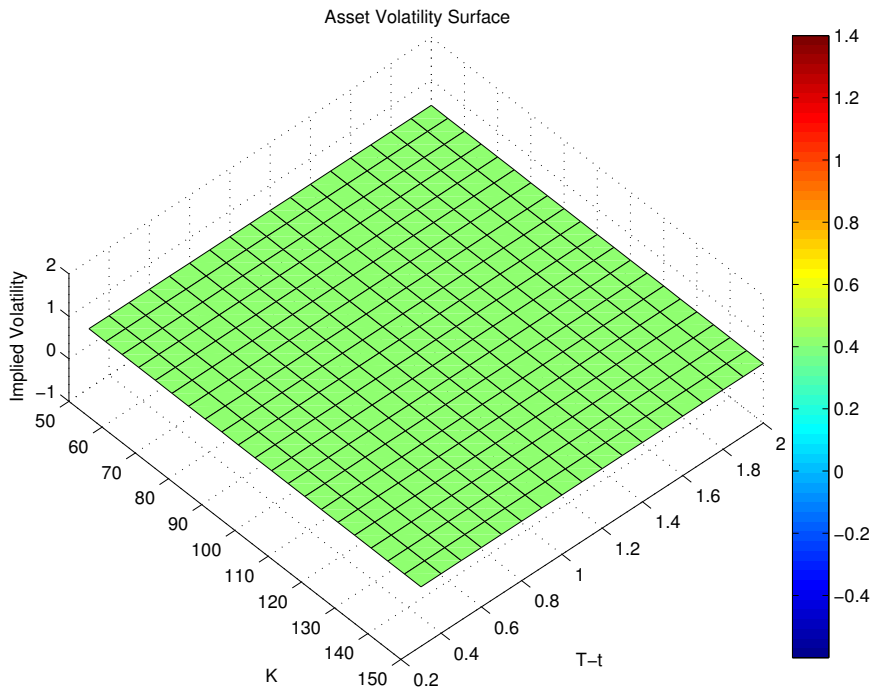

(a)

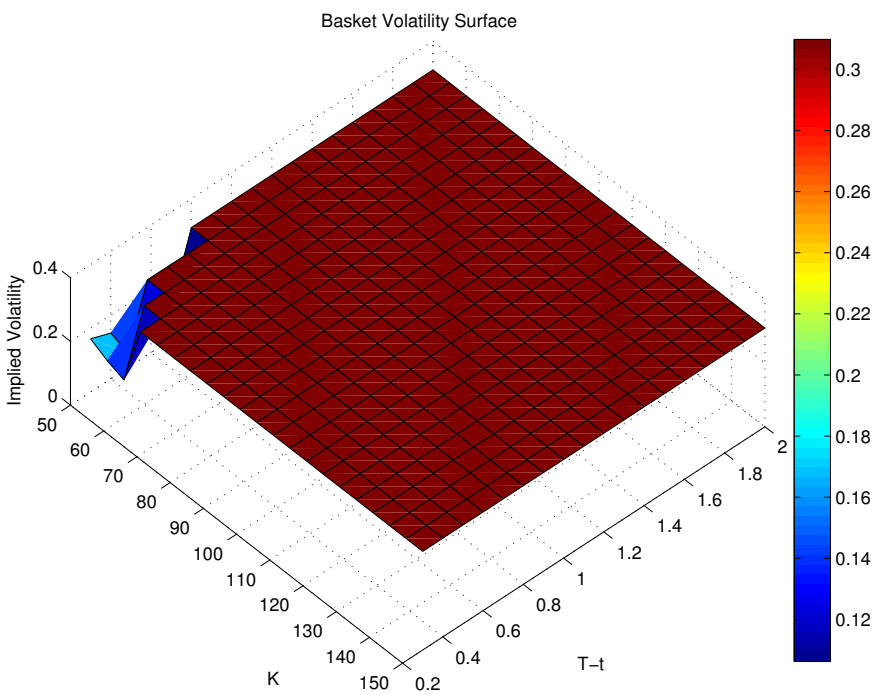

(b)

FIGURE 2. The volatility surface computed for one asset (a) compared to the surface computed for the basket (b).

The last group of numerical tests considers a non-Gaussian model: the jump diffusion model in formula (51). Model parameters are set as follows:

$$r = 0.01, \quad T - t = 1, \quad n = 4, \quad \lambda = 1, \quad \mathbf{S}(t) = [100; 100; 100; 100],$$
$$q_k = 0, \quad \alpha_k = -0.05, \quad \alpha_{kk} = -0.05, \quad \xi_k = 0.5, \quad \xi_{kk} = 0.3, \quad \lambda_k = 0.5, \quad k = 1, \ldots, n,$$
$$\rho_{kj} = 0.5, \quad \rho^Y_{kj} = 0.5, \quad k \neq j.$$

Again a Monte Carlo simulation with 10^6 trials is used as a benchmark. The results are shown in Tables 10 to 13 and confirm the results obtained in the Gaussian setting. The complexity of jump diffusion dynamics does not affect the quality of the pricing method. The method seems to be more accurate when we have positive weights (Tables 10 and 11), but the error is small even with negative weights (Tables 12 and 13).

Finally, we show the volatility surface of a single asset and that of the whole basket in the jump diffusion setting. The model parameters are set as above. We compute the implied volatility surface for $T - t \in [0.3, 2]$ and $K \in [50, 150]$. The results are shown in Figure 3. Both surfaces show a smile for short maturities and flatten when $T - t$ increases.

TABLE 10. In this table $\mathbf{w} = [0.25; 0.25; 0.25; 0.25]$.

K	$\hat{C}^{\mathbf{w}}_K(t)$	MC	IC length
50	51.8308	51.9409	0.0054
60	43.4117	43.5845	0.0074
70	35.9380	36.1770	0.0092
80	29.5579	29.8506	0.0107
90	24.2847	24.6209	0.0122
100	20.0267	20.3932	0.0135
110	16.6370	17.0241	0.0147
120	13.9554	14.3489	0.0155
130	11.8337	12.2239	0.0163
140	10.1463	10.5322	0.0171
150	8.7932	9.1745	0.0178

TABLE 11. In this table $\mathbf{w} = [0.1; 0.2; 0.3; 0.4]$.

K	$\hat{C}^{\mathbf{w}}_K(t)$	MC	IC length
50	51.9290	52.0429	0.0062
60	43.5869	43.7589	0.0079
70	36.1999	36.4301	0.0097
80	29.8988	30.1796	0.0116
90	24.6850	25.0034	0.0127
100	20.4631	20.8000	0.0136
110	17.0885	17.4437	0.0145
120	14.4058	14.7670	0.0150
130	12.2719	12.6289	0.0157
140	10.5661	10.9177	0.0164
150	9.1913	9.5354	0.0168

TABLE 12. In this table $\mathbf{w} = [1; 2; -1; -1]$.

K	$\hat{C}_K^{\mathbf{w}}(t)$	MC	IC length
50	78.6610	80.9336	0.1209
60	72.9709	75.0441	0.1177
70	67.6566	69.5829	0.1122
80	62.7123	64.5501	0.1093
90	58.1280	59.9357	0.1082
100	53.8906	55.6950	0.1061
110	49.9841	51.8095	0.1038
120	46.3909	48.2431	0.1017
130	43.0919	45.0147	0.0971
140	40.0676	42.0448	0.0914
150	37.2981	39.3566	0.0913

TABLE 13. In this table $\mathbf{w} = [1; 0.5; 0.5; -1]$.

K	$\hat{C}_K^{\mathbf{w}}(t)$	MC	IC length
50	62.5819	64.2222	0.0989
60	55.9870	57.4383	0.0946
70	49.9674	51.2696	0.0902
80	44.5278	45.7233	0.0720
90	39.6555	40.8078	0.0654
100	35.3239	36.4893	0.0649
110	31.4964	32.7106	0.0626
120	28.1301	29.4110	0.0620
130	25.1792	26.5345	0.0617
140	22.5977	24.0332	0.0596
150	20.3415	21.8462	0.0597

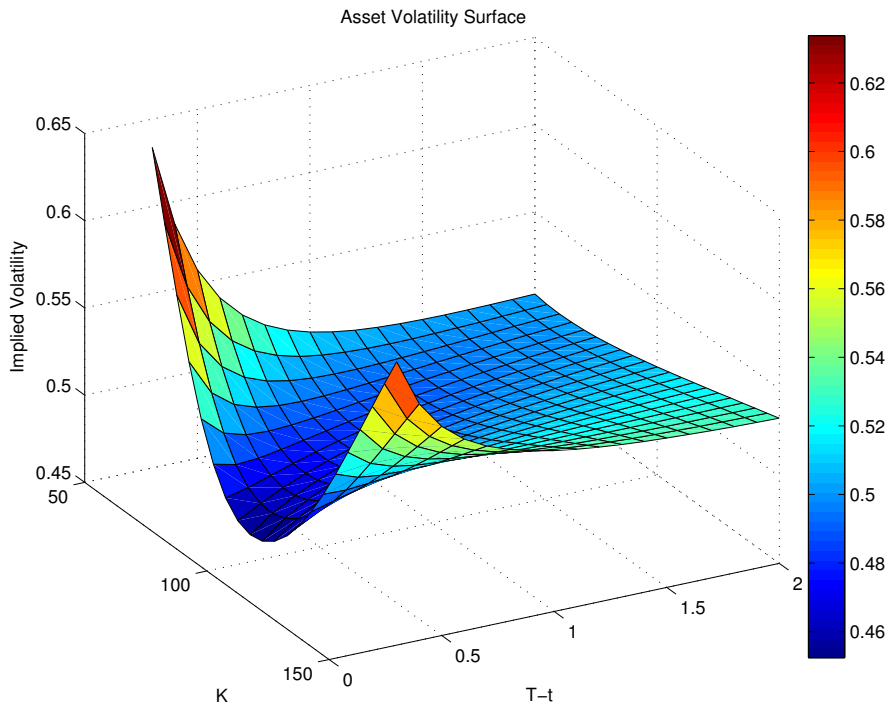

(a)

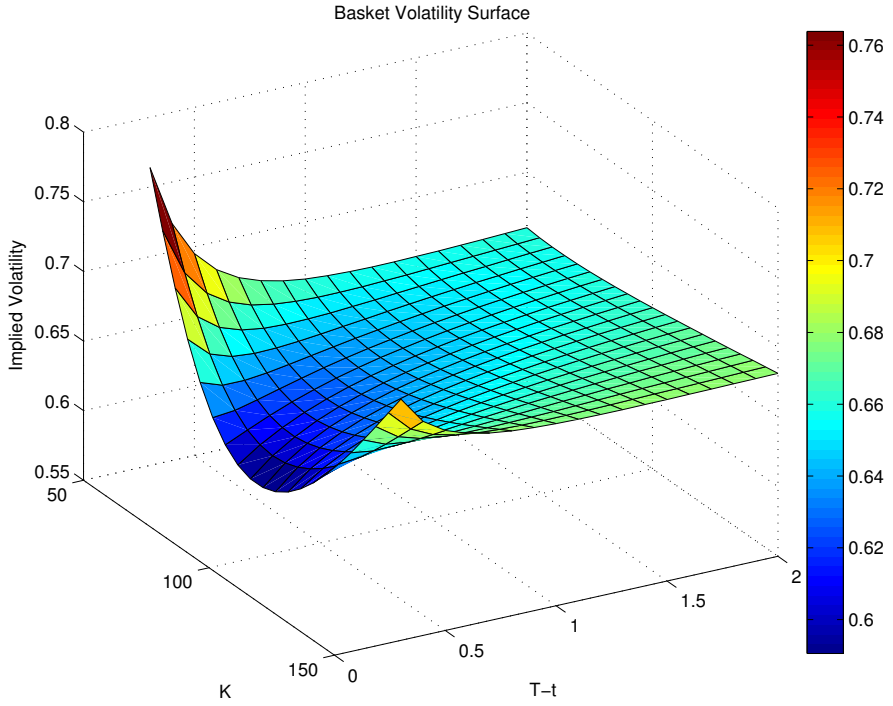

(b)

FIGURE 3. The volatility surface computed for one asset (a) compared to that computed for the basket (b).

CHAPTER 4

Interconnecting Electricity Markets

Any fact becomes important when it's connected to another.
Umberto Eco (1932–)

In the European power market, interconnections between different countries play an important role in obtaining energy balance and maintaining security of supply. Countries are connected by a complex web of transmission lines and the exchange of electricity between European states is increasing. Two main driving factors are behind this development: First, there is an uneven spatial distribution of load centers and generation plants across Europe, which requires energy transport over long distances. Second, there is a mix of different-generation technologies between the countries because of different environmental and political conditions, which leads to different energy price levels during the day. This price difference is an economic incentive to transport electric power between European countries. As discussed in the literature (see, for example, Benth et al. (2008) and Clewlow and Strickland (2000)), electricity prices are characterized by extreme volatility and large upward and downward jumps, as well as fast mean reversion to seasonal trends. This extreme behavior is also present in the differences between the prices of two locations and explains why interconnecting two markets can be profitable.

Energy transmission between European power markets is characterized by load patterns, structural patterns that are a function of supply sources, regional supply and demand balances, and the relative costs of supply. For example, France typically exports low-cost base load power generated by its nuclear plants to its neighbors. In addition, the direction and level of flow between major markets is very changeable. Figure 1 compares the inter-country flows at 10:00 on two dates in 2011. We note the stable exporting status of France but also the dynamic changes in direction of certain flows and countries changing from being net exporters to net importers (e.g., Germany). In Germany, fluctuations in renewable energy production need to be supported by generation flexibility from neighboring markets. Flows from flexible hydropower capacity in Scandinavia and the Alpine region and flexible thermal capacity in the Netherlands and Eastern Europe help maintain the system balance. Energy market integration through interconnection offers economic benefits: increased competition, enhanced liquidity, and greater diversity of supply. Power interconnections, or transportation capacities, are a core component of European companies' energy portfolios. Energy companies seek to reduce economic rents and risk and enhance security of supply. Furthermore, interconnectors will become increasingly important as intermittent renewable capacity grows in Europe. It is therefore essential for companies to understand energy transportation capacity value and how it can be used in portfolio optimization and risk management.

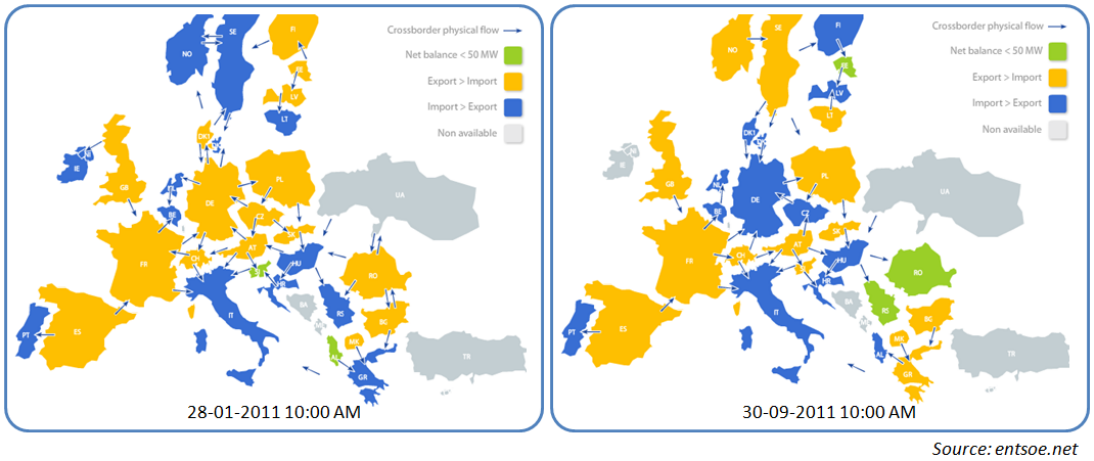

FIGURE 1. Comparison of European power load flows.

An interconnector is an asset that gives the owner the right, but not the obligation, to transmit electricity between two locations each hour of the day over a prefixed time period. Therefore the financial value of the interconnector is determined by a series of options that are written on the price differential between two electricity markets, that is, a strip of European options on the spread. Spread option valuation is a popular task in financial modeling, as discussed in Chapter 2. However, evaluating interconnections between power markets is a very recent issue and is discussed only in a few studies. The most valuable paper on this topic is that of Cartea and Pedraz (2012), who directly model the spread between markets with a mean-reverting jump diffusion process. They also propose a valuation tool that uses real options theory to price hypothetical interconnectors between five pairs of European neighboring countries.

This chapter proposes a valuation procedure that uses real options theory to price interconnections between energy markets. We select a bidimensional stochastic model to describe the energy price dynamics of a specified hour of interconnected countries and calibrate it to historical spot prices and forward market data. The forward price curve bootstrapping methodology proposed in Chapter 1 plays a fundamental role during the calibration step. Finally, by using the semi-closed option formula proposed in Chapter 2 to evaluate spread options, we price interconnections between five European countries.

This chapter is organized as follows: Section 1 introduces the pricing framework for evaluating transmission capacity contracts. Section 2 discusses the stochastic model used to describe energy prices. Section 3 discusses market data involved in the model calibration. Section 4 calibrates the model and, finally, Section 5 presents the numerical results of evaluating interconnections.

1. Pricing interconnection capacity contracts

This section introduces the general pricing framework for the valuation of transmission capacity contracts. Let $S_{1,h}(t)$ and $S_{2,h}(t)$ be two stochastic processes representing the spot[1] prices of the hth hour of the day for two interconnected locations at time t. We model the dynamic of each hour of the day separately. Indeed, as noted by Huisman et al. (2007), hourly electricity prices in day-ahead markets do not follow a time series process but are a panel of 24 cross-sectional hours that vary from day to day. We now consider the spread between prices of the hth hour of the day. Recall that an European spread option with strike price L pays at maturity date T the amount

$$(S_{1,h}(T) - S_{2,h}(T) - L)^+$$

and its time 0 no-arbitrage fair price is the discounted conditional expectation

$$C_L^h(0,T) = e^{-rT}\mathbb{E}_0\Big[(S_{1,h}(T) - S_{2,h}(T) - L)^+\Big]. \tag{54}$$

An interconnection capacity contract gives the owner the right, but not the obligation, to transmit electricity between two locations during a predetermined set of days $\{T_1, \ldots, T_n\}$ and hours. Without loss of generality, we consider contracts that allow the transmission of base load flows of energy; so in our setting $h = 1, \ldots, 24$. The owner of the contract gains the positive difference of prices between the two countries, net of transmission costs. We assume here an equal transmission cost K for every hour of the day and all times of the year. As noted by Cartea and Pedraz (2012), when the difference between the two prices is too large, in at least one of the locations it does not seem plausible to take positions at the prices that produced such large spreads. Following the approach of Cartea and Pedraz (2012), we assume that during times of extreme price deviations, the owner of the interconnector can take positions in both markets; however, we limit the extent to which the owner can profit from the situation. We denote by M the maximum spread level at which it is feasible to take positions in both locations. For simplicity, we assume that this liquidity cap is the same for every hour of the day and all times of the year. Assume that the buyer of the contract can transmit energy from location 2 to location 1. Every hour h of the day T, the owner of the right can buy energy from location 2, paying $S_{2,h}(T)$, and sell it in location 1 at $S_{1,h}(T)$, with a transmission cost K. The profit of such a strategy will be $S_{1,h}(T) - S_{2,h}(T) - K$, if positive. Thus, we can model the right to transmit energy from location 2 to location 1 using options on the spread $S_{1,h}(t) - S_{2,h}(t)$. However, the payoff of an interconnection contract depends not only on the transmission costs but also on the depth of the interconnected power markets; so we structure it as a difference of call options written on the spread (bull spread strategy). In financial terms, the payoff of an energy transmission right from location 2 to location 1 is composed of 24 strips of capped spread options with maturity T_i for $i = 1, \ldots, n$ and its value at time 0 is

$$IC(0) = \sum_{h=1}^{24}\sum_{i=1}^{n}\left(C_K^h(0,T_i) - C_M^h(0,T_i)\right). \tag{55}$$

[1]The owner of the interconnector capacity needs to schedule flows according to market prices in the two interconnected locations. In practice these decisions are usually made based on the day-ahead market and transmission costs. Thus, we assume that the decision to use the interconnector to dispatch electricity from location 1 to location 2, or vice versa, is based on the hourly market prices observed in the day-ahead market, net of transmission costs. The convention in the market and the literature is to treat day-ahead prices as spot prices, even though the former have the structure of a forward contract.

The value of the energy transmission right from location 1 to location 2 is obtained using the formula (55) and switching the position of $S_{1,h}(T)$ and $S_{2,h}(T)$ in the formula (54). The computation of (55) comes from $24 \times n$ evaluations of equation (54). In Chapter 2, Proposition 1 proposes a general method to solve the problem in (54) when the T_i joint characteristic function of the log-returns of the two prices

$$\Phi^h_{T_i}(\mathbf{u}) = \Phi^h_{T_i}(u_1, u_2) = \mathbb{E}\left[e^{iu_1 \ln S_{1,h}(T_i) + iu_2 \ln S_{2,h}(T_i)}\right]$$

is known explicitly. The following section discusses a spot price model and defines its characteristic function $\Phi^h_{T_i}(\mathbf{u})$.

2. Stochastic spot price model

This section introduces the stochastic model we use to describe energy spot prices. The classic process for the spot dynamics of commodity prices is described by the so-called Schwartz (1997) model, defined as the exponential of an Ornstein–Uhlenbeck process. Schwartz's seminal paper considers storable commodities and does not deal with seasonality, but it serves as a starting point for a number of articles proposing no-arbitrage models for the dynamics of electricity prices. The model proposed by Schwartz is a geometric one because of the exponential involved in its definition. Lucia and Schwartz (2002), Cartea and Figueroa (2005) and Geman and Roncoroni (2006), among others, provide examples of geometric no-arbitrage models. Another choice is to consider the no-arbitrage arithmetic models, where the price dynamic is modeled as a linear combination of pure jump processes (e.g., Benth et al. (2007a)). This framework involves no exponential function and the positivity of the spot is achieved by allowing positive jumps only. The advantage of this formulation is that semi-analytic formulas for option prices on forwards with a delivery period can be derived. However, a full analysis of this class of models still seems to be in its early stages. Other models examined in the literature are the so-called equilibrium and hybrid models (e.g., Bessembinder and Lemmon (2002); Barlow (2002); Pirrong and Jermakyan (2008); Cartea and Villaplana (2008)). Our work discusses a bivariate geometric spot price model characterized by seasonality, mean reversion, and jumps. The unidimensional version of this model in energy price modeling is discussed by many authors (e.g., Deng (1999); Villaplana (2003); Hambly et al. (2009)). Our model is able to reproduce typical features of electricity spot price dynamics, such as seasonality, mean reversion, and the occurrence of spikes.

Consider a couple of interconnected power markets. We model the two prices of every hour h for $h = 1, \ldots, 24$ and consider a bidimensional continuous time process for each hour. Since the payoff we want to evaluate depends on prices for the same hour h, we assume independence between the dynamics concerning the different hours of the day. We model 24 independent pairs of prices. For $j = 1, 2$ and $h = 1, \ldots, 24$, the risk-neutral spot price process $S_{j,h}(t)$ is defined as the exponential of the sum of three components, namely, a deterministic function $f_{j,h}(t)$, a Gaussian Ornstein–Uhlenbeck process $X_{j,h}(t)$, and a mean-reverting process with a jump component $Y_{j,h}(t)$:

$$\begin{aligned} S_{j,h}(t) &= \exp\left(f_{j,h}(t) + X_{j,h}(t) + Y_{j,h}(t)\right), \\ dX_{j,h} &= -\alpha_{j,h} X_{j,h}(t)dt + \sigma_{j,h} dW_{j,h}, \\ dY_{j,h} &= -\alpha_{j,h} Y_{j,h}(t-)dt + J^+_{j,h} dN^+_{j,h} - J^-_{j,h} dN^-_{j,h}. \end{aligned} \tag{56}$$

The parameter $\sigma_{j,h}$ is strictly positive and $W_{j,h}$, is a risk-neutral Brownian motion. We assume a speed of mean reversion $\alpha_{j,h} > 0$ for both the diffusion process $X_{j,h}(t)$ and the jump process $Y_{j,h}(t)$.

The two Brownian motions have instantaneous correlation $\rho, |\rho| < 1$. The Poisson processes $N^+_{j,h}$ and $N^-_{j,h}$ have intensity $\lambda^+_{j,h}$ and $\lambda^-_{j,h}$, respectively, and describe the positive and negative jump arrivals separately. The independent identically distributed random variables $J^+_{j,h}$ and $J^-_{j,h}$ represent the jump size and we assume they are exponentially distributed with parameters $0 < \mu^+_{j,h} < 1$ and $\mu^-_{j,h} > 0$, respectively. Note that the model requires $\mu^+_{j,h} < 1$. This restriction is to be expected, since the T forward price at time 0 is given by

$$F_{j,h}(0,T) = \mathbb{E}_0[S_{j,h}(T)] = \mathbb{E}_0[\exp\left(f_{j,h}(T) + X_{j,h}(T) + Y_{j,h}(T)\right)]. \tag{57}$$

Since $Y_{j,h}(T)$ contains terms involving jumps with an exponential distribution, the expectation in (59) diverges if the upper tail of the jump distribution is sufficiently large. The model in (56) is able to reproduce typical features of electricity spot price dynamics such as seasonality, mean reversion, and the occurrence of spikes. However, this model does not claim to fully represent all of the features of electricity prices. Historical data indicate varying volatility over time and hence would require the introduction of an additional stochastic volatility process. A further process describing the stochastic component of the seasonality might be needed to better capture the forward price dynamics. Finally, the risk of spike occurrence is likely to be seasonal rather than constant, as in our choice.

If we assume independence between the jump processes, the joint characteristic function of the model in (56) is

$$\begin{aligned}
\Phi^h_T(\mathbf{u}) \quad = \quad & \exp\Big[iu_1\left(\left(X_{1,h}(0) + Y_{2,h}(0)\right)e^{-\alpha_{1,h}T} + f_{1,h}(T)\right) + \\
& iu_2\left(\left(X_{2,h}(0) + Y_{2,h}(0)\right)e^{-\alpha_{2,h}T} + f_{2,h}(T)\right) - \\
& \frac{u_1^2\sigma^2_{1,h}}{4\alpha_{1,h}}\left(1 - e^{-2\alpha_{1,h}T}\right) - \frac{u_2^2\sigma^2_{2,h}}{4\alpha_{2,h}}\left(1 - e^{-2\alpha_{2,h}T}\right) - \rho\frac{u_1u_2\sigma_{1,h}\sigma_{2,h}}{\alpha_{1,h} + \alpha_{2,h}}\left(1 - e^{-(\alpha_{1,h}+\alpha_{2,h})T}\right) + \\
& \frac{\lambda^+_{1,h}}{\alpha_{1,h}}\ln\left(\frac{1 - i\mu^+_{1,h}u_1e^{-\alpha_{1,h}T}}{1 - i\mu^+_{1,h}u_1}\right) + \frac{\lambda^+_{2,h}}{\alpha_{2,h}}\ln\left(\frac{1 - i\mu^+_{2,h}u_2e^{-\alpha_{2,h}T}}{1 - i\mu^+_{2,h}u_2}\right) + \\
& \frac{\lambda^-_{1,h}}{\alpha_{1,h}}\ln\left(\frac{1 + i\mu^-_{1,h}u_1e^{-\alpha_{1,h}T}}{1 + i\mu^-_{1,h}u_1}\right) + \frac{\lambda^-_{2,h}}{\alpha_{2,h}}\ln\left(\frac{1 + i\mu^-_{2,h}u_2e^{-\alpha_{2,h}T}}{1 + i\mu^-_{2,h}u_2}\right)\Bigg].
\end{aligned} \tag{58}$$

We can evaluate each spread option, plugging (58) into our pricing formula (see Chapter 2, Proposition 1). Moreover, we can easily obtain an expression for the forward price from the characteristic function, which will be useful during the calibration of the model to a market forward curve. We have

$$F_{1,h}(0,T) = \Phi^h_T([-i,0]^\intercal) \quad \text{and} \quad F_{2,h}(t,T) = \Phi^h_T([0,-i]^\intercal);$$

so the forward price for $j = 1, 2$ is

$$\begin{aligned}
F_{j,h}(0,T) = \quad = \quad & \exp\Bigg[\left(X_{j,h}(0) + Y_{j,h}(0)\right)e^{-\alpha_{j,h}T} + f_{j,h}(T) + \frac{\sigma^2_{j,h}}{4\alpha_{j,h}}\left(1 - e^{-2\alpha_{j,h}T}\right) + \\
& \frac{\lambda^+_{j,h}}{\alpha_{j,h}}\ln\left(\frac{1 - \mu^+_{j,h}e^{-\alpha_{j,h}T}}{1 - \mu^+_{j,h}}\right) + \frac{\lambda^-_{j,h}}{\alpha_{j,h}}\ln\left(\frac{1 + \mu^-_{j,h}e^{-\alpha_{j,h}T}}{1 + \mu^-_{j,h}}\right)\Bigg].
\end{aligned} \tag{59}$$

3. Market data

This section presents an example of interconnection capacity valuation using the pricing framework previously described. It also describes the market data we use to calibrate the model and the interconnection pricing. We consider five European countries: Italy, Germany, France, Switzerland, and the Czech Republic. We evaluate the following interconnections between these countries:

- Transmission of energy from Switzerland to Italy ($SWI \to ITA$) and from Italy to Switzerland ($ITA \to SWI$),
- Transmission of energy from France to Italy ($FRA \to ITA$) and from Italy to France ($ITA \to FRA$),
- Transmission of energy from Germany to France ($GER \to FRA$) and from France to Germany ($FRA \to GER$),
- Transmission of energy from France to Switzerland ($FRA \to SWI$) and from Switzerland to France ($SWI \to FRA$),
- Transmission of energy from Czech Republic to Germany ($CZR \to GER$) and from Germany to Czech Republic ($GER \to CZR$).

We consider one-year-long base load interconnections, which give the right to transmit 1 MWh of energy for every hour of the year 2011. The evaluation date of the contracts is December 31, 2010. We use two kinds of market data to calibrate the models. The first kind consists of the historical series of day-ahead spot prices. We consider the following day-ahead prices for five European energy spot markets, starting at different dates:

- Italy (MGP), data since January 1, 2005;
- Germany (EEX), data since January 1, 2005;
- France (PNXT), data since January 1, 2006;
- Switzerland (SWISSX), data since December 12, 2006;
- Czech Republic (CZ), data since January 1, 2008.

Time series are considered in the euro currency for all markets. The last price of each series refers to the evaluation date. Any missing data are replaced by the last available quote preceding the hour in question. This case occurs, for instance, when changing from a legal to a solar hour count.

Exponential models such as (56) do not allow negative or zero prices. However, some markets have energy prices that are less than or equal to zero. Negative prices mean that the destruction of a commodity has more value than its creation. Indeed, a balance between supply and demand must always exist in a power network. Power supply can be higher than demand primarily at night. This nightly imbalance is caused, for instance, by the installation of non-flexible power plants. Reducing the output of such generators is hardly possible from a technical point of view or involves high shutdown costs. Thus, negative prices are acceptable to power suppliers because the opportunity costs of a shutdown period would be much higher. Generally, prices are negative or equal to zero during only a short period of time and mainly at night. As a practical choice, should any of our data be less or equal to zero, we replace it with the value of one. Fanone et al. (2011) presents an empirical study of the reasons for negative prices.

The second market data input consists of a list of forward contract quotations, provided in Table 1. This table shows the prices converted in euros per megawatt–hour (€/MWh), for the Swiss and Czech markets. The lack of liquidity of forward markets around Christmas leads to biased prices on the evaluation date. We therefore consider prices quoted on December 23, 2010. Forward contract quotations are fundamental in calibrating the risk-neutral version of the model. We do so using the bootstrapping procedure described in Chapter 1, obtaining an hourly market estimation of the quantity $F_j(t,T)$ in formula (59), denoted $F^{mkt}_{j,h}(0,T)$. This estimation depends on a weight parameter we set equal to 0.8 to estimate the seasonality contribution, solving equation (4). The pricing model is calibrated according to the information of such hourly forward price curves.[2]

TABLE 1. Forward market data.

Start Date	End Date	F^{base}_{ITA}	F^{peak}_{ITA}	F^{base}_{GER}	F^{peak}_{GER}	F^{base}_{FRA}	F^{peak}_{FRA}	F^{base}_{SWI}	F^{peak}_{SWI}	F^{base}_{CZR}	F^{peak}_{CZR}
01/01/11	31/01/11	68.25	80.50	56.38	71.63	62.40	79.20	68.09	80.56	53.15	71.50
01/02/11	28/02/11	68.25	80.50	54.61	68.14	58.80	70.00	65.51	74.56	52.05	67.00
01/03/11	31/03/11	66.50	78.50	52.23	62.20	54.40	67.50	59.70	69.19	50.50	61.75
01/04/11	30/06/11	63.60	74.10	47.19	57.32	47.10	60.50	49.40	61.56	45.60	57.25
01/07/11	30/09/11	71.00	82.75	48.44	58.48	48.55	59.50	49.00	60.05	46.70	58.85
01/10/11	31/12/11	70.90	82.25	54.59	66.42	60.60	73.70	65.00	76.45	52.60	66.55

The Italian market has some peculiarities. Interconnection capacity contracts do not concern the Italian national single price but they do affect zonal prices. In the Italian day-ahead market, the national single price is the average of zonal prices weighted for total purchases and net of purchases for pumped-storage units and purchases by neighboring countries' zones. A zonal price is defined as the electricity price that is set in the energy market for each of Italy's geographical and virtual zones.[3] These zonal prices are highly correlated with the national single price. However, the available forward contract quotations refer to the Italian national price. In interconnection contract valuation, it is popular for practitioners to compute Italian hourly forward curves for the national price. Then they modify the computed curves to reproduce the relation between the national price and a zonal price, using statistical tools. For simplicity's sake, we neglect this detail and consider the national price as underlying the spread options, as in other markets under examination.

4. Model estimation

The model in formula (56) is discussed in a no-arbitrage risk-neutral setting, but the calibration of the model parameters in such a framework is not trivial. Due to the non-storability of electricity, the underlying cannot be used to replicate derivative products in energy markets. The market is incomplete; therefore arbitrage arguments do not immediately lead to a unique price for derivatives. To calibrate the model and obtain a unique price for a particular derivative we want to trade in the market, we need many liquidly traded derivatives in addition to the underlying. In practice, liquid energy option markets are still rare and such information is not readily available. Only information from average-based forward contracts is available in our valuation example and we use historical data to overcome this problem. To calibrate the model, we obtain data from the real-world probability measure $\mathbb{P}$ and transfer their information to an equivalent risk-neutral measure $\mathbb{Q}$ setting. Since the

[2]Forward contracts quotations are even considered by Cartea and Pedraz (2012), who discuss how to obtain no-arbitrage lower bounds on the value of a bidirectional interconnector, using forward market data.

[3]See Gestore Mercati Energetici's website at http://www.mercatoelettrico.org.

market is incomplete, the measure $\mathbb{Q}$ is not uniquely determined and needs to be chosen according to certain criteria. Kluge (2006) discusses in more detail the change in probability measure for the model in formula (56): The author restricts the set of possible risk-neutral measures to remain in the same class of models and provides a link between real-world and risk-neutral parameters. Once the relation between the $\mathbb{P}$ model and $\mathbb{Q}$ model is identified, one way of choosing a measure $\mathbb{Q}$ is to pick that which is closest to $\mathbb{P}$ in a metric sense.[4] However, following Hambly et al. (2009) and Kluge (2006), we adopt a pragmatic approach: We estimate all parameters from historical data and then calibrate the function $f_{j,h}(t)$ to the observed forward curve. In other words we are assuming that the price under the historical probability measure $\mathbb{P}$ is defined as

$$\begin{aligned} S_{j,h}(t) &= \exp\left(f^*_{j,h}(t) + X_{j,h}(t) + Y_{j,h}(t)\right), \\ dX_{j,h} &= -\alpha_{j,h} X_{j,h}(t)dt + \sigma_{j,h} dW_{j,h}, \\ dY_{j,h} &= -\alpha_{j,h} Y_{j,h}(t-)dt + J^+_{j,h} dN^+_{j,h} - J^-_{j,h} dN^-_{j,h}, \end{aligned} \tag{60}$$

where the only difference from the risk neutral model in equation (56) is the function $f^*_{j,h}(t)$ and we assume

$$f_{j,h}(t) = f^*_{j,h}(t) + g_{j,h}(t),$$

$$g_{j,h}(t) \quad s.t. \quad F_{j,h}(0,T) = F_{j,h}(0,T)^{mkt}$$

and the forward price $F_{j,h}(0,T)$ is computed under $\mathbb{Q}$. This is equivalent to saying we choose a risk-neutral measure $\mathbb{Q}$ that changes as few parameters of the $\mathbb{P}$ model as possible. We now propose a procedure to calibrate the model to market data.

We consider the market data described in Section 3. We first estimate the model parameters for each market and then determine the correlation coefficient between every pair of interconnected market hour prices. We consider separately each hour of each market, so we can omit the subscript j in our model specification, but we emphasize that the procedure we discuss leads to different estimated parameters for each hour of each market. Since model (60) consists of three components, $S_h(t) = \exp\left(f^*_h(t) + X_h(t) + Y_h(t)\right)$, and only $S_h(t)$ is observable, estimating parameters becomes non-trivial: We have to separate the three components to estimate their parameters. We consider the logarithm of the spot price of each hour $h = 1, \ldots, 24$:

$$\ln S_h(t) = f^*_h(t) + X_h(t) + Y_h(t).$$

The function $f^*_h(t)$ models the trend and season components of the logarithmic spot price:

$$f^*_h(t) = trend_h(t) + seasonality_h(t).$$

The trend is estimated using a Hodrick–Prescott filter, denoted $H_{h,\lambda_h}(t)$. Using Pedersen's method, the parameter λ_h of the filter is set to filter out recurrent components with a period equal to or exceeding a year and a half. The rationale behind this choice is that economic movements of more than a year are supposed to be related to macroeconomic phenomena, whereas pure seasonalities must be searched for in shorter periods. The practical choice to set the period equal to a year and a half instead of just one year is due to the risk, when filtering a time series, of introducing distortions near the cutoff frequency. A brief description of the Hodrick–Prescott filter and Pedersen's criterion for the optimal choice of λ_h is given in Appendix A.

[4]Hubalek and Sgarra (2009) discuss the different choices of an equivalent martingale measure with reference to Lévy processes.

Seasonality is estimated with the parametric function

$$\Lambda_h(t) = a_h \cos\left(\frac{4\pi}{365}t + b_h\right) + \mathbf{D}_{day}\mathbf{d}_h + \mathbf{D}_{month}\mathbf{m}_h,$$

where the dummy variables $\mathbf{D}_{day}$ and $\mathbf{D}_{month}$ are defined for each of the twelve months and each of the seven days under analysis. Official holidays are treated as typical Sundays. We add up even a cosine with a six-month period. The function $\Lambda_h(t)$ reproduces a semiannual periodicity plus daily and monthly dummies and is estimated to fit $\ln S_h(t) - H_{h,\lambda_h}(t)$ with a non-linear regression. We show in Tables 2 to 6 the estimated Hodrick–Prescott filter parameter λ_h and the seasonality parameters of the function $\Lambda_h(t)$ for each hour and each market. First, we note that, depending on the historical series under concern, Pedersen's method gives different estimates for λ_h, but their order of magnitude is always between 10^7 and 10^8. The absolute value of the coefficient a_h in the definition of $\Lambda_h(t)$ gives us information about the magnitude of semiannual seasonality. From one hour to the next, semiannual seasonality is very similar in every market, except for the Czech one. We observe higher values of a_h during the morning at about sunrise and during the evening at about sunset. The Czech market follows this pattern as well, but the magnitude of a_h early in the morning is three to four times higher than in the other markets. Regarding weekly seasonality, the estimate of daily dummies provides the same information for all markets. We note a common behavior during the central hours of the day: The Saturday parameter d_7 and especially the Sunday parameter d_1 are usually lower than the weekday parameters. However, we do not observe such behavior for the early morning or late night hours. Seasonalities are very different from one market to another and, due to the large number of parameters, are not easily interpreted. However, we note a few similarities. For all markets during the summer, seasonality coefficients tend to be greater in July than in the other months. This is likely caused by a higher energy demand due to air conditioning usage during the hottest month of the year. The Swiss and French market seasonality parameters are definitely higher during winter, while those of the German market are high from October to February, except for December and January. Energy demand is probably lower during December and January because of holidays. Finally, Italy and the Czech Republic exhibit similar seasonality, but the contribution of their summer parameters to the seasonality function is higher than in Germany.

TABLE 2. Estimated parameters for the Italian market.

ITA	$h=1$	$h=2$	$h=3$	$h=4$	$h=5$	$h=6$	$h=7$	$h=8$	$h=9$	$h=10$	$h=11$	$h=12$
λ	8.11×10^7	8.23×10^7	8.09×10^7	7.87×10^7	7.9×10^7	8.34×10^7	8.5×10^7	8.55×10^7	8.43×10^7	8.9×10^7	9.49×10^7	9.66×10^7
a	−0.0687	0.0817	0.0822	0.036	0.0344	0.00621	−0.0313	0.0507	0.0177	0.054	−0.0879	−0.111
b	2.98	−0.295	−0.33	0.692	1.15	1.23	−0.757	0.973	1.27	−0.702	2.33	2.56
m_1	0.0123	−0.145	0.0565	0.223	0.176	−0.0968	0.363	−0.586	−0.216	0.135	−0.0356	−0.536
m_2	0.0822	−0.0718	0.0603	0.202	0.153	−0.115	0.387	−0.542	−0.207	0.203	−0.00205	−0.489
m_3	0.0912	−0.0732	0.0591	0.216	0.172	−0.148	0.271	−0.634	−0.268	0.169	−0.00655	−0.468
m_4	0.0407	−0.107	0.0616	0.0968	0.0327	−0.227	0.18	−0.736	−0.337	0.179	0.035	−0.42
m_5	−0.00701	−0.216	−0.0543	0.0027	−0.054	−0.346	0.116	−0.79	−0.346	0.21	0.0807	−0.393
m_6	−0.018	−0.24	−0.079	0.00371	−0.0451	−0.424	0.0892	−0.839	−0.375	0.113	0.0396	−0.424
m_7	0.0498	−0.0845	0.0664	0.162	0.116	−0.224	0.2	−0.74	−0.322	0.169	0.134	−0.306
m_8	0.142	−0.0168	0.112	0.279	0.226	−0.111	0.214	−0.764	−0.385	0.0171	−0.111	−0.519
m_9	0.0874	−0.061	0.146	0.249	0.204	−0.126	0.274	−0.616	−0.24	0.219	0.11	−0.294
m_{10}	0.0444	−0.123	0.0501	0.118	0.0659	−0.215	0.287	−0.586	−0.242	0.239	0.105	−0.329
m_{11}	0.00682	−0.152	−0.00316	0.0731	0.0247	−0.209	0.28	−0.671	−0.26	0.147	0.00535	−0.461
m_{12}	−0.00543	−0.181	−0.00585	0.127	0.0843	−0.193	0.283	−0.677	−0.292	0.102	−0.0683	−0.567
d_1	0.024	0.183	−0.0217	−0.121	−0.11	0.0628	−0.596	0.213	−0.137	−0.601	−0.445	0.0702
d_2	−0.11	0.0305	−0.121	−0.241	−0.195	0.115	−0.196	0.768	0.364	−0.106	0.0198	0.475
d_3	−0.103	0.0625	−0.095	−0.201	−0.126	0.219	−0.151	0.81	0.413	−0.0102	0.123	0.579
d_4	−0.0777	0.09	−0.0581	−0.171	−0.109	0.253	−0.147	0.808	0.408	−0.00597	0.133	0.579
d_5	−0.0717	0.0946	−0.0565	−0.162	−0.0981	0.258	−0.152	0.809	0.408	−0.0246	0.116	0.567
d_6	−0.0627	0.0941	−0.0655	−0.17	−0.103	0.253	−0.154	0.799	0.401	−0.0356	0.0983	0.549
d_7	0.0821	0.294	0.141	0.0391	0.0693	0.287	−0.247	0.663	0.267	−0.236	−0.13	0.286

ITA	$h=13$	$h=14$	$h=15$	$h=16$	$h=17$	$h=18$	$h=19$	$h=20$	$h=21$	$h=22$	$h=23$	$h=24$
λ	8.36×10^7	8.4×10^7	8.66×10^7	8.97×10^7	8.85×10^7	8.64×10^7	8.95×10^7	8.85×10^7	8.44×10^7	8.07×10^7	8.14×10^7	7.92×10^7
a	0.0835	0.066	0.0948	0.0852	−0.117	0.161	0.143	0.0459	−0.014	−0.0557	0.0567	0.064
b	−0.469	−0.729	−0.802	−0.889	2.77	−0.0278	−0.128	−0.426	0.149	2.78	−0.101	−0.577
m_1	0.0285	−0.268	0.000392	−0.132	−0.00265	0.0616	0.329	0.234	0.5	0.606	0.133	−0.0308
m_2	0.0473	−0.253	−0.00223	−0.191	−0.098	−0.0239	0.417	0.296	0.469	0.605	0.158	−0.00867
m_3	0.0735	−0.245	0.0392	−0.152	−0.0745	−0.119	0.301	0.292	0.463	0.625	0.197	0.0225
m_4	0.0739	−0.257	0.057	−0.152	−0.0998	−0.209	−0.0202	−0.0499	0.444	0.651	0.17	0.00713
m_5	0.0706	−0.237	0.0836	−0.104	−0.0983	−0.257	−0.0609	−0.113	0.311	0.603	0.131	0.00246
m_6	0.0603	−0.23	0.0667	−0.108	−0.124	−0.338	−0.131	−0.157	0.219	0.523	0.082	−0.0653
m_7	0.204	−0.0845	0.255	0.116	0.111	−0.143	−0.0309	−0.0627	0.309	0.578	0.155	0.00545
m_8	0.156	−0.149	0.0842	−0.122	−0.0618	−0.12	0.0981	0.0613	0.532	0.745	0.241	0.0592
m_9	0.205	−0.122	0.19	0.0431	0.12	−0.0159	0.154	0.158	0.489	0.648	0.172	−0.00101
m_{10}	0.182	−0.14	0.139	−0.0194	0.0463	−0.0627	0.296	0.327	0.447	0.628	0.15	0.0226
m_{11}	0.104	−0.198	0.111	−0.0618	0.0699	0.153	0.435	0.25	0.419	0.592	0.126	−0.00192
m_{12}	0.0311	−0.264	0.0122	−0.145	−0.00142	0.0513	0.305	0.197	0.432	0.552	0.112	−0.0289
d_1	−0.283	−0.0283	−0.428	−0.313	−0.397	−0.244	−0.375	−0.207	−0.44	−0.583	−0.113	0.00917
d_2	−0.0805	0.269	0.0241	0.213	0.152	0.188	−0.121	−0.102	−0.398	−0.608	−0.164	−0.0187
d_3	−0.0302	0.298	0.058	0.261	0.196	0.221	−0.0912	−0.0791	−0.388	−0.603	−0.158	−0.00721
d_4	−0.0327	0.295	0.0455	0.246	0.191	0.215	−0.0948	−0.0821	−0.399	−0.609	−0.164	−0.00757
d_5	−0.0473	0.283	0.0411	0.234	0.165	0.195	−0.107	−0.0954	−0.41	−0.615	−0.163	−0.000756
d_6	−0.0453	0.279	0.0229	0.202	0.134	0.17	−0.133	−0.122	−0.431	−0.621	−0.153	0.0191
d_7	−0.169	0.0751	−0.305	−0.17	−0.239	−0.0818	−0.251	−0.127	−0.466	−0.66	−0.16	0.0129

TABLE 3. Estimated parameters for the German market.

GER	$h=1$	$h=2$	$h=3$	$h=4$	$h=5$	$h=6$	$h=7$	$h=8$	$h=9$	$h=10$	$h=11$	$h=12$
λ	7.46×10^7	7.11×10^7	6.47×10^7	6.25×10^7	6.46×10^7	7.34×10^7	7.94×10^7	8.28×10^7	8.12×10^7	8.12×10^7	8.17×10^7	7.91×10^7
a	0.00241	−0.0422	−0.0579	−0.0664	−0.115	0.124	−0.216	0.132	−0.0764	−0.0526	0.0411	0.0432
b	−0.471	0.0294	−0.838	−0.347	−0.249	2.76	−0.358	2.08	−0.457	0.622	−1.79	0.386
m_1	0.0444	−0.122	0.211	0.308	0.351	0.395	−0.444	0.212	0.25	0.395	0.171	0.414
m_2	0.108	−0.029	0.358	0.437	0.453	0.505	−0.229	0.376	0.327	0.441	0.214	0.487
m_3	−0.0163	−0.267	0.0577	0.178	0.206	0.306	−0.504	0.0984	0.129	0.317	0.123	0.414
m_4	0.000344	−0.272	−0.0592	0.103	0.16	0.302	−0.498	0.0586	0.197	0.413	0.235	0.494
m_5	−0.153	−0.41	−0.209	−0.289	−0.179	0.0508	−0.629	−0.0109	0.159	0.388	0.198	0.414
m_6	0.00765	−0.187	−0.0118	0.0269	0.112	0.16	−0.416	0.0852	0.266	0.483	0.299	0.54
m_7	0.0641	−0.0966	0.192	0.275	0.307	0.374	−0.244	0.245	0.308	0.482	0.289	0.503
m_8	−0.0786	−0.327	−0.0507	−0.0292	0.0398	0.206	−0.436	0.127	0.145	0.28	0.0867	0.417
m_9	0.016	−0.219	0.0572	0.121	0.145	0.293	−0.34	0.281	0.285	0.431	0.247	0.58
m_{10}	0.0546	−0.178	0.108	0.173	0.202	0.317	−0.308	0.354	0.396	0.591	0.399	0.645
m_{11}	−0.0299	−0.296	−0.102	−0.00173	0.0901	0.267	−0.51	0.103	0.292	0.524	0.329	0.513
m_{12}	−0.0184	−0.236	0.021	0.12	0.156	0.234	−0.659	0.00864	0.192	0.447	0.246	0.423
d_1	−0.138	−0.0331	−0.379	−0.491	−0.632	−0.974	−0.814	−1.36	−1.05	−1.02	−0.727	−0.896
d_2	−0.164	0.0424	−0.213	−0.311	−0.262	−0.214	0.769	0.173	−0.0189	−0.273	−0.0965	−0.325
d_3	0.0241	0.269	0.0178	−0.06	−0.0637	−0.083	0.816	0.209	0.0176	−0.238	−0.067	−0.336
d_4	0.0417	0.309	0.0311	−0.000287	−0.0476	−0.0811	0.778	0.167	−0.00773	−0.25	−0.0765	−0.33
d_5	0.0784	0.335	0.0972	0.0421	0.0191	−0.0599	0.803	0.178	−0.0197	−0.272	−0.101	−0.378
d_6	0.0528	0.292	0.0405	−0.0326	−0.0379	−0.0797	0.797	0.158	−0.0256	−0.271	−0.103	−0.385
d_7	0.131	0.373	0.135	0.0953	−0.0753	−0.361	0.142	−0.414	−0.461	−0.587	−0.389	−0.676

GER	$h=13$	$h=14$	$h=15$	$h=16$	$h=17$	$h=18$	$h=19$	$h=20$	$h=21$	$h=22$	$h=23$	$h=24$
λ	7.99×10^7	8.23×10^7	8.27×10^7	8.16×10^7	8.34×10^7	8.6×10^7	8.64×10^7	8.6×10^7	8.14×10^7	7.86×10^7	7.77×10^7	7.56×10^7
a	−0.0432	0.0414	0.0282	0.0528	0.111	0.148	0.101	0.0192	−0.0756	−0.0601	−0.00753	0.0162
b	−2.81	−0.214	−0.0382	−0.085	0.349	0.395	−0.0109	−2.04	0.202	0.011	1.71	0.016
m_1	0.182	−0.0992	−0.0132	−0.257	0.00606	0.0366	−0.076	−0.191	−0.0354	0.0413	0.113	0.179
m_2	0.247	−0.041	0.0537	−0.21	0.012	−0.00932	0.000721	−0.163	−0.0583	0.0209	0.121	0.216
m_3	0.159	−0.122	−0.05	−0.292	−0.056	−0.14	−0.143	−0.195	−0.133	−0.0476	0.087	0.173
m_4	0.213	−0.0691	−0.00536	−0.248	−0.068	−0.221	−0.335	−0.457	−0.169	0.00256	0.0855	0.18
m_5	0.151	−0.131	−0.0617	−0.287	−0.176	−0.329	−0.42	−0.499	−0.25	−0.04	0.0488	0.105
m_6	0.226	−0.042	0.0649	−0.205	−0.0978	−0.305	−0.403	−0.418	−0.167	−0.00217	0.105	0.182
m_7	0.234	−0.0107	0.11	−0.152	0.0052	−0.208	−0.364	−0.389	−0.127	0.0578	0.153	0.245
m_8	0.157	−0.148	−0.0367	−0.275	−0.0508	−0.194	−0.384	−0.49	−0.22	0.00551	0.0423	0.128
m_9	0.298	0.0266	0.122	−0.0965	0.141	0.0081	−0.159	−0.24	−0.0139	0.0674	0.112	0.193
m_{10}	0.373	0.105	0.183	−0.0423	0.152	0.0558	0.0713	0.0398	0.0621	0.0866	0.146	0.233
m_{11}	0.269	0.0386	0.135	−0.0947	0.163	0.266	0.157	−0.0596	−0.00885	0.0309	0.122	0.175
m_{12}	0.195	−0.0534	0.0223	−0.203	0.078	0.0953	−0.0411	−0.153	−0.00803	0.0548	0.12	0.138
d_1	−0.601	−0.428	−0.599	−0.389	−0.566	−0.32	−0.113	0.0701	−0.0811	−0.137	−0.146	−0.258
d_2	−0.076	0.24	0.166	0.415	0.189	0.239	0.308	0.372	0.188	0.0473	−0.0792	−0.149
d_3	−0.109	0.229	0.17	0.413	0.191	0.241	0.286	0.366	0.194	0.0544	−0.0677	−0.139
d_4	−0.0805	0.232	0.175	0.415	0.197	0.234	0.292	0.366	0.189	0.0592	−0.0647	−0.132
d_5	−0.112	0.19	0.132	0.386	0.167	0.21	0.296	0.35	0.18	0.0324	−0.0774	−0.139
d_6	−0.141	0.104	0.0157	0.254	0.0506	0.109	0.171	0.246	0.0917	−0.0303	−0.103	−0.154
d_7	−0.382	−0.156	−0.256	−0.00266	−0.186	−0.0802	0.0458	0.147	−0.0664	−0.165	−0.186	−0.263

TABLE 4. Estimated parameters for the French market.

FRA	$h=1$	$h=2$	$h=3$	$h=4$	$h=5$	$h=6$	$h=7$	$h=8$	$h=9$	$h=10$	$h=11$	$h=12$
λ	1.1×10^8	1.08×10^8	1.15×10^8	1.2×10^8	1.17×10^8	1.18×10^8	1.13×10^8	1.19×10^8	1.24×10^8	1.24×10^8	1.25×10^8	1.25×10^8
a	0.0773	0.0927	0.102	0.142	0.175	−0.147	−0.202	−0.117	−0.0548	0.0193	−0.00756	0.0331
b	−1.95	−1.87	−1.91	−2.05	−2.44	0.192	−0.231	−0.754	−0.505	−2.87	−2.67	−0.203
m_1	0.0476	0.469	0.063	0.0924	0.164	0.53	0.296	0.392	0.128	0.191	0.343	0.217
m_2	0.012	0.456	0.0606	0.165	0.19	0.493	0.238	0.326	0.0684	0.158	0.305	0.188
m_3	−0.0489	0.385	−0.0446	0.0558	0.0188	0.316	0.00833	0.0843	−0.072	0.0447	0.196	0.0953
m_4	−0.109	0.303	−0.127	−0.0267	−0.1	0.213	−0.116	−0.0252	−0.0974	0.0526	0.204	0.124
m_5	−0.181	0.158	−0.316	−0.273	−0.234	0.0797	−0.246	−0.0911	−0.165	−0.011	0.149	0.096
m_6	−0.0935	0.255	−0.249	−0.219	−0.191	0.00178	−0.234	−0.0479	−0.119	0.0683	0.259	0.204
m_7	−0.0198	0.349	−0.114	−0.037	0.0354	0.32	0.0319	0.089	−0.0448	0.141	0.347	0.299
m_8	−0.36	−0.0497	−0.575	−0.587	−0.569	−0.155	−0.382	−0.204	−0.308	−0.123	0.108	0.0416
m_9	−0.112	0.255	−0.246	−0.221	−0.264	0.151	−0.0211	0.149	−0.0282	0.112	0.319	0.264
m_{10}	0.093	0.486	0.0348	0.126	0.0515	0.34	0.121	0.356	0.214	0.353	0.504	0.434
m_{11}	0.0994	0.507	0.0298	0.0972	0.0933	0.397	0.152	0.281	0.132	0.279	0.408	0.302
m_{12}	0.138	0.566	0.151	0.256	0.247	0.531	0.252	0.334	0.105	0.218	0.354	0.24
d_1	0.0243	−0.389	0.0266	−0.102	−0.159	−0.738	−0.843	−1.08	−0.704	−0.668	−0.748	−0.626
d_2	−0.139	−0.565	−0.116	−0.22	−0.169	−0.329	0.16	0.13	0.227	0.0316	−0.158	−0.0683
d_3	0.0753	−0.317	0.152	0.102	0.153	−0.0863	0.267	0.177	0.261	0.0681	−0.118	−0.0356
d_4	0.0438	−0.331	0.127	0.0838	0.086	−0.124	0.226	0.114	0.221	0.0459	−0.146	−0.0673
d_5	0.0822	−0.288	0.184	0.145	0.16	−0.072	0.257	0.142	0.236	0.0421	−0.144	−0.0669
d_6	0.09	−0.286	0.175	0.126	0.15	−0.0894	0.241	0.119	0.2	0.0215	−0.17	−0.111
d_7	0.137	−0.228	0.248	0.232	0.154	−0.327	−0.163	−0.326	−0.16	−0.277	−0.447	−0.388

FRA	$h=13$	$h=14$	$h=15$	$h=16$	$h=17$	$h=18$	$h=19$	$h=20$	$h=21$	$h=22$	$h=23$	$h=24$
λ	1.22×10^8	1.21×10^8	1.21×10^8	1.23×10^8	1.24×10^8	1.25×10^8	1.24×10^8	1.22×10^8	1.17×10^8	1.16×10^8	1.15×10^8	1.14×10^8
a	−0.0347	0.0324	0.0273	−0.0381	0.0855	0.16	0.137	0.0607	−0.0491	−0.0194	0.0387	−0.0539
b	−2.92	−0.358	0.228	−2.25	0.76	0.671	0.601	0.914	−0.133	−0.0901	−0.676	2.36
m_1	−0.424	0.539	0.0776	0.205	0.0903	0.227	0.371	0.132	0.229	0.332	−0.326	0.329
m_2	−0.465	0.494	0.0303	0.15	0.0287	0.119	0.362	0.118	0.116	0.234	−0.382	0.298
m_3	−0.562	0.408	−0.065	0.043	−0.0828	−0.0347	0.138	0.0386	0.0322	0.193	−0.383	0.296
m_4	−0.534	0.422	−0.0687	0.0205	−0.169	−0.179	−0.101	−0.332	−0.141	0.163	−0.439	0.229
m_5	−0.544	0.416	−0.0796	0.0137	−0.197	−0.263	−0.207	−0.402	−0.216	0.103	−0.444	0.196
m_6	−0.461	0.506	0.0378	0.135	−0.087	−0.218	−0.181	−0.344	−0.146	0.0846	−0.429	0.206
m_7	−0.375	0.593	0.159	0.302	0.0938	−0.029	−0.0188	−0.215	−0.041	0.182	−0.372	0.261
m_8	−0.568	0.381	−0.0658	0.0724	−0.0789	−0.0738	−0.0418	−0.285	−0.146	0.164	−0.461	0.142
m_9	−0.387	0.588	0.133	0.267	0.132	0.159	0.198	−0.00938	0.138	0.32	−0.329	0.294
m_{10}	−0.27	0.7	0.233	0.339	0.186	0.233	0.401	0.306	0.285	0.427	−0.169	0.497
m_{11}	−0.371	0.621	0.141	0.226	0.143	0.342	0.531	0.189	0.251	0.354	−0.228	0.439
m_{12}	−0.417	0.565	0.0887	0.194	0.0913	0.261	0.364	0.105	0.24	0.358	−0.259	0.408
d_1	0.117	−0.908	−0.511	−0.676	−0.59	−0.509	−0.493	−0.167	−0.214	−0.35	0.306	−0.362
d_2	0.565	−0.382	0.109	0.00345	0.168	0.115	−0.00721	0.17	0.0513	−0.176	0.394	−0.267
d_3	0.582	−0.365	0.128	0.0335	0.21	0.146	0.0104	0.169	0.0391	−0.183	0.387	−0.272
d_4	0.564	−0.375	0.113	0.0204	0.189	0.113	−0.0239	0.148	0.0227	−0.18	0.383	−0.279
d_5	0.555	−0.385	0.108	0.0131	0.191	0.123	−0.0101	0.156	0.0183	−0.196	0.371	−0.284
d_6	0.518	−0.448	0.0221	−0.0916	0.0636	0.00798	−0.136	0.0542	−0.0499	−0.247	0.353	−0.275
d_7	0.314	−0.682	−0.224	−0.332	−0.183	−0.2	−0.308	−0.0625	−0.176	−0.343	0.278	−0.343

TABLE 5. Estimated parameters for the Swiss market.

SWI	$h=1$	$h=2$	$h=3$	$h=4$	$h=5$	$h=6$	$h=7$	$h=8$	$h=9$	$h=10$	$h=11$	$h=12$
λ	9.91×10^{7}	9.62×10^{7}	9.61×10^{7}	9.75×10^{7}	9.57×10^{7}	9.95×10^{7}	1.03×10^{8}	1.02×10^{8}	1.02×10^{8}	1.02×10^{8}	1.02×10^{8}	1.02×10^{8}
a	−0.0508	0.0911	0.0758	−0.00629	0.0348	−0.0642	0.112	0.052	0.0911	−0.0957	0.105	0.133
b	2.39	−1.01	−0.942	0.504	1.22	−1.49	1.33	0.945	0.933	−2.43	0.591	0.489
m_1	0.0992	0.831	0.366	0.396	0.0447	0.202	0.293	0.183	0.211	0.343	0.274	−0.35
m_2	0.0848	0.857	0.373	0.347	0.0621	0.205	0.339	0.233	0.235	0.387	0.31	−0.302
m_3	0.0184	0.814	0.311	0.279	0.0133	0.0862	0.144	0.0783	0.105	0.273	0.2	−0.395
m_4	−0.146	0.668	0.162	0.0805	−0.229	−0.114	−0.13	−0.128	−0.102	0.0594	0.00574	−0.582
m_5	−0.347	0.4	−0.186	−0.316	−0.697	−0.412	−0.412	−0.268	−0.237	−0.0744	−0.119	−0.704
m_6	−0.308	0.386	−0.153	−0.236	−0.531	−0.453	−0.31	−0.225	−0.152	0.0351	0.0168	−0.519
m_7	−0.263	0.486	−0.0145	−0.0363	−0.341	−0.261	−0.233	−0.256	−0.136	0.037	0.0138	−0.523
m_8	−0.315	0.419	−0.11	−0.174	−0.45	−0.29	−0.193	−0.239	−0.169	0.00723	−0.00902	−0.541
m_9	−0.132	0.661	0.156	0.0617	−0.191	−0.0999	−0.0122	−0.0258	0.00635	0.17	0.13	−0.423
m_{10}	0.0888	0.895	0.387	0.315	−0.0081	0.0422	0.155	0.23	0.198	0.355	0.291	−0.307
m_{11}	0.0543	0.787	0.283	0.213	−0.128	0.0458	0.0604	0.125	0.111	0.254	0.171	−0.452
m_{12}	0.0798	0.818	0.331	0.297	−0.0742	0.0514	0.0905	0.126	0.0975	0.265	0.177	−0.466
d_1	0.0485	−0.752	−0.298	−0.28	−0.0833	−0.429	−0.771	−0.783	−0.585	−0.591	−0.493	0.11
d_2	−0.0569	−0.882	−0.36	−0.3	0.105	0.156	0.227	0.222	0.147	−0.0564	−0.00839	0.586
d_3	0.12	−0.631	−0.125	−0.0657	0.28	0.241	0.253	0.238	0.165	−0.0417	0.00251	0.597
d_4	0.0824	−0.667	−0.145	−0.0893	0.25	0.208	0.224	0.224	0.15	−0.047	0.000959	0.593
d_5	0.0998	−0.636	−0.124	−0.0544	0.289	0.233	0.23	0.221	0.149	−0.0481	−0.00268	0.584
d_6	0.112	−0.63	−0.105	−0.0321	0.322	0.224	0.215	0.204	0.118	−0.0817	−0.0382	0.54
d_7	0.216	−0.485	0.0509	0.124	0.363	0.0462	−0.0975	−0.0773	−0.132	−0.29	−0.245	0.304

SWI	$h=13$	$h=14$	$h=15$	$h=16$	$h=17$	$h=18$	$h=19$	$h=20$	$h=21$	$h=22$	$h=23$	$h=24$
λ	1.02×10^{8}	1.01×10^{8}	1.01×10^{8}	1.01×10^{8}	1.03×10^{8}	1.05×10^{8}	1.06×10^{8}	1.05×10^{8}	1.03×10^{8}	1.02×10^{8}	1×10^{8}	1×10^{8}
a	0.103	0.0988	0.0898	0.0915	0.108	−0.162	0.147	0.114	0.0754	0.054	0.0331	0.0567
b	0.358	0.289	0.305	0.349	0.199	−2.87	0.406	0.767	1.3	1.08	0.248	−0.162
m_1	0.741	0.293	0.793	0.233	0.0964	0.104	0.39	0.487	0.424	0.268	0.33	0.428
m_2	0.763	0.314	0.801	0.235	0.0989	0.11	0.413	0.483	0.38	0.244	0.314	0.451
m_3	0.677	0.24	0.732	0.151	0.0145	−0.00513	0.276	0.385	0.268	0.141	0.277	0.379
m_4	0.497	0.0352	0.494	−0.124	−0.299	−0.384	−0.136	−0.0363	0.00494	−0.0799	0.0512	0.139
m_5	0.409	−0.0751	0.371	−0.259	−0.473	−0.572	−0.301	−0.192	−0.185	−0.243	−0.0669	−0.0115
m_6	0.515	0.0293	0.494	−0.134	−0.361	−0.479	−0.216	−0.085	−0.117	−0.226	−0.0409	0.00678
m_7	0.529	0.0472	0.519	−0.0919	−0.302	−0.373	−0.109	−0.00183	−0.0633	−0.193	−0.0238	0.0417
m_8	0.521	0.0499	0.503	−0.101	−0.286	−0.294	−0.0427	0.0365	−0.0547	−0.147	−0.0313	0.053
m_9	0.651	0.196	0.655	0.049	−0.112	−0.136	0.107	0.216	0.158	−0.0148	0.099	0.201
m_{10}	0.782	0.343	0.831	0.234	0.0832	0.0346	0.341	0.491	0.323	0.155	0.308	0.437
m_{11}	0.654	0.213	0.721	0.143	0.0631	0.0911	0.369	0.366	0.26	0.135	0.279	0.37
m_{12}	0.653	0.199	0.69	0.121	0.0359	0.0536	0.302	0.369	0.326	0.186	0.288	0.354
d_1	−0.893	−0.486	−1.02	−0.46	−0.263	−0.135	−0.328	−0.356	−0.247	−0.0905	−0.207	−0.306
d_2	−0.522	−0.0452	−0.508	0.0973	0.251	0.26	−0.0308	−0.151	−0.0989	0.0218	−0.12	−0.205
d_3	−0.51	−0.0354	−0.493	0.113	0.26	0.273	−0.0146	−0.141	−0.0931	0.0178	−0.118	−0.215
d_4	−0.52	−0.0421	−0.502	0.0958	0.243	0.253	−0.0364	−0.154	−0.0967	0.0133	−0.129	−0.225
d_5	−0.528	−0.0492	−0.505	0.0977	0.247	0.257	−0.0372	−0.14	−0.0983	0.0138	−0.129	−0.211
d_6	−0.563	−0.0949	−0.561	0.0324	0.172	0.175	−0.116	−0.213	−0.138	−0.0179	−0.149	−0.224
d_7	−0.728	−0.288	−0.775	−0.167	−0.0106	0.0278	−0.228	−0.299	−0.224	−0.0856	−0.188	−0.272

TABLE 6. Estimated parameters for the Czech market.

CZR	$h=1$	$h=2$	$h=3$	$h=4$	$h=5$	$h=6$	$h=7$	$h=8$	$h=9$	$h=10$	$h=11$	$h=12$
λ	6.92×10^7	7.7×10^7	6.05×10^7	5.66×10^7	5.07×10^7	5.34×10^7	5.74×10^7	5.77×10^7	5.89×10^7	5.8×10^7	5.8×10^7	5.76×10^7
a	0.413	−0.696	0.673	−0.718	−0.685	−0.656	−0.506	−0.441	−0.288	−0.174	0.126	−0.0927
b	2.83	−0.406	2.97	−0.269	−0.311	−0.561	−1.01	−0.666	−0.415	0.169	3.03	−0.621
m_1	0.0304	0.738	0.817	0.718	0.932	0.238	0.137	0.583	−0.0519	−0.129	−0.173	0.0696
m_2	−0.355	0.3	0.371	0.305	0.542	0.113	0.0728	0.338	−0.17	−0.191	−0.252	−0.033
m_3	−0.533	−0.0916	−0.316	−0.249	0.146	−0.507	−0.366	0.00977	−0.39	−0.387	−0.429	−0.158
m_4	−0.474	−0.193	−0.375	−0.308	−0.0399	−0.755	−0.642	−0.0361	−0.467	−0.254	−0.341	−0.116
m_5	−0.27	0.17	0.00603	−0.241	−0.0178	−0.781	−0.625	0.087	−0.265	−0.11	−0.24	−0.0479
m_6	0.315	0.925	0.696	0.715	0.715	−0.416	−0.338	0.516	0.0486	0.109	−0.0239	0.188
m_7	0.49	1.45	1.11	1.11	1.16	0.194	0.212	0.779	0.138	0.0559	−0.0264	0.206
m_8	0.148	0.887	0.463	0.495	0.715	0.0364	0.208	0.533	−0.116	−0.206	−0.219	0.0708
m_9	−0.101	0.415	0.173	0.243	0.45	−0.184	0.197	0.508	−0.112	−0.0926	−0.132	0.159
m_{10}	−0.533	−0.0832	−0.376	−0.177	0.175	−0.527	−0.202	0.287	−0.12	0.0236	−0.0711	0.157
m_{11}	−0.437	−0.0967	−0.0143	−0.243	0.00412	−0.561	−0.419	0.286	−0.205	−0.0392	−0.194	−0.0134
m_{12}	−0.297	0.364	0.42	0.368	0.687	−0.319	−0.36	0.337	−0.126	−0.00336	−0.13	0.0222
d_1	−0.238	−1.01	−0.881	−0.848	−1.5	−1.16	−1.85	−1.97	−0.668	−0.42	−0.201	−0.368
d_2	−0.346	−0.906	−0.996	−1.06	−1.05	0.342	0.675	0.09	0.363	0.241	0.273	0.0417
d_3	0.352	−0.185	−0.0263	0.0551	−0.0242	0.728	0.744	0.121	0.426	0.284	0.34	0.106
d_4	0.331	−0.261	−0.111	−0.0638	−0.154	0.708	0.726	0.0939	0.402	0.27	0.323	0.0796
d_5	0.361	−0.123	0.089	0.121	−0.0363	0.73	0.718	0.0913	0.401	0.257	0.31	0.0712
d_6	0.361	−0.162	0.112	0.0943	−0.0893	0.743	0.712	0.0726	0.388	0.255	0.308	0.0546
d_7	0.427	−0.0263	0.204	0.224	−0.121	0.276	0.00174	−0.58	−0.052	−0.0543	0.0358	−0.206

CZR	$h=13$	$h=14$	$h=15$	$h=16$	$h=17$	$h=18$	$h=19$	$h=20$	$h=21$	$h=22$	$h=23$	$h=24$
λ	5.76×10^7	5.66×10^7	5.65×10^7	5.56×10^7	5.51×10^7	5.58×10^7	5.67×10^7	5.68×10^7	5.67×10^7	5.69×10^7	5.78×10^7	5.91×10^7
a	−0.101	0.0893	0.132	−0.175	0.171	0.202	0.202	−0.177	0.124	0.081	0.0448	−0.0832
b	−0.717	1.85	1.73	−1.67	1.35	1.24	1.49	−1.01	2.49	2.33	1.99	−0.178
m_1	0.0897	0.354	0.299	0.425	−0.0622	0.196	0.21	0.214	0.638	0.03	0.155	−0.101
m_2	−0.0263	0.263	0.188	0.367	−0.25	0.0417	0.162	0.000295	0.528	−0.0166	0.0985	−0.301
m_3	−0.154	0.169	0.0705	0.22	−0.353	−0.148	0.0201	−0.00439	0.38	−0.121	0.0299	−0.299
m_4	−0.152	0.134	0.00704	0.094	−0.455	−0.319	−0.448	−0.344	0.364	−0.0579	0.0578	−0.244
m_5	−0.0626	0.188	0.006	0.0517	−0.51	−0.403	−0.426	−0.357	0.306	−0.0555	0.081	−0.166
m_6	0.144	0.348	0.203	0.246	−0.331	−0.252	−0.263	−0.154	0.437	0.0201	0.175	−0.00181
m_7	0.184	0.427	0.337	0.438	−0.165	−0.0735	−0.0718	−0.0155	0.487	0.0541	0.22	0.0263
m_8	0.0842	0.361	0.291	0.43	−0.153	0.018	−0.0054	−0.0578	0.481	0.0868	0.182	−0.0959
m_9	0.131	0.46	0.379	0.525	−0.0448	0.117	0.0897	0.0867	0.666	0.147	0.236	−0.0759
m_{10}	0.0921	0.377	0.222	0.329	−0.236	−0.0549	0.0969	0.188	0.617	0.0408	0.159	−0.126
m_{11}	−0.0433	0.204	0.0371	0.143	−0.312	−0.00336	−0.0104	−0.0803	0.41	−0.0913	0.0548	−0.251
m_{12}	0.0221	0.26	0.133	0.222	−0.22	−0.0191	−0.072	−0.0458	0.465	−0.0564	0.0501	−0.261
d_1	−0.349	−0.673	−0.596	−0.718	−0.119	−0.212	−0.127	−0.104	−0.586	−0.0511	−0.139	0.107
d_2	0.0689	−0.189	−0.0775	−0.193	0.35	0.131	0.125	0.105	−0.402	0.0558	−0.0796	0.23
d_3	0.11	−0.129	0.000995	−0.111	0.431	0.233	0.179	0.155	−0.404	0.0593	−0.0817	0.231
d_4	0.0978	−0.146	−0.0168	−0.125	0.408	0.208	0.163	0.131	−0.429	0.0476	−0.102	0.214
d_5	0.0893	−0.16	−0.0205	−0.133	0.408	0.203	0.17	0.134	−0.419	0.0401	−0.1	0.197
d_6	0.0693	−0.196	−0.0878	−0.209	0.328	0.114	0.0194	0.0218	−0.498	−0.027	−0.16	0.117
d_7	−0.194	−0.486	−0.373	−0.443	0.086	−0.0798	−0.0621	−0.0787	−0.61	−0.101	−0.21	0.0135

Once the non-parametric trend and parametric seasonality are estimated, we separate them from the stochastic process component

$$Z_h(t) = \ln S_h(t) - H_{h,\lambda_h}(t) - \Lambda_h(t) = X_h(t) + Y_h(t).$$

The last value of the time series of $Z_h(t)$ concerns our evaluation date and is input data for our pricing formula. Such values are shown in Table 7.

TABLE 7. The computed process $Z(t)$ on December 31, 2010.

α_h	ITA	GER	FRA	SWI	CZR
$h = 1$	−0.26342	0.12408	−0.12838	−0.28483	0.27097
$h = 2$	−0.40381	0.10700	−0.10825	−0.50895	0.31080
$h = 3$	−0.55397	0.096343	−0.25398	−0.62438	0.22027
$h = 4$	−0.56940	−0.072232	−0.41036	−0.70699	0.11620
$h = 5$	−0.55491	−0.15925	−0.37509	−0.61493	−0.20572
$h = 6$	−0.69825	−0.099510	−0.34517	−0.73811	−0.17784
$h = 7$	−0.52263	0.16580	−0.21596	−0.59989	−0.71336
$h = 8$	−0.42415	−0.19487	−0.37086	−0.21618	−0.59366
$h = 9$	−0.40267	−0.31108	−0.29207	−0.29901	−0.88127
$h = 10$	−0.35237	−0.29792	−0.22043	−0.15052	−0.67571
$h = 11$	−0.34732	−0.30027	−0.15457	−0.11360	−0.47048
$h = 12$	−0.33569	−0.19689	−0.12401	−0.11507	−0.40785
$h = 13$	−0.29660	−0.25311	−0.096574	−0.17319	−0.45823
$h = 14$	−0.27726	−0.18952	−0.12180	−0.17148	−0.42755
$h = 15$	−0.39077	−0.21674	−0.21991	−0.34519	−0.35042
$h = 16$	−0.39664	−0.24581	−0.24722	−0.35762	−0.29813
$h = 17$	−0.45776	−0.33727	−0.32087	−0.18563	−0.33782
$h = 18$	−0.55312	−0.38230	−0.42248	−0.31100	−0.56164
$h = 19$	−0.44668	−0.33276	−0.46318	−0.25530	−0.87593
$h = 20$	−0.34675	−0.42027	−0.24619	−0.17941	−0.97530
$h = 21$	−0.30591	−0.37114	−0.20882	−0.17820	−0.84224
$h = 22$	−0.25487	−0.20853	−0.17415	−0.30863	−0.59191
$h = 23$	−0.26881	−0.14483	−0.17129	−0.23479	−0.22134
$h = 24$	−0.15347	−0.19261	−0.095600	−0.20527	0.069359

The dynamic of $Z_h(t)$ is given by

$$dZ_h(t) = -\alpha_h Z_h(t)dt + \sigma_h dW_h + J_h^+ dN_h^+ - J_h^- dN_h^-. \tag{61}$$

The exact discrete time model of (61) is

$$Z_h(t+\delta t) = \exp(-\alpha_h \delta t) Z_h(t) + \sigma_h \sqrt{\frac{1-\exp(-2\alpha_h \delta t)}{2\alpha_h}} \epsilon_h(t), \tag{62}$$

where δt is equal to 1/365. The model in (62) is a discrete time AR(1) model with a non-normal error term $\epsilon_h(t)$. Indeed, $\epsilon_h(t)$ reflects the information given by Brownian motion and the exponential jumps. The quantity $\xi_h = \exp(-\alpha_h \delta t)$ can be easily estimated by ordinary least squares. Rearranging terms, we use the following estimator for the mean reversion parameter

$$\alpha_h = -\frac{\ln \xi_h}{\delta t}.$$

However, the following remark is necessary. When the residual term $\epsilon_h(t)$ is white noise, the ordinary least squares estimator of α_h corresponds to a maximum likelihood estimator. However, when

the residual term is not normal, ordinary least squares provides only a quasi-maximum likelihood estimate: The estimator is biased and should be corrected. We do not discuss this issue further, but see Ullah et al. (2010).[5] For every market, the augmented Dickey–Fuller test on deseasonalized prices (every hour using different lags, from one to 21) suggests the rejection of the unit root hypothesis in favor of mean-reverting alternatives in all cases. Table 8 shows the estimated speed of mean reversion. Values are estimated on a yearly basis. They are very high and the processes mean-revert to their equilibrium level very rapidly. The half-life of the exponential decays varies from 12 hours to almost three days, depending on the market and the hour considered. On average, the speed of mean reversion is higher in the Czech market and lower in the Swiss one. In the Czech market, the speed of mean reversion is high during the entire day. The other four markets exhibit a clustering of the mean reversion speeds. We see high mean reversion levels in the morning (particularly from 7:00 to 9:00) and relatively low values during the evening (from 18:00 to 23:00).

Table 8. Estimated mean reversion parameters.

α_h	ITA	GER	FRA	SWI	CZR
$h = 1$	268.25	480.40	317.41	208.16	504.40
$h = 2$	288.94	434.76	260.91	234.97	474.64
$h = 3$	369.42	400.09	257.95	274.77	392.09
$h = 4$	260.16	448.64	314.94	255.85	404.11
$h = 5$	255.31	442.08	302.25	302.91	409.10
$h = 6$	261.96	459.78	290.59	295.56	449.73
$h = 7$	406.46	502.25	390.49	428.15	597.59
$h = 8$	393.52	534.12	355.74	345.50	641.54
$h = 9$	307.82	385.14	257.68	268.79	449.50
$h = 10$	328.71	278.84	206.40	172.90	746.97
$h = 11$	308.50	248.59	179.15	163.41	717.69
$h = 12$	296.37	385.87	158.97	155.47	645.23
$h = 13$	259.67	441.24	138.84	151.95	689.16
$h = 14$	263.14	246.18	122.49	167.44	715.15
$h = 15$	293.85	350.97	129.52	172.71	665.37
$h = 16$	299.48	341.62	156.19	182.46	441.47
$h = 17$	270.13	371.26	203.38	171.43	708.55
$h = 18$	236.71	217.97	161.60	135.76	661.87
$h = 19$	210.47	234.50	136.61	112.73	817.77
$h = 20$	254.05	191.30	150.63	100.78	807.96
$h = 21$	271.51	195.32	184.07	102.30	253.94
$h = 22$	280.71	205.96	143.65	134.00	308.45
$h = 23$	233.06	223.20	333.28	143.30	385.44
$h = 24$	257.78	373.79	352.74	198.92	575.08

We now examine the residuals of the autoregressive model. It is very difficult to remove every sign of the autocorrelation generated by the seasonality in our data using such a simple model, especially at higher frequencies (e.g., weekly). However, the analysis of autocorrelation and partial autocorrelation is satisfactory for every market. The residuals are mostly small fluctuations around

[5]For example, if $\epsilon_h(t)$ follows an asymmetric Laplace distribution, few theoretical results are also available. Trindade et al. (2010) derive the marginal distribution of the process and calculate the exact confidence bands for minimum mean-squared error linear predictors. The authors also discuss the conditional maximum likelihood-based inference and provide corresponding asymptotic results.

zero, but from time to time they are rather extreme jumps. Moreover, the residuals are far from being normally distributed, as proven by many statistical tests we performed. This motivates our model's use of a mix of Brownian motion and a jump process. The next step is to identify the jumps and to separate them from the Brownian motion. We apply recursive filtering to implement this procedure. The filter identifies as a jump all data whose absolute value is more than three standard deviations from the mean. The filtering is performed recursively, in the sense that after the jumps are identified, these are removed, the level is computed again, and new jumps are identified. The procedure is iterated until the level remains the same and no new jumps are found.

Once the jumps are identified, we estimate their intensity and distribution. We separate positive from negative jumps. The parameter λ_h^+ is given by the ratio of the number of positive jumps to the number of total observations. Similarly, the parameter λ_h^- is estimated by the ratio of the number of negative jumps to the number of total observations. Then, dividing by 365, we obtain a yearly basis estimation. The parameters μ_h^+ and μ_h^- are, respectively, the means of the positive and negative jump distributions (in absolute value). One drawback of the algorithm is that it is unable to detect small jumps within a few standard deviations of the change in the mean-reverting process. The implication is that the jump mean parameter will be upward biased. This bias needs to be taken into account when estimating the parameters of the jump size distribution. We cannot find a sample from the jump distributions J^+ and J^-. We have a sample from the conditional distributions $J_h^+|J_h^+ > \gamma_h^+$ and $J_h^-|J_h^- > \gamma_h^-$, where we denote by $[\gamma_h^-, \gamma_h^+]$ the thresholds used in the iterative jump filtering procedure. The parameters are estimated using the following expressions for the conditional mean of the exponential distribution:

$$\mathbb{E}[J_h^+|J_h^+ > \gamma_h^+] = \gamma_h^+ + \mu_h^+, \qquad \mathbb{E}[J_h^-|J_h^- > \gamma_h^-] = \gamma_h^- + \mu_h^-.$$

We obtain μ_h^+ and μ_h^- by calculating the difference between the sample mean of detected jumps and the last thresholds used in the jump filtering.

Table 9 shows the results of the jump filtering procedure. The upper panel shows the annual intensities of positive and negative jumps for each market. The lower panel shows the estimated exponential distribution parameters. The jump intensities vary considerably with the market and the hour. The average number of (positive and negative) jumps per day varies between 7 (Italy) and 17 (Czech Republic); the minimum jump intensity is estimated for the 18th hour of the Italian market (almost three jumps per year) and the greatest jump intensity is estimate for the seventh hour of the Italian market (50 jumps per year). Jumps occur with the lowest frequency in the Italian market and with the highest frequency in the Czech market. The highest frequency of jumps occurs in the earliest hours of the day (from 00:00 to 9:00) for the German and Czech markets. A higher arrival rate of jumps in the Swiss market occurs between 6:00 and 9:00, while we see no such clustering in the Italian or French markets. On average, the positive jumps (sudden increases in price) are a bit more likely than the negative ones (sudden price drops) for all the markets we analyze. In Germany, Switzerland, and the Czech Republic, the jump distributions lead to more negative extreme values than positive ones and jumps are likely to be larger during the first half of the day than during the second half. In Italy and France the distribution of positive and negative jumps is more symmetric and we do not notice a pronounced difference between the distribution of jumps across the hours of the day.

TABLE 9. Estimated jump intensity parameters.

	ITA	ITA	GER	GER	FRA	FRA	SWI	SWI	CZR	CZR
	λ_h^+	λ_h^-	λ_h^+	λ_h^-	λ_h^+	λ_h^-	λ_h^+	λ_h^-	λ_h^+	λ_h^-
$h=1$	2.5	10.7	2	9.67	0.8	10.8	2.96	6.9	5.33	19.3
$h=2$	1.67	5.33	3.17	14.7	1.6	12.4	1.48	7.15	5.33	25.6
$h=3$	1.83	3.66	5.17	18	1.2	11.6	1.48	9.12	5	30
$h=4$	2.67	3.83	4.17	21	0.6	5.4	2.46	7.89	3.33	24.3
$h=5$	2.67	3.5	3.83	21	0.8	4.8	3.2	8.38	4.66	24
$h=6$	2.33	2.5	4.83	16.2	0.8	6.4	3.7	6.9	11.3	18
$h=7$	3.33	11.5	6.67	16.2	5.6	10.4	9.86	8.87	32	18.6
$h=8$	3	5.66	9	11.2	5.2	7.2	12.8	9.86	25	16
$h=9$	3	5.33	5.83	6.67	4.8	8	4.93	5.18	6.99	9.66
$h=10$	3.17	2.67	6.67	4.33	6.4	5.2	4.93	4.44	3	5.66
$h=11$	3.17	3.17	7.33	3.5	5.2	3.8	5.67	4.44	3	2.66
$h=12$	2.33	2.5	9.5	2.5	5.8	2.6	7.64	4.68	4	3.33
$h=13$	6.33	3.33	5.67	3	6	3	4.93	3.94	2	4
$h=14$	6.83	4.16	5.33	4.33	5	3	5.18	3.94	2	5.33
$h=15$	3.66	4.5	5.33	4.67	4.4	4.6	4.44	4.93	2.66	8.66
$h=16$	3.33	4.83	5.17	6.5	4.4	6.6	2.71	4.93	4.66	10.3
$h=17$	3.33	4.5	5.17	6.67	5.6	8.2	3.45	4.19	2.66	6.66
$h=18$	2.33	0.833	6.33	5.33	6	6.8	5.42	3.2	3	6.33
$h=19$	3.83	3.66	7.5	4.5	7.2	5.8	4.93	3.45	2.66	5.66
$h=20$	4	2.5	5.5	4.5	4.4	3.8	3.45	2.71	1.67	7.66
$h=21$	4.5	2.33	2.5	3	4.8	4.8	2.22	4.68	3.66	3.66
$h=22$	3	2.5	3	3.33	3.6	4.6	2.46	6.9	3.66	6.33
$h=23$	5	3.83	2.83	2.83	4.8	2.4	4.19	5.18	3.33	8.66
$h=24$	3.33	7.5	3.33	8.33	4.8	2.4	2.46	7.15	2.66	12.7
	μ_h^+	μ_h^-	μ_h^+	μ_h^-	μ_h^+	μ_h^-	μ_h^+	μ_h^-	μ_h^+	μ_h^-
$h=1$	0.0622	0.137	0.264	0.712	0.628	0.386	0.0506	0.205	0.525	2.1
$h=2$	0.0762	0.138	0.324	1.1	0.364	0.336	0.304	0.368	0.479	2.01
$h=3$	0.364	0.539	0.329	1.23	0.607	0.398	0.464	0.532	0.549	1.74
$h=4$	0.161	0.195	0.321	1.14	1	1.08	0.297	0.61	0.513	1.65
$h=5$	0.153	0.173	0.345	1.02	0.843	1.16	0.283	0.763	0.481	1.85
$h=6$	0.133	0.169	0.22	0.897	0.756	0.49	0.218	0.498	0.303	1.87
$h=7$	0.0808	0.154	0.195	1.19	0.189	0.527	0.223	0.674	0.553	2.07
$h=8$	0.0939	0.204	0.191	1.26	0.178	0.436	0.209	0.512	0.376	2.19
$h=9$	0.0904	0.197	0.337	0.925	0.273	0.286	0.139	0.496	0.361	1.55
$h=10$	0.0877	0.157	0.346	0.577	0.326	0.347	0.148	0.239	0.282	1.4
$h=11$	0.0551	0.112	0.333	0.483	0.424	0.322	0.158	0.215	0.202	2.45
$h=12$	0.103	0.0928	0.338	0.679	0.385	0.41	0.169	0.173	0.18	1.48
$h=13$	0.112	0.0743	0.326	0.508	0.244	0.222	0.114	0.131	0.278	1.31
$h=14$	0.101	0.105	0.327	0.284	0.168	0.146	0.107	0.174	0.297	1.21
$h=15$	0.117	0.159	0.387	0.629	0.189	0.171	0.0971	0.211	0.282	0.706
$h=16$	0.117	0.135	0.315	0.528	0.211	0.186	0.0932	0.23	0.155	0.46
$h=17$	0.0852	0.099	0.312	0.523	0.224	0.321	0.0978	0.159	0.299	0.873
$h=18$	0.084	0.204	0.329	0.205	0.209	0.24	0.203	0.161	0.269	0.948
$h=19$	0.0647	0.0898	0.325	0.267	0.259	0.165	0.225	0.148	0.253	1.18
$h=20$	0.0709	0.0809	0.249	0.144	0.291	0.271	0.131	0.1	0.158	0.884
$h=21$	0.0717	0.0727	0.148	0.129	0.252	0.212	0.0816	0.112	0.153	0.193
$h=22$	0.0975	0.0485	0.0608	0.0784	0.219	0.134	0.0712	0.124	0.14	0.264
$h=23$	0.0921	0.0694	0.094	0.133	0.203	0.652	0.0478	0.0996	0.139	0.263
$h=24$	0.0741	0.139	0.18	0.372	0.193	0.746	0.0728	0.104	0.313	0.761

Once we separate diffusion and jumps, the following step is the estimation of the diffusion parameters. We compute the diffusion coefficient χ_h of the Gaussian noise, removing jumps from residuals and computing a standard deviation on the remaining data. Equation (62) describes the link between the discrete parameter χ_h and the continuous parameter σ_h, that is,

$$\sigma_h = \chi_h \sqrt{\frac{2\alpha_h}{1 - \exp(-2\alpha_h \delta t)}}.$$

Table 10 shows the estimated volatilities. We note very high volatility levels: On average, they are higher in the Czech market and lower in the Italian and Swiss markets. Regarding the distribution of volatilities during the day, we observe the same pattern in almost all markets, with higher volatilities during the early morning, particularly between 3:00 and 9:00.

TABLE 10. Estimated volatility parameters.

σ_h	ITA	GER	FRA	SWI	CZR
$h = 1$	3.1023	5.4948	5.0568	3.9176	11.475
$h = 2$	4.4694	6.6205	5.2665	5.2853	15.316
$h = 3$	5.4539	7.8292	6.2965	6.1833	15.958
$h = 4$	4.9683	9.7609	8.9593	7.1848	20.072
$h = 5$	4.9791	9.1509	9.4772	7.8882	18.728
$h = 6$	4.9585	8.0090	7.8209	6.5877	14.412
$h = 7$	4.3078	10.711	7.9917	6.1831	11.511
$h = 8$	4.3794	9.2339	6.8065	4.5297	11.472
$h = 9$	3.8727	6.3036	4.8936	4.1829	6.6376
$h = 10$	4.5266	4.7048	4.0550	3.3616	7.2690
$h = 11$	4.4108	4.3376	3.6891	3.2599	6.6783
$h = 12$	4.4388	5.2137	3.5529	3.3268	6.0353
$h = 13$	3.2115	5.1595	3.0399	2.9828	5.9059
$h = 14$	3.0905	4.1829	3.0225	3.1207	6.0983
$h = 15$	3.8446	5.0069	3.2016	3.2414	5.7313
$h = 16$	4.1264	5.0079	3.5586	3.4775	4.4312
$h = 17$	4.1872	5.0759	4.0831	3.4348	5.8064
$h = 18$	4.0668	3.9716	3.6402	3.0284	5.7393
$h = 19$	3.4528	3.9244	3.3145	2.6991	6.5874
$h = 20$	3.3275	3.5022	3.0727	2.3787	6.1820
$h = 21$	3.0540	3.4013	2.9826	1.9947	2.8352
$h = 22$	2.9282	3.2053	2.8800	2.1673	2.6883
$h = 23$	2.1530	3.1228	3.6001	2.2165	2.8412
$h = 24$	2.1897	3.8093	3.9991	3.1446	4.7419

The next step is the computation of the function $f_h(T)$ in model (56). Since we have a model for each hour, we compute 24 separate functions. We already estimated such quantities from historical data preceding the valuation date:

$$f_h^*(t) = H_{h,\lambda_h}(t) + \Lambda_h(t).$$

We now need its risk-neutral specification $f_h(T)$ that will allow us to reproduce forward market quotations at the maturity date T. Therefore, each function is defined by a vector of the daily values of the days for which each option should be evaluated, that is, T_i for $i = 1, \ldots, n$. For each hour in question, the forward curve bootstrapping algorithm output is an n-dimensional vector with

elements $F_h(0,T_i)$. Rearranging the terms of equation (59), we obtain, for $i = 1, \ldots, n$,

$$\begin{aligned} f_h(T_i) &= \ln F_h(0,T_i) - (X_h(0) + Y_h(0))\, e^{-\alpha_h T_i} - \frac{\sigma_h^2}{4\alpha_h}\left(1 - e^{-2\alpha_h T_i}\right) - \\ &\quad \frac{\lambda_h^+}{\alpha_h} \ln\left(\frac{1-\mu_h^+ e^{-\alpha_h T_i}}{1-\mu_h^+}\right) - \frac{\lambda_h^-}{\alpha_h} \ln\left(\frac{1+\mu_h^- e^{-\alpha_h T_i}}{1+\mu_h^-}\right). \end{aligned} \tag{63}$$

The risk adjusted trend-seasonality function is computed using formula (63).

The last parameter in formula (58) is the correlation coefficient ρ_h between two prices of a given hour h for a pair of markets. The parameter is estimated by a sample correlation between the Gaussian residuals of the two markets. We computed such correlations on our dataset and show the results in Table 11. We see that estimated parameters are always positive: Under our model's assumptions, the energy prices of the five markets tend to move simultaneously up or down. The higher correlations involve the Germany–Czech Republic and France–Switzerland pairs. The Italian market seems to be the least correlated of the other four countries. For almost all pairs of markets, the correlation is higher during peak load hours than off peak. Evaluating the interconnections, we do not need all the parameters estimated in Table 11, only the correlation between neighboring interconnections. However, for the sake of completeness, we provide information for every possible market pair to appreciate more details. For example, Italy's correlations with neighboring countries (France and Switzerland) are, on average, slightly higher than those with Germany and the Czech Republic.

Table 11. Estimated correlation parameters.

ρ_h	ITA-GER	ITA-FRA	ITA-SWI	ITA-CZR	GER-FRA	GER-SWI	GER-CZR	FRA-SWI	FRA-CZR	SWI-CZR
$h=1$	0.119	0.114	0.125	0.084	0.42	0.281	0.326	0.352	0.219	0.146
$h=2$	0.125	0.137	0.193	0.115	0.365	0.279	0.31	0.376	0.242	0.209
$h=3$	0.135	0.145	0.217	0.0779	0.435	0.295	0.312	0.432	0.296	0.24
$h=4$	0.0911	0.151	0.174	0.065	0.436	0.301	0.283	0.409	0.281	0.208
$h=5$	0.0858	0.129	0.187	0.054	0.367	0.298	0.278	0.402	0.301	0.291
$h=6$	0.0846	0.0931	0.115	0.0944	0.368	0.32	0.309	0.356	0.318	0.233
$h=7$	0.0952	0.132	0.0971	0.105	0.362	0.247	0.395	0.379	0.275	0.263
$h=8$	0.13	0.141	0.214	0.0607	0.422	0.278	0.466	0.412	0.15	0.166
$h=9$	0.19	0.176	0.19	0.26	0.412	0.307	0.529	0.438	0.356	0.323
$h=10$	0.138	0.164	0.148	0.227	0.379	0.287	0.49	0.457	0.425	0.329
$h=11$	0.124	0.193	0.208	0.173	0.416	0.366	0.478	0.498	0.435	0.377
$h=12$	0.145	0.211	0.257	0.175	0.438	0.443	0.53	0.534	0.442	0.404
$h=13$	0.197	0.256	0.296	0.315	0.403	0.365	0.552	0.508	0.395	0.355
$h=14$	0.182	0.234	0.272	0.29	0.366	0.335	0.403	0.466	0.387	0.312
$h=15$	0.175	0.223	0.219	0.297	0.388	0.338	0.518	0.446	0.405	0.361
$h=16$	0.158	0.199	0.177	0.221	0.421	0.359	0.519	0.398	0.433	0.36
$h=17$	0.166	0.229	0.195	0.199	0.477	0.356	0.474	0.367	0.386	0.307
$h=18$	0.175	0.248	0.223	0.174	0.402	0.351	0.362	0.437	0.36	0.327
$h=19$	0.168	0.166	0.23	0.196	0.376	0.328	0.372	0.426	0.348	0.333
$h=20$	0.138	0.197	0.202	0.208	0.338	0.282	0.338	0.443	0.341	0.324
$h=21$	0.123	0.151	0.133	0.193	0.365	0.255	0.365	0.347	0.385	0.274
$h=22$	0.115	0.102	0.094	0.149	0.293	0.187	0.321	0.228	0.319	0.185
$h=23$	0.0792	0.0961	0.0833	0.106	0.334	0.204	0.262	0.262	0.336	0.213
$h=24$	0.0396	0.0604	0.0471	0.092	0.372	0.186	0.324	0.287	0.25	0.123

The following algorithm summarizes the calibration procedure on M interconnected markets:

```
for h = 1:24
    for m = 1:M
        filter Hodrick-Prescott cyclical trend for market m, hour h;
        estimate the seasonality function for market m, hour h;
        estimate the mean reversion coefficient with an AR(1) for market m, hour h;
        filter jumps for market m, hour h;
        estimate jump parameters for market m, hour h;
        estimate Gaussian volatility for market m, hour h;
        estimate the function f(t) for market m, hour h;
    end
    compute correlation between Gaussian residuals of every market for hour h;
end
```

5. Numerical results

This section discusses the results of valuing interconnection capacity in neighboring European countries. Based on the market data described in Section 3 and parameters estimated in Section 4, we compute the market value of a one-year-long interconnection that gives the owner the right to transmit 1 MWh of electricity between two markets during base load times in the year 2011. As argued by Cartea and Pedraz (2012), it does not seem plausible to exploit large price spreads, due to liquidity reasons in the two markets. We cap the maximum spread at different levels: $M \in \{10, 20, 30, 40, 50, \infty\}$ €/MWh, where we allow $M = \infty$ to include the case where there are no liquidity constraints. The transmission cost K can vary across different interconnections. The value of the interconnector is affected by changes in K: The higher K, the lower the value of the interconnection. For simplicity's sake, we consider three cases in our analysis: zero transmission costs, $K = 0$ €/MWh, and fixed transmission costs of 5 €/MWh and 10 €/MWh for each possible interconnection.[6]

Table 12 shows the results of our valuation. The most valuable interconnections concern the right to transmit energy to Italy, because prices in the Italian market are usually much higher than in France or Switzerland. Consequently, the same connections are not worth much when used to transmit energy from Italy to France and Switzerland: there are not many profitable hours during the year for such dealing. The other three interconnections under analysis do not show such a big difference between the values of the two interconnector's directions. The interconnections between France and Germany and between Germany and the Czech Republic are almost equally profitable in both directions. However, there are differences. At the valuation date, the transmission of energy from the Czech Republic to Germany was expected to be worth more than the option to transmit energy in the opposite direction. Similarly, the option to buy energy in Germany and sell it in France was expected to be more profitable than the reverse. Finally, price levels in Switzerland are usually lower than in France and the valuation results confirm that the option to transmit

[6]In some markets (e.g., the Italian market), energy transmission can be subject to costs and profits involving green certificates, which can affect the parameter K setting. Therefore the parameter K is not required to be strictly positive.

energy from France to Switzerland is more convenient than the reverse. Table 12 shows the effect of the liquidity cap is different across the markets in our study. For example, consider the case where $K = 0$ €/MWh and we buy energy in Germany and sell it in France. On the evaluation date, the price levels between these two markets are close. If the cap is reduced from $M = \infty$ to $M = 10$ €/MWh, the value of the interconnection decreases by almost 35%. If we draw the same comparison transmitting energy from France to Italy, the value of the interconnection decreases by more than 55%. This is because the difference in forward prices between Italy and France is larger. We note a similar pattern when comparing the same interconnections with different transmission costs. Consider the $M = 50$ €/MWh case. Going from $K = 0$ to $K = 5$ €/MWh, the value of the interconnection GER→FRA (buying energy in Germany and selling it in France) decreases by about 40%. The same analysis on the interconnection ITA→FRA show a value reduction of only 23%. As a general result, different effects of the liquidity cap and transmission costs are due to the particular features of the spread in each market, that is, differences in forward prices, mean reversion rates, volatilities, jump intensities, and jump sizes.

TABLE 12. Values of a one-year interconnector lease for different strike prices K and liquidity caps M.

$K = 0$	$M = 10$	$M = 20$	$M = 30$	$M = 40$	$M = 50$	$M = \infty$
FRA → ITA	62,503	105,632	129,068	139,285	143,113	145,085
ITA → FRA	10,927	15,426	17,202	17,912	18,211	18,621
SWI → ITA	55,697	91,409	109,747	117,581	120,556	122,123
ITA → SWI	14,864	20,856	22,988	23,703	23,942	24,101
FRA → SWI	38,870	55,458	60,910	62,478	62,916	63,127
SWI → FRA	22,565	30,553	33,089	33,929	34,245	34,676
FRA → GER	25,356	34,129	36,758	37,589	37,889	38,253
GER → FRA	35,383	50,667	56,288	58,288	59,025	59,685
CZR → GER	33,031	47,743	53,195	55,094	55,704	56,145
GER → CZR	25,757	35,162	38,488	39,901	40,619	41,944
$K = 5$	$M = 10$	$M = 20$	$M = 30$	$M = 40$	$M = 50$	$M = \infty$
FRA → ITA	29,169	72,298	95,733	105,950	109,779	111,751
ITA → FRA	4,317	8,816	10,592	11,302	11,601	12,011
SWI → ITA	25,483	61,195	79,533	87,367	90,342	91,909
ITA → SWI	5,903	11,895	14,027	14,742	14,980	15,140
FRA → SWI	16,087	32,676	38,128	39,696	40,133	40,344
SWI → FRA	8,681	16,669	19,205	20,046	20,362	20,793
FRA → GER	9,780	18,553	21,182	22,013	22,313	22,677
GER → FRA	14,518	29,801	35,423	37,423	38,160	38,820
CZR → GER	13,687	28,399	33,852	35,751	36,361	36,802
GER → CZR	10,016	19,421	22,747	24,159	24,878	26,202
$K = 10$	$M = 10$	$M = 20$	$M = 30$	$M = 40$	$M = 50$	$M = \infty$
FRA → ITA	0	43,129	66,565	76,781	80,610	82,582
ITA → FRA	0	4,499	6,275	6,985	7,284	7,693
SWI → ITA	0	35,712	54,050	61,884	64,860	66,427
ITA → SWI	0	5,992	8,124	8,839	9,078	9,237
FRA → SWI	0	16,589	22,041	23,608	24,046	24,257
SWI → FRA	0	7,988	10,524	11,364	11,680	12,111
FRA → GER	0	8,773	11,402	12,233	12,533	12,897
GER → FRA	0	15,283	20,905	22,904	23,642	24,302
CZR → GER	0	14,712	20,165	22,064	22,673	23,115
GER → CZR	0	9,405	12,731	14,144	14,862	16,187

Bibliography

C. Alexander and A. Venkatramanan. Analytic approximations for multi-asset option pricing. *Mathematical Finance*, DOI: 10.1111/j.1467-9965.2011.00481.x, 2011.

F. B. Anderson and M. Deacon. *Estimating and Interpreting the Yield Curve.* John Wiley and Sons, Chichester, 1996.

L. Ballotta and E. Bonfiglioli. Multivariate asset models using Lévy processes and applications. Available at http://ssrn.com/abstract=1695527, 2012.

M. T. Barlow. A diffusion model for electricity prices. *Mathematical Finance*, 12:287–298, 2002.

J. Beisser. *Topics in Finance—A Conditional Expectation Approach to Value Asian, Basket and Spread options.* PhD thesis, Johannes Gutenberg University Mainz, 2001.

F. E. Benth, J. Kallsen, and T. Meyer-Brandis. A non-Gaussian Ornstein–Uhlenbeck process for electricity spot price modeling and derivative pricing. *Applied Mathematical Finance*, 14(2): 153–169, 2007a.

F. E. Benth, S. Koekebakker, and F. Ollmar. Extracting and applying smooth forward curves from average-based commodity contracts with seasonal variation. *Journal of Derivatives*, 15(1):52–66, Fall 2007b.

F. E. Benth, J. S. Benth, and S. Koekebakker. *Stochastic Modelling of Electricity and Related Markets.* World Scientific Publishing, Singapore, 2008.

H. Bessembinder and M. L Lemmon. Equilibrium pricing and optimal hedging in electricity forward markets. *Journal of Finance*, 57(3):1347–1382, 2002.

P. Bjerksund and G. Stensland. Closed form spread option valuation. *Quantitative Finance*, iFirst: 1–10, 2011.

F. Black and M. Scholes. The Pricing of Option and Corporate Liabilities. *Journal of Political Economy*, 81(3):637–654, 1973.

S. Borovkova, F. J. Permana, and H. Weide. A closed-form approach to the valuation and hedging of basket and spread options. *Journal of Derivatives*, 14(4):8–24, 2007.

R. Carmona and V. Durrelman. Pricing and hedging spread option in a log-normal model. Available at http://orfe.princeton.edu/ rcarmona/download/fe/spread.pdf, 2003a.

R. Carmona and V. Durrelman. Pricing and hedging spread options. *SIAM Review*, 45, 2003b.

P. Carr and D. Madan. Option valuation using the fast Fourier transform. *Journal of Computational Finance*, 2:61–73, 2000.

A. Cartea and M. G. Figueroa. Pricing in electricity markets: A mean reverting jump diffusion model with seasonality. *Applied Mathematical Finance*, 12(4):313–335, 2005.

A. Cartea and C. G. Pedraz. How much should we pay for interconnecting electricity markets? A real options approach. *Energy Economics*, 34(1):14–30, 2012.

A. Cartea and P. Villaplana. Spot price modeling and the valuation of electricity forward contracts: The role of demand and capacity. *Journal of Banking & Finance*, 32:2502–2519, 2008.

G. H. L. Cheang and C. Chiarella. Exchange option under jump-diffusion dynamics. *Applied Mathematical Finance*, 18:245–276, 2011.

L. Clewlow and C. Strickland. *Energy Derivatives: Pricing and Risk Management*. Lacima Publications, London, 2000.

M. Curran. Valuing Asian and portfolio options by conditioning on the geometric mean price. *Managment Science*, 40:1705–1711, 1994.

G. Deelstra, J. Liinev, and M. Vanmaele. Pricing of arithmetic basket options by conditioning. *Insurance: Mathematics and Economics*, 31(1):55–77, 2004.

G. Deelstra, A. Petkovic, and M.Vanmaele. Pricing and hedging Asian basket spread options. *Journal of Computational and Applied Mathematics*, 234:2814–2830, 2010.

M. A. H. Dempster and S. S. G. Hong. Spread option valuation and the fast Fourier transform. In *Mathematical Finance—Bachelier Congress 2000*, pages 203–220. Springer, Berlin, 2002.

M. A. H. Dempster, E. Medova, and K. Tang. Long term spread option valuation and hedging. *Journal of Banking & Finance*, 32:2530–2540, 2008.

S. Deng. Stochastic models of energy commodity prices and their applications: Mean-reversion with jumps and spikes. Available at http://www.ieor.berkeley.edu/ oren/pubs/Deng

S. Deng, M. Li, and E. Zhou. Closed-form approximation for spread option prices and Greeks. *Journal of Derivatives*, 15:58–80, 2008.

J. Dhaene, M. Denuit, M. J. Goovaerts, R. Kaas, and D. Vyncke. The concept of comonotonicity in actuarial science and finance: Theory. *Insurance: Mathematics and Economics*, 31:3–33, 2002a.

J. Dhaene, M. Denuit, M. J. Goovaerts, R. Kaas, and D. Vyncke. The concept of comonotonicity in actuarial science and finance: applications. *Insurance: Mathematics and Economics*, 31:133–161, 2002b.

E. Fanone, A. Gamba, and M. Prokopczuk. The case of negative day-ahead electricity prices. Available at http://ssrn.com/abstract=1839208, 2011.

D. Flamouris and D. Giamouridis. Approximate basket option valuation for a simplified jump process. *Journal of Futures Markets*, 27:819– 837, 2007.

S. Fleten and J. Lemming. Constructing forward price curves in electricity markets. *Energy Economics*, 25:409–424, 2003.

G. Fusai and A. Roncoroni. *Implementing Models in Quantitative Finance: Methods and Cases*. Springer, Berlin, 2008.

H. Geman and A. Roncoroni. Understanding the fine structure of electricity prices. *Journal of Business*, 79(3):1225–1261, 2006.

D. Gentle. Basket weaving. *Risk*, 6(6):51–52, 1993.

P. B. Girma and A. S. Paulson. Seasonality in petroleum futures spreads. *Journal of Futures Markets*, 18:581–598, 1998.

P. B. Girma and A. S. Paulson. Risk arbitrage opportunities in petroleum futures spreads. *Journal of Futures Markets*, 19:931–955, 1999.

B. Hambly, S. Howison, and T. Kluge. Modelling spikes and pricing swing options in electricity markets. *Quantitative Finance*, 9(8):937–949, 2009.

M. Hildmann, J. Cornel, D. Stokic, G. Andersson, and F. Herzog. Robust calculation and parameter estimation of the hourly price forward curve. Available at http://www.eeh.ee.ethz.ch/uploads/tx_ethpublications/Hildmann_PSCC2011.pdf, 2011.

R. J. Hodrick and E. C. Prescott. Postwar U.S. business cycles: An empirical investigation. *Journal of Money, Credit and Banking*, 29(1):1–16, February 1997.

Z. Huang and S.G. Kou. First passage times and analytical solutions for options on two assets with jump risk. Available at http://www.cfe.columbia.edu/pdf-files/Kou_05_06.pdf, 2006.

F. Hubalek and C. Sgarra. On the Esscher transforms and other equivalent martingale measures for Barndorff–Nielsen and Shephard stochastic volatility models with jumps. *Stochastic Processes and their Applications*, 119(7):2137–2157, 2009.

R. Huisman, C. Huurman, and R. Mahieu. Hourly electricity prices in day-ahead markets. *Energy Economics*, 29:240–248, 2007.

T. R. Hurd and Z. Zhou. A Fourier transform method for spread option pricing. *SIAM Journal of Financial Mathematics*, 1:142–157, 2009.

C. B. Huynh. Back to baskets. *Risk*, 7(5):59–61, 1993.

N. L. Johnson. Systems of frequency curves generated by methods of translation. *Biometrika*, 36: 149–176, 1949.

R. L. Johnson, C. R. Zulauf, S. Irwin, and M. Gerlow. The soy-bean complex spread: An examination of market efficiency from the viewpoint of a production process. *Journal of Futures Markets*, 11:25–37, 1991.

E. Ju. Pricing Asian and basket options via Taylor expansion. *Journal of Computational Finance*, 5(3):79–103, 2002.

E. Kirk. Correlation in the energy market. In *Managing energy price risk*, pages 71–78. Risk Publication, London, first edition, 1995.

T. Kluge. *Pricing Swing Options and other Electricity Derivatives.* PhD thesis, University of Oxford, Available at http://kluge.in-chemnitz.de/docs/phd/dphil_thesis.pdf, 2006.

S. Kotz, T. J. Kozubowski, and K. Podgorsky. *The Laplace Distribution and Generalizations: A Revisit With Applications to Communications, Economics, Engineering, and Finance.* Birkhauser, Boston, 2001.

M. Krekel, J. De Kock, R. Korn, and T.K. Man. An analysis of pricing methods for baskets options. *Wilmott*, 3:82–89, 2004.

P. Laurence and T. Wang. Distribution-free upper bounds for spread options and market-implied antimonotonicity gap. *The European Journal of Finance*, 14(8):717–734, 2008.

E. Levy. Pricing European average rate currency options. *Journal of International Money and Finance*, 11:474–491, 1992.

R. Lord. Partially exact and bounded approximations for arithmetic Asian options. *Journal of Computational Finance*, 10:1–52, 2006.

J. J. Lucia and E. S. Schwartz. Electricity prices and power derivatives: Evidence from the Nordic Power Exchange. *Review of Derivatives Research*, 5:5–50, 2002.

W. Margrabe. The value of an option to exchange one asset for another. *Journal of Finance*, 33: 177–186, 1978.

J. H. McCulloch. Measuring the term structure of interest rates. *Journal of Business*, 44:19–31, 1971.

R. C. Merton. Option pricing when underlying stock returns are discontinous. *Journal of Financial Economics*, 3:125–144, 1976.

M. A. Milevsky and S. E. Posner. A closed-form approximation for valuing basket options. *Journal of Derivatives*, 5:54–61, 1998a.

M. A. Milevsky and S. E. Posner. Valuing Exotic Options by Approximating the SPD with Higher Moments. *Journal of Financial Engineering*, 7(2):109–125, 1998b.

J. A. Nielsen and K. Sandmann. Pricing bounds on Asian options. *Journal of Financial and Quantitative Analysis*, 38:449–473, 2003.

N. D. Pearson. An efficient approach for pricing spread options. *Journal of Derivatives*, 3:76–91, 1995.

T. M. Pedersen. The Hodrick–Prescott filter, the Slutzky effect, and the distortionary effect of filters. *Journal of Economic Dynamics & Control*, 25:1081–1101, 2001.

C. Pirrong and M. Jermakyan. The price of power: The valuation of power and weather derivatives. *Journal of Banking & Finance*, 32:2520–2529, 2008.

L. C. G. Rogers and Z. Shi. The value of an Asian option. *Journal of Applied Probability*, 32: 1077–1088, 1995.

E. S. Schwartz. The stochastic behavior of commodity prices: Implications for valuation and hedging. *Journal of Finance*, 52:923–973, 1997.

G. W. P. Thompson. *Topics in Mathematical Finance*. PhD thesis, University of Cambridge, 1999.

A. A. Trindade, Y. Zhu, and B. Andrews. Time series models with asymmetric Laplace innovations. *Journal of Statistical Computation and Simulation*, 80(12):1317–1333, 2010.

S. Truck, R. Weron, and R. Wolff. Outlier treatment and robust approaches for modeling electricity spot prices. Technical report, Hugo Steinhaus Center, Wroclaw University of Technology, Available at http://mpra.ub.uni-muenchen.de/4711/, 2007.

S. M. Turnbull and L. M. Wakeman. A quick algorithm for pricing European average options. *Journal of Financial and Quantitative Analysis*, 26(3):377–389, 1991.

A. Ullah, Y. Wang, and J. Yu. Bias in the mean reversion estimator in the continuous time Gaussian and Lèvy processes. Available at http://apps.olin.wustl.edu/MEGConference/Files/pdf/2010/18.pdf, 2010.

M. Vanmaele, G. Deelstra, and G. Liinev. Approximation of stop-loss premiums involving sums of lognormals by conditioning on two variables. *Insurance: Mathematics and Economics*, 35: 343–367, 2004.

A. Venkatramana and C. Alexander. Closed form approximations for spread options. *Applied Mathematical Finance*, 18:447–472, 2011.

P. Villaplana. Pricing power derivatives: A two-factor jump-diffusion approach. EFMA 2004 Basel Meetings. Available at http://orff.uc3m.es/bitstream/10016/87/1/wb031805.pdf, 2003.

D. Vyncke, M. J. Goovaerts, and J. Dhaene. An accurate analytical approximation for the price of a European-style arithmetic Asian option. *Finance*, 25:121–139, 2004.

G. Xu and H. Zheng. Approximate basket options valuation for a jump-diffusion model. *Insurance: Mathematics and Economics*, 45:188–194, 2009.

G. Xu and H. Zheng. Basket options valuation for a local volatility jump-diffusion model with the asymptotic expansion method. *Insurance: Mathematics and Economics*, 47:415–422, 2010a.

G. Xu and H. Zheng. Lower bound approximation to basket option values for local volatility jump-diffusion models. Available at http://papers.ssrn.com/sol3/papers.cfm?abstract_id=2137502, 2010b.

APPENDIX A

The Hodrick–Prescott filter

The Hodrick–Prescott filter (Hodrick and Prescott (1997)) is a mathematical tool used in macroeconomics, especially business cycle theory, to separate the cyclical component of a time series from raw data. It is used to obtain a smoothed-curve representation of a time series, one that is more sensitive to long-term than to short-term fluctuations. The idea of the filter is to additively decompose a time series $\{x_i\}$ into a trend $\{\tau_i\}$ and a noise component $\{\epsilon_i\}$ using an optimization algorithm. Two quantities are necessary:

(1) Measure of **convexity**

$$\bigtriangledown^2 t_i := t_{i+1} - 2t_i + t_{t-1}.$$

(2) Measure of **smoothness**

$$\sum_{i=2}^{t_{end}-1} (\bigtriangledown^2 t_i)^2.$$

The purpose of the filter is to find a trend $T := \{\tau_i\}$ that is as close as possible to the observed price path $\{x_i\}$, that is, solve

$$\min_{(\tau_t)_{t=1}^{t_{end}}} \sum_{i=1}^{t_{end}} (x_i - \tau_i)^2.$$

We even require the filter within the class of time-dependent functions showing a fixed degree of smoothness. Hodrick and Prescott (1997) show that this problem allows an analytic solution—hence the name Hodrick–Prescott filter—obtained through the Lagrange formulation

$$\min_{\{\tau_t\}} \left[\sum_{t=1}^{t_{end}} (x_t - \tau_t)^2 + \lambda \sum_{t=1}^{t_{end}} [(\tau_{t+1} - \tau_t) - (\tau_t - \tau_{t-1})]^2 \right].$$

The solution is

$$T = [I + \lambda * F]^{-1} X,$$

where

- $I :=$ identity matrix,
- $F :=$ sparse matrix with non-zero elements given by

$$
\begin{array}{ll}
F(1,1) = F(n,n) = 1, & \\
F(1,2) = F(n,n-1) = -2, & \\
F(2,1) = F(n-1,n) = -2, & \\
F(2,2) = F(n-1,n-1) = 5, & \\
F(i,i) = 6, & i = 3...n-2, \\
F(i,i+2) = F(i+2,i) = 1, & i = 1...n-2, \\
F(i,i+1) = F(i+1,i) = -4, & i = 2...n-2 \neq 1,2.
\end{array}
$$

The Hodrick–Prescott filter is a low-pass filter and, depending on the parameter λ, filters trend functions at different frequencies. To filter specific frequencies of the time series, we need a criterion to determine the optimal value of the smoothing parameter λ. The criterion we briefly describe is proposed by Pedersen (2001). Let $H^*(\omega)$ be the power transfer function of an ideal business cycle filter at frequency ω, where ω comprises n discrete equally $\Delta\omega$-spaced values with steps between zero and π, $\omega \in W = (\omega_1 < \omega_2 < \cdots < \omega_n)$ with $\omega_1 = 0$ and $\omega_n = \pi$, and let $H(\omega)$ be the power transfer function of some distorting business cycle filter. We than have

$$
H(\omega) = \left| \frac{4\lambda(1-\cos(\omega))^2}{4\lambda(1-\cos(\omega))+1} \right|^2,
$$

$$
H^*(\omega) = 1(\omega \geq \omega_c).
$$

We indicate by $S_x(\omega)$ the power spectral density function of the signal $\{x_i\}$. Suppose we want to filter out frequencies lower than a threshold ω_c. The optimal criterion is λ such that Q_w is minimum, where

$$
Q_w = \sum_{\omega \in W} |H(\omega) - H^*(\omega)| v(\omega)
$$

and

$$
v(\omega) = \frac{2S_x(\omega)\Delta\omega}{\sum_{\omega \in W} 2S_x(\omega)\Delta\omega}.
$$

The Q-statistics could be interpreted as the variance of the difference between the ideal filtered spectrum and the suboptimal filtered spectrum.

APPENDIX B

Proofs for Chapter 2

1. Proof of Proposition 1

We observe that $\mathbb{E}\Big[S_2^{\alpha}(T)\Big] = \Phi_T(0, -i\alpha)$, so we can rewrite the set A defined in (24) as

$$\begin{aligned} A &= \{\omega : \ln S_1(T) - \alpha \ln S_2(T) > k - \ln \Phi_T(0, -i\alpha)\} \\ &= \{\omega : X_1(T) - \alpha X_2(T) + \ln \Phi_T(0, -i\alpha) > k\}. \end{aligned}$$

Following Carr and Madan (2000) and Dempster and Hong (2002), we multiply the expected value of the option approximation (26) by an exponentially decaying term, tuned by a parameter δ, so that it is square integrable in k over the negative axis. Then we apply the Fourier transform to this modified lower bound price:

$$\begin{aligned} & \Psi(\gamma; \delta, \alpha) = \int_{\mathbb{R}} e^{i\gamma k + \delta k} \mathbb{E}\left[(S_1(T) - S_2(T) - K)\, 1_{(A)}\right] dk \\ = & \int_{\mathbb{R}} e^{i\gamma k + \delta k} \left[\int_{\mathbb{R}} \int_{k - \ln \Phi_T(0, -i\alpha) + \alpha X_2(T)}^{+\infty} \left(e^{X_1(T)} - e^{X_2(T)} - K\right) f(X_1, X_2)\, dX_1 dX_2\right] dk \\ = & \int_{\mathbb{R}} \int_{\mathbb{R}} \left[\int_{-\infty}^{X_1(T) + \ln \Phi_T(0, -i\alpha) - \alpha X_2(T)} e^{i\gamma k + \delta k} dk\right] \left(e^{X_1(T)} - e^{X_2(T)} - K\right) f(X_1, X_2)\, dX_1 dX_2 \\ = & \frac{1}{i\gamma + \delta} \int_{\mathbb{R}} \int_{\mathbb{R}} e^{i(\gamma - i\delta)(X_1(T) - \alpha X_2(T) + \ln \Phi_T(0, -i\alpha))} \left(e^{X_1(T)} - e^{X_2(T)} - K\right) f(X_1, X_2)\, dX_1 dX_2 \\ = & \frac{e^{i(\gamma - i\delta) \ln(\Phi_T(0, -i\alpha))}}{i(\gamma - i\delta)} \Big[\mathbb{E}\big[e^{i(\gamma - i\delta - i)X_1(T) - i\alpha(\gamma - i\delta)X_2(T)}\big] - \mathbb{E}\big[e^{i(\gamma - i\delta)X_1(T) + i(-\alpha\gamma + i\alpha\delta - i)X_2(T)}\big] \\ & - K\mathbb{E}\big[e^{i(\gamma - i\delta)(X_1(T) - \alpha X_2(T))}\big]\Big] \\ = & \frac{e^{i(\gamma - i\delta) \ln(\Phi_T(0, -i\alpha))}}{i(\gamma - i\delta)} \Big[\Phi_T(\gamma - i(\delta + 1), -\alpha(\gamma - i\delta)) - \Phi_T(\gamma - i\delta, -\alpha\gamma + i\alpha\delta - i) \\ & - K\Phi_T(\gamma - i\delta, -(\gamma - i\delta)\alpha)\Big]. \end{aligned}$$

The lower bound is given by an inverse transform and depends on the parameters α and k. The optimal lower bound is achieved using the maximization

$$\max_{k,\alpha} e^{-\delta k - rT} \frac{1}{\pi} \int_0^{+\inf} e^{-i\gamma k} \Psi(\gamma; \delta, \alpha) d\gamma.$$

In practice, the optimization can be replaced by an educated guess, as suggested by Bjerksund and Stensland (2011), setting

$$\alpha = \frac{F_2(0,T)}{F_2(0,T)+K}, \qquad k = \ln(F_2(0,T)+K),$$

where $F_2(0,T)$ is the forward price of the second asset at time 0 for delivery at a future date T.

2. Proof of Proposition 2

Using the same arguments as in the previous Section, we have

$$\begin{aligned}
&\Xi(\gamma;\delta,\alpha) = \int_{\mathbb{R}} e^{i\gamma k+\delta k}\mathbb{E}\left[(S_1(T)-S_2(T)-L)^2 1_{(A)}\right]dk \\
= &\int_{\mathbb{R}} e^{i\gamma k+\delta k}\left[\int_{\mathbb{R}}\int_{k-\ln\Phi_T(0,-i\alpha)+\alpha X_2(T)}^{+\infty}\left(e^{X_1(T)}-e^{X_2(T)}-L\right)^2 f(X_1,X_2)\,dX_1dX_2\right]dk \\
= &\int_{\mathbb{R}}\int_{\mathbb{R}}\left[\int_{-\infty}^{X_1(T)+\ln\Phi_T(0,-i\alpha)-\alpha X_2(T)} e^{i\gamma k+\delta k}dk\right]\Big(e^{2X_1(T)}+e^{2X_2(T)}+L^2-2Le^{X_1(T)} \\
&-2e^{X_1(T)+X_2(T)}+2Le^{X_2(T)}\Big)f(X_1,X_2)\,dX_1dX_2 \\
= &\frac{1}{i\gamma+\delta}\int_{\mathbb{R}}\int_{\mathbb{R}} e^{i(\gamma-i\delta)(X_1(T)-\alpha X_2(T)+\ln\Phi_T(0,-i\alpha))}\Big(e^{2X_1(T)}+e^{2X_2(T)}+L^2-2Le^{X_1(T)} \\
&-2e^{X_1(T)+X_2(T)}+2Le^{X_2(T)}\Big)f(X_1,X_2)\,dX_1dX_2 \\
= &\frac{e^{i(\gamma-i\delta)\ln(\Phi_T(0,-i\alpha))}}{i(\gamma-i\delta)}\Big[\mathbb{E}\big[e^{i(\gamma-i\delta-2i)X_1(T)-i\alpha(\gamma-i\delta)X_2(T)}\big]-\mathbb{E}\big[e^{i(\gamma-i\delta)X_1(T)+i(-\alpha\gamma+i\alpha\delta-2i)X_2(T)}\big] \\
&+L^2\mathbb{E}\big[e^{i(\gamma-i\delta)(X_1(T)-\alpha X_2(T))}\big]-2L\mathbb{E}\big[e^{i(\gamma-i\delta-i)X_1(T)-i\alpha(\gamma-i\delta)X_2(T)}\big]+ \\
&2L\mathbb{E}\big[e^{i(\gamma-i\delta)X_1(T)+i(-\alpha\gamma+i\alpha\delta-i)X_2(T)}\big]-2\mathbb{E}\big[e^{i(\gamma-i\delta-i)X_1(T)+i(-\alpha\gamma+i\alpha\delta-i)X_2(T)}\big]\Big] \\
= &\frac{e^{i(\gamma-i\delta)\ln(\Phi_T(0,-i\alpha))}}{i(\gamma-i\delta)}\Big[\Phi_T((\gamma-i\delta)-2i,-\alpha(\gamma-i\delta)) \\
&+\Phi_T(\gamma-i\delta,-\alpha(\gamma-i\delta)-2i)+L^2\Phi_T(\gamma-i\delta,-\alpha(\gamma-i\delta)) \\
&-2L\Phi_T(\gamma-i\delta-i,-\alpha(\gamma-i\delta))+2L\Phi_T(\gamma-i\delta,-\alpha(\gamma-i\delta)-i) \\
&-2\Phi_T(\gamma-i\delta-i,-\alpha(\gamma-i\delta)-i)\Big].
\end{aligned}$$

We can obtain $Q(0)$ by an inverse Fourier transform, discounting and setting parameters $\alpha = 1$ and $k = \ln(F_2(0,T))$.

3. Derivation of formula (35)

The characteristic function is

$$\begin{aligned}\mathbb{E}[e^{i\mathbf{u}^\intercal \mathbf{X}(T)}] &= e^{i\mathbf{u}^\intercal(\mathbf{X}(0)+\gamma T)}\mathbb{E}\Big[\exp\Big\{iu_1\big(\sigma_1 W_1(T)+\sum_{m=1}^{N_1(T)} Z_1(m)+\sum_{n=1}^{N(T)} Y_1(n)\big)\\ &\quad +iu_2\big(\sigma_2 W_2(T)+\sum_{m=1}^{N_2(T)} Z_2(m)+\sum_{n=1}^{N(T)} Y_2(n)\big)\Big\}\Big]\\ &= e^{i\mathbf{u}^\intercal(\mathbf{X}(0)+\gamma T)}\sum_{n=0}^{\infty}\sum_{n_1=0}^{\infty}\sum_{n_2=0}^{\infty}\frac{e^{-\lambda T}(\lambda T)^n}{n!}\frac{e^{-\lambda_1 T}(\lambda_1 T)^{n_1}}{n_1!}\frac{e^{-\lambda_2 T}(\lambda_2 T)^{n_2}}{n_2!}\beta(n,n_1,n_2),\end{aligned}$$

where

$$\begin{aligned}\beta(n,n_1,n_2) &= \mathbb{E}\Big[\exp\Big\{iu_1\big(\sigma_1 W_1(T)+\sum_{m=1}^{N_1(T)} Z_1(m)+\sum_{n=1}^{N(T)} Y_1(n)\big)+iu_2\big(\sigma_2 W_2(T)+\sum_{m=1}^{N_2(T)} Z_2(m)+\\ &\quad \sum_{n=1}^{N(T)} Y_2(n)\big)\Big\}\Big|N(T)=n, N_1(T)=n_1, N_2(T)=n_2\Big].\end{aligned}$$

Conditioning to the event $\{N(T)=n, N_1(T)=n_1, N_2(T)=n_2\}$, $\beta(n,n_1,n_2)$ is the characteristic function of a bivariate normal variable $B(n,n_1,n_2)$, where

$$B(n,n_1,n_2)\sim \mathcal{MN}\left(\begin{pmatrix} n_1\alpha_{11}+n\alpha_1\\ n_2\alpha_{22}+n\alpha_2\end{pmatrix},\begin{pmatrix} n_1\xi_{11}^2+n\xi_1^2+\sigma_1^2T & n\rho_Y\xi_1\xi_2+\sigma_1\sigma_2\rho T\\ n\rho_Y\xi_1\xi_2+\sigma_1\sigma_2\rho T & n_2\xi_{22}^2+n\xi_2^2+\sigma_2^2T\end{pmatrix}\right).$$

We therefore obtain

$$\begin{aligned}\beta(n,n_1,n_2) &= \exp\big\{iu_1(n_1\alpha_{11}+n\alpha_1)+iu_2(n_2\alpha_{22}+n\alpha_2)-u_1^2(n_1\xi_{11}^2+n\xi_1^2+\sigma_1T)/2-\\ &\quad u_2^2(n_2\xi_{22}^2+n\xi_2^2+\sigma_2T)/2-u_1u_2(n\rho_Y\xi_1\xi_2+\sigma_1\sigma_2\rho T)\big\},\end{aligned}$$

which results in

$$\begin{aligned}\mathbb{E}[e^{i\mathbf{u}^\intercal \mathbf{X}(T)}] &= e^{i\mathbf{u}^\intercal(\mathbf{X}(0)+\gamma T)-T(\lambda+\lambda_1+\lambda_2+u_1^2\sigma_1^2/2+u_2^2\sigma_2^2/2+u_1u_2\sigma_1\sigma_2)}\sum_{n_1=0}^{\infty}\frac{e^{n_1(\ln(\lambda_1T)+iu_1\alpha_{11}-u_1^2\xi_{11}^2/2)}}{n_1!}\times\\ &\quad \sum_{n_2=0}^{\infty}\frac{e^{n_2(\ln(\lambda_2T)+iu_2\alpha_{22}-u_2^2\xi_{22}^2/2)}}{n_2!}\sum_{n=0}^{\infty}\frac{e^{n(\ln(\lambda T)+iu_1\alpha_1+iu_2\alpha_2-u_1^2\xi_1^2/2-u_2^2\xi_2^2/2-u_1u_2\xi_1\xi_2\rho_Y)}}{n!}.\end{aligned}$$

Straightforward calculations lead to the formula (35).

APPENDIX C

Proofs for Chapter 3

1. Proof of Proposition 3

We denote by $f(X_k, Y_n)$ the joint bivariate probability density of $X_k(T)$ and the log-geometric average $Y_n(T)$. We consider the lower bound to the basket option payoff in T, as in formula (40):

$$\mathbb{E}\left[(A_n(T) - K)\, I(\mathcal{G})\right],$$

where $\mathcal{G} = \{\omega : Y_n(T) > \kappa\}$. We introduce the dumping factor $\exp(\delta\kappa)$ according to Carr and Madan (2000) and compute the Fourier transform with respect to κ. We obtain

$$\begin{aligned}
\Psi(\gamma;\delta) &= \int_{\mathbb{R}} e^{i\gamma\kappa+\delta\kappa}\mathbb{E}\left[(A_n(T) - K)\, I(\mathcal{G})\right] d\kappa \\
&= \int_{\mathbb{R}} e^{i\gamma\kappa+\delta\kappa}\left[\sum_{k=1}^{n} w_k \mathbb{E}\left[(S_k(T) - K)\, I(\mathcal{G})\right]\right] d\kappa \\
&= \int_{\mathbb{R}} e^{i\gamma\kappa+\delta\kappa}\left[\sum_{k=1}^{n} w_k \int_{\mathbb{R}}\int_{\kappa}^{+\infty}\left(S_k(t)\, e^{X_k(T)} - K\right) f(X_k, Y_n)\, dX_k dY_n\right] d\kappa \\
&= \sum_{k=1}^{n} w_k \int_{\mathbb{R}}\int_{\mathbb{R}}\left[\int_{-\infty}^{Y_n} e^{i\gamma\kappa+\delta\kappa}\left(S_k(t)\, e^{X_k(T)} - K\right) f(X_k, Y_n)\, d\kappa\right] dX_k dY_n \\
&= \sum_{k=1}^{n} w_k \int_{\mathbb{R}}\int_{\mathbb{R}}\left[\int_{-\infty}^{Y_n} e^{i\gamma\kappa+\delta\kappa} d\kappa\right]\left(S_k(t)\, e^{X_k(T)} - K\right) f(X_k, Y_n)\, dX_k dY_n \\
&= \frac{1}{i\gamma+\delta}\sum_{k=1}^{n} w_k \int_{\mathbb{R}}\int_{\mathbb{R}} e^{i(\gamma-i\delta)Y_n(T)}\left(S_k(t)\, e^{X_k(T)} - K\right) f(X_k, Y_n)\, dX_k dY_n \\
&= \frac{1}{i\gamma+\delta}\left[\sum_{k=1}^{n} w_k\left[S_k(t)\,\mathbb{E}\left(e^{i(\gamma-i\delta)Y_n(T)+X_k(T)}\right) - K\mathbb{E}\left(e^{i(\gamma-i\delta)Y_n(T)}\right)\right]\right] \\
&= \frac{1}{i\gamma+\delta}\left[\sum_{k=1}^{n} w_k\left(S_k(t)\,\Phi_T(\gamma - i\delta, -i\mathbf{e}_k, \mathbf{w}) - K\Phi_T(\gamma - i\delta, \mathbf{0}, \mathbf{w})\right)\right].
\end{aligned}$$

Remembering the dumping factor, we read the Fourier inversion as

$$\frac{e^{-\delta\kappa}}{\pi}\int_0^{+\infty} e^{-i\gamma\kappa}\Psi(\gamma;\delta)d\gamma.$$

Formula (42) is obtained by discounting, applying the positive part function, and maximizing with respect to κ.